Order Number 9009788

The remobilization of the interfaces of moving bubbles and droplets retarded by surfactant adsorption

Stebe, Kathleen Joan, Ph.D.

City University of New York, 1989

U·M·I
300 N. Zeeb Rd.
Ann Arbor, MI 48106

THE REMOBILIZATION OF THE INTERFACES OF MOVING BUBBLES AND DROPLETS RETARDED BY SURFACTANT ADSORPTION

by

KATHLEEN J. STEBE

A dissertation submitted to the Graduate Faculty in Engineering in partial fulfillment of the requirements for the degree of Doctor of Philosophy, The City University of New York.

1989

This manuscript has been read and accepted for the Graduate Faculty in Engineering in satisfaction of the dissertation requirement for the degree of Doctor of Philosophy.

September 28, 1989

Professor Charles Maldarelli

September 28, 1989

Dean Jacques E. Benveniste

Professor Andreas Acrivos

Professor Zeev Dagan

Professor Kevin McKeigue

Dr. Paul Gherson, Technicon Inc.
Supervisory Committee

The City University of New York

ABSTRACT

THE REMOBILIZATION OF THE INTERFACES OF MOVING BUBBLES AND DROPLETS RETARDED BY SURFACTANT ADSORPTION

by

Kathleen J. Stebe

Advisor: Professor Charles Maldarelli

This thesis addresses the influence of surfactant molecules on fluid particle flows in a three part study ((I.), (II.) and (III.)). Surfactant molecules adsorb onto the interfaces of moving fluid particles and are convected to the rear pole of the droplet. Adsorbed surfactant molecules accumulate at this stagnation point if the time scale for interfacial convection is faster than those governing the kinetic exchange of surfactant and bulk diffusion. Surfactant accumulation in this region gives rise to a surface tension gradient along the interface which retards the surface velocity. In this thesis, conditions under which surface velocities of surfactant laden fluid particles can remain unhindered are investigated.

The remobilization of fluid particle interfaces is demonstrated experimentally in (I.) and (II.) using a three phase capillary slug flow in which a train of air and aqueous surfactant solution slugs

ride on an annular wetting film of fluorocarbon oil. Surfactant adsorbs along and retards the aqueous-oil interface, significantly increasing the pressure drop required to drive the flow at constant velocity.

In (I.), a fluid particle flow is shown to remain unhindered in the presence of a single adsorbed surfactant. A surfactant with no desorption kinetic barriers, present in concentrations such there are no barriers to diffusive mass transport, adsorbs uniformly along the interface. No gradients in surface tension arise to retard the surface velocity; the flow behaves as it would in the absence of surfactant, save that it has a reduced, uniform surface tension.

The remobilization of fluid particle flows hindered by adsorbed impurities is demonstrated in (II.). A fast adsorbing and desorbing surfactant with no barriers to diffusive transport preferentially adsorbs along the particle interface, preventing the adsorption of an impurity. The remobilizing surfactant establishes a uniform surface concentration (and therefore a uniform surface tension). Thus, competitive adsorption of a fast sorption kinetic surfactant allows fluid particle flows in the presence of impurities to behave hydrodynamically as they would in their absence.

In (III.) a spectrophotometric technique for measuring the oil film thickness around the aqueous slug in the three phase slug flow is described. Initial results indicate that the films are on the order of tens of microns, and decrease with the surface mobility of the oil-aqueous interface. This is attributed to a reduction of the leak rate and the constant rate of oil induction.

Table of Contents

LIST OF TABLES

LIST OF FIGURES

APPENDIX

Chapter 3

Chapter 4

LIST OF PLATES

INTRODUCTION

This thesis studies the influence of surfactant molecules on fluid particle flows. Surfactant molecules adsorb on fluid particle interfaces, where they reduce the interfacial tension. Adsorbed surfactant molecules on moving drops or bubbles are swept along the interface toward converging stagnation points, where, due to bulk diffusion barriers or slow desorption kinetics, they can accumulate. At steady state a surface distribution of surfactant is realized with some higher surface concentration near the converging stagnation zone than elsewhere on the interface if desorption or bulk diffusion barriers are present. The surface tension gradients which arise due to the nonuniform surface concentration set up a Marangoni stress which opposes and retards the surface velocity and acts to retard the drop velocity. This is the effect commonly associated with surfactants in fluid particle flows.

In this dissertation, conditions under which the surface velocities of fluid particles can remain unhindered in the presence of adsorbed surfactant are investigated in a three part study. The flow used to demonstrate the remobilization of fluid particle interfaces is a three phase capillary slug flow. In the flow, a train of alternating air and aqueous surfactant solution slugs are drawn through a teflon capillary tube. The slug train rides on an annular fluorocarbon oil film which preferentially wets the tube wall. Surfactant solutions are used to form the aqueous phase. Adsorbed surfactant acts to retard the surface velocity along the aqueous-oil interface. The oil which forms the thin annular film is

introduced at a low, constant flow rate which precludes any thickening of the annular film to relieve the shearing in this region. The retarding effects of adsorbed surfactant are threfore strongly felt in this flow geometry. Since the three phase slug flow is drawn at a constant velocity through the capillary tube, the drag resisting the flow due to the presence of surface concentration gradients of adsorbed surfactant makes itself felt in an increased pressure drop required to drive the flow.

In the first part of this study, it is shown that a fluid particle flow can remain unhindered in the presence of a single adsorbed surfactant. A surfactant with no desorption kinetic barriers, present in large enough concentrations that barriers to diffusive mass transport have been eliminated, adsorbs uniformly along a fluid particle interface. No gradients in surface tension arise to retard the surface velocity; the fluid particle flow behaves hydrodynamically as it would in the absence of surfactant, save that it has a reduced, uniform surface tension.

This is demonstrated in a series of experiments in which a fast sorption kinetic surfactant, Triton-X 100, is dissolved in the aqueous phase in the three phase slug flow. At Triton-X 100 concentrations high enough that barriers to diffusive mass transport have been eliminated, the pressure drop required to drive the three phase slug flow reduces to that required to drive the flow in the absence of absorbed surfactant. As a counter example, it is shown that the elimination of diffusion barriers for a slow desorption surface adsorber does not result in a remobilized fluid particle

interface. The surface adsorber used in those experiments was the protein Bovine Serum Albumin. (B.S.A.)

In the second part of this study, the remobilization of fluid particle flows hindered by adsorbed surface active impurities is investigated. If a fast adsorbing and desorbing surfactant is present at concentrations such that it has no barriers to diffusive transport from the sublayer of the interface to the bulk, it will preferentially adsorb along the particle interface, preventing the adsorption of a surface active impurity. The remobilizing surfactant will establish a uniform surface concentration (and therefore a uniform surface tension) in equilibrium with its bulk concentration. In this manner, competitive adsorption of a fast sorption kinetic surfactant is demonstrated to allow fluid particle flows in the presence of surface active impurities to behave hydrodynamically as they would in the absence of surfactant.

The remobilization of the interfaces of fluid particles retarded by adsorbed impurities was demonstrated experimentally in the three phase slug flow. In each series of experiments, two surface adsorbers were dissolved in the aqueous slug phase. The first was present as a "contaminant"; the adsorber B.S.A. or the commercial surfactant Brij-35 was dissolved at concentrations where they act to significantly increase the pressure drop required to drive the flow. In each series of experiments in the competitive adsorption study, Triton-X 100 was used as the second adsorber in solution. Its concentration was increased from extremely low values to concentrations where the barriers to diffusive mass flux disappear.

In the third part of this study a spectrophotometric technique for measuring the wetting layer thickness around the aqueous slug in the three phase slug flow is described. Initial results indicate that the wetting layers are on the order of tens of microns, and decrease as the surface mobility of the oil-aqueous interface is decreased. This effect is attributed to a reduction of the leak rate and the fact that the oil induction rate is maintained constant.

This dissertation is divided into four chapters. Chapter 1 details a literature review on the subjects of the influence of surfactants on fluid particle flows and the hydrodynamics of slug flows. The remobilization of fluid particle interfaces in the presence of a single adsorbed surfactant is detailed in Chapter 2. The results of the second part of this study, in which it is demonstrated that the interfaces of fluid particles retarded by the adsorption of surface active impurities can be remobilized by competitive adsorption of a remobilizing surfactant, are given in Chapter 3. The scope of future work, including the measurement of wetting layers in capillary tubes using a spectrophotometric method, along with some preliminary results on the effect of adsorbed surfactant on the film thicknesses realized in the three phase slug flow are presented in Chapter 4. The scope of future work is outlined, including a study of surfactant effects in two phase slug flows, surfactants being present in the continuous (wetting) phase.

Chapter 1

Literature Review

The aim of this chapter is to review the prior investigations which are relevant to the proposed studies. It is convenient to divide this review into two sections. In the first, a review of investigations of the influence of surfactants on fluid particle flows is presented. In the second section, the results from prior investigations of the hydrodynamics of slug flows in fluid filled capillaries are detailed.

1. Surfactants in Fluid Particle Flows

Surfactant molecules have hydrophobic and hydrophillic chemical moities and therefore find it energetically favorable to adsorb on fluid particle interfaces where they reduce the interfacial tension. The hydrodynamics of fluid particle flows, in which bubbles or droplets move in a continuous fluid, is altered by surfactant adsorption. Fluid particle velocities are found to decrease, or the drag opposing the particle motion is found to increase in the presence of adsorbed surfactant. The physicochemical basis for these effects is the nonuniform distribution of surfactant adsorbed along the particle interface. Surfactant adsorbed on fluid particle interfaces accumulates near converging stagnation zones if the rate of desorption is slow compared to that of surface convection, or if bulk diffusion barriers are present. Accumulated surfactant reduces

the surface tension in this region. The stress resulting from the surface tension gradient, a Marangoni tension, opposes and reduces the surface velocity, reducing the particle velocity in turn. This is the explanation put forth by Frumkin and Levich (1947) for the reduction in terminal velocity of a fluid droplet settling in an otherwise quiescent medium in the presence of surfactants. All investigations of the retarding effect of surfactants on fluid particle flows have considered their effect in the context of this problem of a spherical fluid droplet settling in an otherwise quiescent medium, except for a few recent studies on slug flows which will be discussed in the following section.

Consider the simple fluid particle flow in which a spherical fluid particle settling at low Re in an otherwise quiescent infinite medium. In the case where the kinetic desorption of surfactant is slow compared to surface convection, adsorbed surfactant molecules are swept by surface convection toward and accumulate in the region of the trailing stagnation point of the sphere.

In the case of fast sorption kinetics, surface convection sweeps adsorbed surfactant to the rear pole of the droplet where it can adsorb and desorb freely, in equilibrium with the local sublayer concentration. If the rate at which surfactant diffuses through the sublayer to the bulk is slow, the local sublayer concentration and therefore the surface concentration at the trailing pole will be higher than elsewhere along the drop interface.

Consider the extreme limits of the two cases described above, in which the rate at which surfactant is swept by surface convection

to the trailing stagnation point is extremely fast compared to the kinetics of adsorption and desorption or diffusive mass transport. In either of these limits, the surface concentration everywhere on the drop surface away from the rear stagnation zone will be zero. This is termed stagnant cap behavior, as in the zone covered with surfactant molecules, the surface velocity is reduced to zero. Several investigators have observed stagnant cap behavior for settling fluid spheres in the presence of surfactant. Savic (1953), using flow visualization techniques, observed streamlines which were asymmetric with respect to the equatorial plane of the fluid sphere, indicating that the surface velocity vanishes near the trailing stagnation point. It the experimental investigations of Horton et al. (1965) a shift in the recirculation vortex in the drop interior away from the cap region was observed, again indicating that the surface velocity is zero in this region. Other experimental investigators who observed stagnant cap behavior near the trailing stagnation point in their studies on the influence of surfactant adsorption on mass transfer are: Garner and Skelland (1955), Elzinga and Banchero (1961), Huang and Kintner (1969) and Beitel and Heideger (1971).

There have been several theoretical and numerical investigations of the problem of a settling fluid droplet with a stagnant cap at the trailing stagnation zone. This requires a mixed boundary condition at the interface, as the surface velocity is zero along the stagnant cap region and moves with the exterior shearing fluid everywhere else on the interface. Savic (1953), Griffith

(1962) and Davis and Acrivos (1966) studied this problem. In Savic's study, the surface tension at the trailing pole was taken to be zero, while that at the leading pole was assumed to be the clean surface value. Griffith used a linearized isotherm to relate the surface concentration at the trailing pole to the surface tension realized there. Davis and Acrivos assumed that the surface tension in the stagnant cap region was equal to the monolayer collapse tension.

Griffith did not treat the full hydrodynamics of the problem, but rather used approximate expressions for the tangential stresses exerted by the interior and exterior phases on the interface to solve for the cap angle. Both Savic and Davis and Acrivos considered the equations governing this flow, expanding the stream function in an infinite series of orthogonal polynomials. Savic truncated the resulting series after 6 terms; Davis and Acrivos truncated at 150 terms. In both studies, cap angle as a function of drag is computed. Sadhal and Johnson (1982) examine the governing equations to this flow in the limits of low Re and high Pe, that is in the limit of convection rate much higher than diffusion rates, one of the limits whereby stagnant caps form. An exact solution for the equations is formulated for arbitrary cap angle, and closed form solution for the drag force as a function of viscosities and cap angle is found. In their study, Sadhal and Johnson used a linearized isotherm to determine the surface tension in the cap region. Closed form solutions are also found for the maximum and minimum surface tensions and amount of surfactant on the surface as

a function of cap angle. Harper (1973, 1982) studied the case of small cap angles and carried out an asymptotic analysis of the governing equations. The results of Sadhal and Johnson agree with Harper's asymptotic results for small cap angle.

In the regime where sorption kinetics, bulk diffusion or surface diffusion are fast but still rate limiting compared to surface convection, the surface distribution of adsorbed surfactant deviates only slightly from its equilibrium value. This is termed the uniform retardation regime. In Frumkin and Levich (1947) and Levich (1962) the three cases in which a single of these mass transport mechanisms is fast but rate limiting are investigated individually. Schlechter anf Farley (1963) computed the drag on a spherical droplet for an assumed surface tension distribution. Newman (1966) studied the retardation of falling drops and derived a unified expression which included both surface desorption and diffusion effects. Newman's results reduce to those of Levich in the appropriate limits. Since the surface velocity is uniformly retarded in this regime and not stagnated, , surface viscosity effects can be included. Agrawal and Wasan (1979) included these effects in their analysis of this problem.

In the regime where bulk diffusion is slow compared to convection, the surface distribution of surfactant deviates significantly from that at equilibrium. Wasserman and Slattery (1969), in their study of diffusion controlled surface aging, solved the equations governing the flow field for only trace amounts of surfactant present in the exterior phase. Their results are a

perturbation of the clean surface solution and are valid only in the region where surface velocity is not significantly retarded. Saville (1973) also took this approach with similar results. In LeVan and Newman (1976), an arbitrary surface tension gradient along the interface is considered. Surfactant is present in trace amount in both the droplet and exterior phases. Decreases in terminal and surface velocities of the droplet are found, with the surface velocity being reduced predominantly in the region of the rear stagnation zone, as is observed experimentally.

Finally, LeVan and Holbrook (1982) treat this problem in a study in which the coupled fluid mechanical equations and mass transfer equations were solved simultaneously. A linearized isotherm is used to describe the relationship between sublayer and surface concentrations. Asymptotic and numerical results for the limiting cases show that the uniform retardation of the interface as posited by Levich (1962) in the case of fast mass transfer, and stagnant cap behavior for extremely slow mass transfer (i.e. either diffusion slow or slow desorption kinetics) are obtained.

2 Hydrodynamics of Slug Flows in Tubes

2.1 Clean Interface Studies

The antecedents to studies of multiphase flows in tubes were the theoretical and experimental investigations of the simpler problem of the steady fingering or drawing of single gas bubbles into horizontal capillaries filled with a viscous liquid. A straightforward nondimensionalization of the Navier Stokes equations

for the film liquid, and the interfacial stress and kinematic boundary conditions at the gas-liquid interface, reveals that there are three independent nondimensional groups determining the problem: (1) $\rho UR/\mu$ (a Reynolds number), (2) $\mu U/\sigma$ (a capillary number) and (3) $\rho gR^2/\sigma$ (a Bond or Weber number). In these groups, μ and ρ denote, respectively, the viscosity and density of the liquid which is being displaced, σ signifies the liquid-gas interfacial tension, U denotes the velocity of the moving bubble, and R and g denote, respectively, the tube radius and the gravitational acceleration.

Consider, for the fingering problem, a creeping flow regime ($\rho UR/\mu \ll 1$) in which the tube radius R is small enough so that gravitational forces are negligible in comparison to interfacial tension forces ($\rho gR^2/\sigma \ll 1$). The hydrodynamics is then determined solely by the capillary number, which is the ratio of viscous to interfacial tension forces. Bretherton (1961) first attempted to develop analytical solutions for the interfacial shape for the case in which the capillary number is small. He recognized that in this latter limit, the bubble profile may be divided into three regions:

(i) a nose section in which viscous tractions acting on the interface are negligible, and the nose profile is determined solely by interfacial tension,

(ii) a transition region in which the viscous tractions become important, and are in fact responsible for bending the interface from the near spherical nose configuration to the

cylidrical configuration which conforms to the tube geometry, and

(iii) an extended region of constant film thickness.

In the transition region, the length scale in the axial direction exceeds that of the radial, and therefore lubrication theory may be used. Recognizing this fact, Bretherton developed asymptotic solutions for the film profile in the lubrication limit and assumed in addition that the film thickness was much smaller than the tube diameter. The zeroth order equation for the film profile which he derived for the transition region was:

$$h_{zzz} = 3Ca(h - h_{\infty})/h^3 \qquad (2.1)$$

where h denotes the local film thickness (scaled by the tube radius R), Ca denotes the capillary number as defined above and z denotes the axial coordinate (scaled with R) of a cylindrical coordinate system centered along the tube axis. Finally, in equation (2.1) h_{∞} is the constant film thickness in the extended region away from the bubble nose. Note, in equation (2.1), the subscripted variable indicates partial differentiation.

Bretherton derived analytical solutions to equation (1) which were valid in the vicinity of the ends of the transition region. The constants of integration of these solutions were obtained by matching with the adjoining exterior zones. Thus the end portion of the transition region which borders the nose was matched to the constant radius of curvature of the nose (assumed to be equal to

2/R), and the solution at the opposite end was matched to the constant film thickness in the extended region. Finally, a numerical integration of equation (2.1) across the transition region provided the relations for matching the end solutions. The final equation determined for the dependence of the capillary number on the film thickness h_∞ was:

$$h_\infty \approx 1.337Ca^{2/3} \qquad (2.2)$$

and for the pressure drop across the center of the bubble nose:

$$\frac{\Delta P}{\sigma/R} \approx 2 + 3.58(3Ca)^{2/3} \qquad (2.3)$$

Equation (2.2) indicates that the thickness of the annular film left behind as the bubble moves through the tube in the limit of small Reynolds, Weber and capillary numbers is proportional to the 2/3 power of the capillary number. Bretherton's analysis was rederived in a more formal manner by Park and Homsy (1984) by using the theory of matched asymptotic expansions. In their analysis, uniform expansions were obtained in the transition region by stretching the axial coordinate. The results of Park and Homsy indicated that Bretherton's expression for the h_∞ is the zeroeth order term in an expansion for the film thickness (scaled with $Ca^{2/3}$) in the extended region in powers of $Ca^{1/3}$.

Numerical solutions of the above problem were undertaken by Reinelt (1984) using finite-differences and Shen and Udell (1985)

using finite elements. Both studies obtained values for h_∞ around a semi-infinite gas slug fingering in a fluid filled capillary tube which were several percent larger than that given by the Bretherton expression. For capillary numbers less than 10^{-3}, the two methods encountered convergence difficulties since for this low range of Ca, film thicknesses become very small, and the flow field discretizations are unable to resolve the variations in the hydrodynamic variables in the thin film region.

Reinelt (1986) also treated the related problem of a long gas bubble rising in a vertical tube under the effect of gravity (i.e. $\rho g R^2/\sigma$ not negligible), using finite differences. The shape of the gas finger and its dependence on Bond number for Ca between 10^{-4} and 10^{-1} are examined. Bretherton solved for the relationship between Ca and the Bond number at small Ca, Reinelt's results asymptote those of Bretherton as Ca→0. Martinez and Udell (1987) extend the work of Reinelt (1984) and Shen and Udell (1985) by considering a gas slug of finite length being drawn through a horizontal capillary tube. Reinelt and Shen and Udell, in considering the semi-infinite gas finger in a tube, solved only for the shape of the leading meniscus. In Martinez and Udell, the complete slug profiles, flow fields and pressure drop across the bubble are examined as functions of Ca using a boundary element approach for Ca between 10^{-1} and 10. Interestingly, at Ca=1.5 the curvature computed for the trailing meniscus becomes negative, perhaps signalling the onset of the

formation of a re-entrant cavity as observed experimentally by Goldsmith and Mason at high Ca. In a third numerical study of the behavior of finite length gas slugs in capillary tubes, Ratulowski and Chang (1989) solve for the shape of the slug, both the leading and trailing menisci, using the lubrication equations for the transition and hemispherical regions. This technique allowed them to extend the Bretherton solution for circular capillaries to higher Ca.

Several experimental investigations have undertaken the measurement of h_∞. Fairbrother and Stubbs (1935) first measured the film thickness surrounding a bubble drawn into a capillary tube. They obtained values for h_∞ by measuring the bubble velocity U, and the volumetric flow rate, Q, of the liquid expelled from the tube. Since the liquid left behind on the tube wall is at rest, h_∞/R is simply $(U - U_m)/2U$, where U_m is the average velocity of the liquid in front of the bubble, and is equal to $Q/(\pi R^2)$. Their data shows good agreement with the Bretherton expression for relatively large Ca (10^{-3} to 10^{-2}). For smaller Ca ($10^{-4} < Ca < 10^{-3}$), the measured values are systematically larger. Fairbrother and Stubbs correlated their results by the following equation:

$$h_\infty/R = .5Ca^{1/2} \qquad (2.4)$$

Bretherton (1961) attempted his own experiments to measure h_∞ for the range $10^{-6} < Ca < 10^{-2}$. He obtained values for h_∞ by measuring the shrinkage of long liquid slugs moving through an empty capillary. As was the case with the Fairbrother and Stubbs results, Bretherton's data agreed with the 2/3 dependence only for Ca between 10^{-3} and 10^{-2}, and showed consistently larger values than that predicted by equation (2.2) for smaller Ca. Marchessault and Mason (1960), using an electrolyte liquid, obtained values for the film thickness by measuring the axial electrical conductance. They studied values of Ca between 10^{-5} and 10^{-4}, and found that the measured values of h_∞ were larger than those given by equation (2.2). They further concluded that there data correlated well with the relation of Fairbrother and Stubbs.

Recent experimental studies by Chen (1986) and Schwartz et al (1986) in the range of low capillary numbers, that is Ca between 10^{-5} and 10^{-3}, also confirm that the Fairbrother and Stubbs correlation agrees well with experiments, and that the Bretherton result underpredicts the film thickness. Schwartz et al. (1986) used Bretherton's technique of measuring the reduction in volume of a long liquid slug in front of the gas to measure the film thickness. Parodoxically, they found that the film thicknesses left behind finite length bubbles of length less than 2R correlate well with the Bretherton expression.

Chen (1986) used the resistance measurement technique of Marchessault and Mason (1960) to obtain residual film thicknesses. His results show that for Ca < 10^{-5}, h_∞ appears to become uniform in Ca, and equal to a value of .73μ. Chen attributes the development of a steady film thickness to intermolecular disjoining (or strongly) wetting forces.

Experimental examinations in the range of relatively high capillary numbers (10^{-2} < Ca < 10^{-1}) have also been undertaken. Goldsmith and Mason (1963) obtained values for the residual film thickness by the direct measurement of a magnified image of the film, and concluded from the data that the empirical correlation given by equation (2.4) is accurate for capillary numbers in the range of 10^{-2} to 10^{-1}. Taylor (1961) concluded the same using Fairbrother and Stubbs' technique of measuring the volumetric flow rate of the liquid expelled from the front end of the bubble. In addition, Taylor and later Cox (1962), again using the Fairbrother and Stubbs technique, demonstrated that for capillary numbers of the order of one or larger, the film thickness in the extended region tends towards an asymptoic value of approximately .6R.

The axisymmetric creeping motion of drops through circular tubes was investigated numerically in Martinez and Udell(1988). Drop to tube radius, viscosity ratio, and capillary number were varied in the study. the dependence of wetting layer thickness on capillary number for Ca between 0 and .15 was solved numerically with the ratio of the viscosity of the drop to that of the

continuous phase as a parameter varied from 0 to 10. The numerical results were found to be in excellent agreement with the film thickness measurements of Fairbrother and Stubbs, Taylor and Goldsmith and Mason. As the drop phase became increasingly viscous, the thickness of the wetting layer was found to increase for a constant capillary number. This would be expected as a thickening of the film region helps to relieve the increased shearing in the film which develop due to the viscous tractions in the drop phase.

2.2 Surfactants in Slug Flows

The fluid mechanics of slug flows in fluid filled capillaries in the presence of surfactants is not as well documented as the clean fluid case. In their study, Marchessault and Mason (1960) found the pressure drop required to drive the flow of long gas slugs in tubes was larger than that predicted by Bretherton, and that the pressure drop increased proportionately to bubble length. While they offered no explanation as to the cause, they postulated that the interface of the gas slug behaved as if it were rigid. It is conjectured that impurities in the flow may have adsorbed onto the interface resulting in this rigidification.

Lawson and Hirasaki (1985) as well as Ginley and Radke (1987) consider the impact of surfactant with slow sorption kinetics on the flow of gas slugs in liquid filled capillaries, for the case where surfactant adsorbed on the interface deviates only slightly from the equilibrium surface concentration. Surface and bulk diffusion

resistances are neglected. Bretherton's low Ca equations for the flow are expanded in a regular perturbation in large adsorption rates. While Lawson and Hirasaki do not allow the film thickness around the cylindrical portion of the slug to vary in their analysis, assuming that surfactant effects are only felt at the ends, Ginley and Radke do allow h_∞ to change in their analysis. The results from both studies indicate that the pressure drop across the bubble increases significantly with added surfactant; in these investigations, both pressure drop and film thickness vary with $Ca^{2/3}$, as in the clean surface results of Bretherton. In the perturbation scheme of Ginley and Radke, the film thickness is found to decreases slightly with added surfactant. This is surprising, as the film thickness would be expected to increase for two reasons: Firstly, the surface tension decreases with added surfactant, resulting in an increased Ca. Since h_∞ varies in the clean surface case as $Ca^{2/3}$ according to Bretherton's result, this should result in an increased film thickness. Secondly, the accumulation of surfactant on an interface acts to retard the surface velocity. If enough surfactant is present on the interface the surface velocity in the cylindrical region will be retarded, greatly increasing the drag as the shearing in the film between the immobilized interface and the tube wall is proportional to $1/h_\infty$. As in two phase slug flows there is no scarcity of the fluid which forms the wetting layer, an increase in film thickness with the addition of surfactant

in the sorption controlled regime would therefore be expected from energy considerations.

An experimental study of this problem has been undertaken by Barthes-Biesel et al. The pressure drop required to drive the flow of a gas slug in a liquid filled capillary is measured, the liquid containing anionic surfactant at constant concentration. The pressure drop is found initially to increase with bubble length, until, at slug length between 20 and 40 radii, it reaches some constant value. This behavior was reported for Ca between $4x10^{-5}$ and $4x10^{-4}$. The maximum pressure drop across a gas slug is found to vary as $Ca^{.54}$, while theory predicts that the pressure drop will vary as $Ca^{2/3}$.

Chapter 2

Unretarded Surface Flow on the Interfaces of Moving Bubbles and Drops in the Presence of Adsorption of a Single, Freely Exchanging Surfactant

1. Introduction

Surfactant molecules which adsorb onto the interfaces of a translating fluid particle are convected towards stagnation regions where the surface flow converges. Accumulation of surfactant in the vicinity of these regions creates a surface pressure which is directed opposite to the direction of convection, and thus retards the surface velocity. The effect of this retardation on the hydrodynamic drag exerted by the continuous phase on the fluid particle is dependent on the compexity of the surface flow pattern, particularly on the presence of multiple stagnation points. However, for cases in which the surface convection is unidirectional, moving from a leading stagnant pole to a trailing one, the retardation of the surface velocity increases the drag exerted on the fluid particle. Examples of this behavior are the motion of a droplet in an otherwise quiescent fluid medium, or the translation of a fluid slug in a tube filled with a liquid at rest. In each of these cases, if the particle is subject to a constant driving force, then this increase in drag manifests itself as a reduction of the translational velocity of the particle.

The focus of this study is to identify, by examining the mechanisms of surfactant transport, conditions where adsorption is

not accompanied by reduction in the surface velocity, and to verify these conditions with a particular surfactant in a carefully controlled experimental fluid particle flow. While more exact arguments will be presented in what follows, it is at least qualitatively clear that desorptive and bulk diffusive resistances to exchange of surfactant between the bulk and the surface are what allows surfactant to collect at converging stagnation points on the fluid particle surface. In the absence of these resistances, the surface concentration would be uniform, and Marangoni stresses would not retard the surface velocity. The central argument of this study is that if the rate of molecular desorption is slow in comparison to the prevailing convective rate at which surfactant is swept to the stagnation zone on the particle interface, and the bulk concentration of surfactant is high enough so as to suppress boundary layer diffusion gradients, then the surfactant freely exchanges between the bulk and the surface and the surface flow is unretarded.

The fluid particle flow used to demonstrate this argument is a three phase periodic slug flow in a capillary. The flow consists of an alternating train of air and aqueous slugs drawn at low capillary number through a teflon capillary tube of order 1 mm in diameter. The slugs ride on a thin cushion of a fluorocarbon oil film which is immiscible with the aqueous slug and which strongly wets the inside teflon surface of the tube wall in preference to gas and water. The thickness of the oil film is of the order of tens of microns, and is controllable by the volumetric induction rate of oil. Surfactant is dissolved in the aqueous slug phase. This flow regime is extremely

sensitive to the presence of surfactant adsorbed onto the aqueous-oil interface. Adsorbed molecules on this interface are convected to the trailing region of the cylindrical surface of the slug where they lower the surface velocity. Since the cushion that the slugs ride on is thin, decreases in the surface velocity greatly increase the shear in the film, and the pressure required to drive the slug flow at a constant velocity increases proportionately. It is this characteristic of the three phase slug flow which makes it ideally suitable for the detection of surface velocity retardation with changes in surfactant concentration.

The surfactant used to verify the mobility conditions is the nonionic polyethoxyether Triton-X 100, a surfactant soluble in the aqueous phase but not in the fluorocarbon oil. Related pendant drop tensiometry studies of this surfactant at the aqueous-air and aqueous-fluorocarbon oil interface in the work by Lin et al. (1989) indicate that the desorption kinetics of this surfactant is sufficently fast so as to be a good candidate for this study. In addition, as a counter example, the protein bovine serum albumin (BSA) is used. The desorption kinetics of this surface adsorber is presumed slow because of denaturation of surface adsorbed protein, and the tendency of this protein to form desorption inhibiting multilayers at elevated bulk concentrations.

An outline of this chapter is as follows. The study is divided into five sections. In the first (Sec. 2), the physicochemical conditions for surface mobility are constructed using a Langmuir formalism to describe the surfactant sorption kinetics. The apparatus used to create the three phase flow regime, the

experimental protocol, and the nondimensional groups which prescribe this flow are described in Sec. 3. The results obtained verifying remobilization are detailed in Sec. 4, and the chapter concludes (Sec. 5) with a summary and a discussion of some of the implications of the ideas advanced.

2. Physicochemical Criteria for Surface Mobility

Two transport processes, occuring in series, govern the exchange of surfactant molecules between the surface and the bulk. These are bulk diffusion and the kinetics of adsorption and desorption of surfactant from the sublayer underneath the surface onto the surface (termed here sorption kinetics). Consider as a simple example these processes as they occur in competition with surface convection at steady state on a fluid particle of length scale ℓ' translating axisymmetrically at low Reynolds number with terminal velocity U' in an otherwise quiescent medium of infinite extent (Fig. 1). For illustration, surfactant is assumed present in the continuous phase at concentration C'_∞ far from the fluid particle. In the absence of motion the surface concentration in equilibrium with C'_∞ is denoted as Γ'_o.

The rate at which surfactant is transported by surface convection through a perimeter of order ℓ' oriented perpendicular to the surface flow is $O(\Gamma'_o U' \ell')$. For scaling arguments, the sorption kinetic exchange may be characterized by a Langmuir formalism; thus the kinetic exchange rate Q' is given by:

$$Q' = \alpha'((\beta'/\alpha')C_s'(\Gamma_\infty' - \Gamma') - \Gamma') \qquad (2.1)$$

In (2.1), α' and β' are desorptive and adsorptive kinetic rate constants, respectively, C_s' is the sublayer concentration of surfactant, and Γ' and Γ_∞' are the surface and the maximum packing concentrations, respectively. The desorption and adsorption rates to the surface are therefore $O(\alpha'\Gamma_o'\ell'^2)$ and $O(\beta'C_\infty'\Gamma_o'\ell'^2)$, respectively, where the surface area of the fluid body exposed to the continuous phase is $O(\ell'^2)$.

The time scale for diffusion through the bulk is dependent upon the relationship between the convective and diffusive fluxes of surfactant in the bulk. A bulk Peclet number ordering these fluxes is defined as $U'\ell'/D'$, where D' is the bulk diffusivity of surfactant. Since the usual circumstance in mass transfer in liquids is the regime of large Peclet number, attention here will be restricted to this regime. When Pe is large, diffusion gradients normal to the surface which carry surfactant between the surface and the bulk exist in a small boundary layer of thickness δ'. Within this layer the diffusive flux normal to the surface is balanced by the convective flux in the direction along the surface. Clearly the scale of the diffusive flux to the surface of area $O(\ell'^2)$ is $O(\ell'^2D'C_\infty'/\delta')$. The size of δ' is dependent upon the characteristics of the flow along the surface. The maximum flux develops when δ' is smallest, and this will be realized for a mobile interface for which δ' is of order $\ell'Pe^{-1/2}$. Thus the scale of the maximum diffusive flux is $O(\ell'^2D'C_\infty'/(\ell'Pe^{-1/2}))$.

The surface of the fluid body of Fig. (1) will remain mobile even in the presence of surfactant adsorption as long as there are no resistances to transport between the bulk and the surface. This will be the case when the convective rate of transport along the surface is much less than both the rates of desorption and diffusion. These conditions will be fulfilled as long as the sorption kinetics are such that surfactant desorbs quickly, $(\alpha'\Gamma_o'\ell'^2)/(\Gamma_o'U'\ell') \gg 1$, and the bulk concentration is large enough so that the surfactant diffuses quickly away from the surface $(D'C_\infty'\ell'^2/(\ell' Pe^{-1/2}))/(\Gamma_o'U'\ell') \gg 1$. The ratio C_∞'/Γ_o' appearing in the last inequality defines the adsorption depth, h', the distance normal to the surface which contains (at equilibrium per unit area) as much surfactant as that adsorbed onto the surface.

Defining by ν the ratio of the rate of surfactant transport by desorption to that by surface convection (i.e. $\nu = (\alpha'\ell')/U'$), the physicochemical conditions for remobilization formulated above may be summarized as: (i) $\nu \gg 1$ and (ii) $(\ell'/h')Pe^{-1/2} \gg 1$. Under fixed values for Pe, U' and ℓ'bilization is realized if the surfactant's kinetics of desorption is intrinsically fast with respect to surface convection ($\nu \gg 1$), and the bulk concentration is large enough so that k and h'/ℓ' are sufficently large to insure that $\nu \gg 1$ and $(\ell'/h')Pe^{-1/2} \gg 1$. These general criteria are placed within the context of the three phase slug flow used in this study in Sec. 3.2.

3. The Three Phase Flow

3.1 Apparatus Design

The apparatus which creates the segmented flow is detailed in Fig.(2A). A three way solenoid valve (Lee Co.) is configured so as to draw either air or aqueous surfactant solution. The solenoid valve is attatched to a piece of glass tubing (ID=1.7mm). Along the length of glass tubing two LED emitter-detector pairs are located a known distance from the solenoid valve. The LED emitter-detector pairs are configured through a relay circuit which allows them to control the solenoid valve. The glass tube is initially filled with aqueous surfactant solution. A small air slug is formed and drawn through the length of tubing. When the aqueous-air interface passes the first LED emitter-detector pair, the solenoid begins to draw in air. When the same aqueous-air interface passes the second detector, the solenoid draws aqueous solution. The length of an air slug is therefore determined by the distance between the two detectors; the length of an air aqueous slug pair is determined by the distance between the solenoid valve and the first detector. This manner of creating the segmented flow is reproducible and creates a periodic flow pattern independent of flow velocity. The glass tubing is attatched to a T section through which oil is injected at a known flow rate. The downstream end of the T section is attached to the experimental test section, which consists of a length of teflon tubing. Since the fluorocarbon oil used preferentially wets teflon, the oil injected by an infusion pump (Sage Instruments) at the T section will wet the teflon tube wall,

forming an annular oil film and establishing the three phase flow pattern.

The experimental test section (Fig.(2B)) to which the segmented flow apparatus is attached consists of a length of teflon tubing whose ID was checked by volume displacement. The tubing, which is oriented horizontally, is attatched at the extreme downstream end to a peristaltic pump (LKB Productor 2132 Microperpex pump). Velocity measurements are made for each unit cell as it passes through the test section by two LED emitter-detector pairs located at either end of the test section. Also located at the upstream and downstream ends of the system are two pressure taps. These are simply T sections which are attatched to fluid filled tubes which lead to either side of a diaphragm type differential pressure transducer (Validyne DP-15). Both the LED emitter-detector pairs and the pressure transducer are attatched to an A/D card (Data Translation DT2805); the pressure drop and the average velocity over the length of test section are monitored continuously during a run.

3.2 Nondimensional Groups

Before the equations which prescribe the slug flow can be formulated, it is necessary to state the assumptions concerning the flow. An idealization of a repeating unit (a periodic cell) of the flow train is given in Fig. (3) in a frame in which the slugs are stationary. The aqueous slug and the lubricating oil film are regarded as incompressible Newtonian fluids with, respectively, viscosities $\mu'_{(a)}$ and $\mu'_{(o)}$, and densities $\rho'_{(a)}$ and $\rho'_{(o)}$. The air slug is assumed to be incompressible and of negligible density and

viscosity. Some topological nomenclature: The spaces occupied by the oil, gas and aqueous phases in the unit cell are denoted by $V'_{(o)}$, $V'_{(g)}$ and $V'_{(a)}$, respectively. The oil-aqueous and oil-gas interfaces are denoted as $\partial V'_{(o/a)}$ and $\partial V'_{(o/g)}$, respectively; the leading and trailing aqueous-gas surfaces are denoted as $\partial V^{\ell}_{(a/g)}$ and $\partial V^{t}_{(a/g)}$ respectively. Finally the tube radius is denoted by R', the train velocity by U' and the clean interfacial tensions of the oil-aqueous, oil-gas and aqueous-gas surfaces by $\gamma'_{(o/a)}$, $\gamma'_{(o/g)}$ and $\gamma'_{(a/g)}$, respectively. The bulk concentration of surfactant from which the slugs are drawn is denoted by C'_{∞} and the surface concentrations in equilibrium with C'_{∞} at the oil-aqueous and aqueous-gas interfaces are denoted by Γ'_o and $\tilde{\Gamma}'_o$, respectively.

The hydrodynamic and surfactant transport equations are formulated with respect to a cylindrical coordinate system (r', θ, z') coincident with the centerline of the capillary. The scaling of these equations is as follows. Spatial coordinates are scaled with the tube radius R', velocity vectors ($\underline{v}$) by U', pressure (p) by the capillary scale $\gamma'_{(o/a)}/R'$, the bulk concentration by C'_{∞}, and surface concentrations by Γ'_o and $\tilde{\Gamma}'_o$, for, respectively, the oil-aqueous and aqueous-gas interfaces. For the aqueous slug phase ($\underline{x} \in V_{(o)}$), the nondimensionalized hydrodynamic field equations and bulk surfactant conservation equation become:

$$\nabla \cdot \underline{v} = 0 \qquad (3.1)$$

$$Re(\underline{v}\cdot\nabla\underline{v}) = -(\kappa Ca_{(o/a)})^{-1}\nabla p + \nabla^2\underline{v} \qquad (3.2)$$

$$Pe(\underline{v}\cdot\nabla C) = \nabla^2 C, \qquad (3.3)$$

while for the film region ($\underline{x} \in V_{(o)}$; variables identified by the tilde superscript) for which the surfactant is not soluble the equations are:

$$\nabla\cdot\tilde{\underline{v}} = 0 \qquad (3.4)$$

$$(Re\chi/\kappa)\tilde{\underline{v}}\cdot\nabla\tilde{\underline{v}} = -Ca_{(o/a)}^{-1}\nabla\tilde{p} + \nabla^2\tilde{\underline{v}} \qquad (3.5)$$

In the above, the dimensionless groups are defined as follows:

$$\kappa = \mu'_{(o)}/\mu'_{(a)}$$

$$\chi = \rho'_{(o)}/\rho'_{(a)}$$

$$Re = R'U'\rho'_{(a)}/\mu'_{(a)}$$

$$Ca_{(o/a)} = \mu'_{(o)}U'/\gamma'_{(o/a)}.$$

$$Pe = U'R'/D'$$

where D' is the bulk diffusion of surfactant in the aqueous slug.

In order to formulate boundary conditions at the interfaces on which surfactant adsorbs, it is necessary to detail the sorption kinetics and to relate the surface tension to the adsorption. While the idea of remobilization is not dependent on a particular kinetic form, Langmuir kinetics (eq. (2.1)) is chosen here since it admits analytically tractable results and is thus a useful illustrative

scheme, and because it proves adequate enough for the description of the kinetic and equilibrium adsorption properties of Triton-X 100, the surfactant used in this study (cf. Appendix A). With this choice of a kinetic scheme, the equilibrium surface concentration Γ'_o is given in terms of the bulk concentration C'_∞ by the relation $\Gamma'_o = \Gamma'_\infty(\beta' C'_\infty/\alpha')/(1+(\beta' C'_\infty/\alpha'))$. Further, the equilibrium dependence of the interfacial tension on the surface concentration can be obtained from the Gibbs-Duhem equation $\Gamma' R' T' = -\frac{\partial \gamma'}{\partial \ell n(a)}$, and results in Frumkin's equation $\gamma'(\Gamma') = \gamma' + R'T'\Gamma'_\infty \ell n(1-\Gamma'/\Gamma'_\infty)$ if it is assumed that the bulk concentration is small enough so that the activity a may be replaced by the bulk concentration. (Here R' denotes the gas constant and T' the absolute temperature.) The Frumkin equation defining $\gamma'(\Gamma')$ and its corollary $\frac{\partial \gamma'}{\partial \Gamma'} = -R'T'(1 - \Gamma'/\Gamma'_\infty)^{-1}$ which is important in the formulation of the Marangoni stress, are applied to the nonequilibrium flow.

The locus of points defining the the oil-aqueous interface $\partial V_{(o/a)}$ is identified by the specification $F_{(o/a)}(r, \theta, z) = r - \zeta(\theta,z) = 0$. Thus the normal to this interface (directed towards the oil film) is given by $\underline{n} = \nabla F/|\nabla F|$, the mean curvature 2H is defined as $-\nabla_s \cdot \underline{n}$ (∇_s denotes the surface gradient operator) and orthogonal tangent vectors $\underline{t}_z$ and $\underline{t}_\theta$ are defined as perpendicular to $\underline{n}$ and with, respectively, (r,z) and (θ,z) components. The boundary conditions on $\partial V_{(o/a)}$ ($\underline{x} \in \partial V_{(o/a)}$) are:

$$\underline{v} = \tilde{\underline{v}} \qquad (3.6)$$

$$\underline{n}\cdot\underline{v} = 0 \qquad (3.7)$$

$$\underline{n}\cdot(-\tilde{p}\underline{I} + Ca_{(o/a)}\tilde{\underline{D}} + p\underline{I} - (Ca_{(o/a)}/\kappa)\underline{D})\cdot\underline{n} +$$

$$2H(1 - Ma\cdot Ca_{(o/a)}\ell n(1 - \Gamma k/(1+k))) + Bo\zeta\sin\theta = 0 \quad (3.8)$$

$$\underline{n}\cdot(\tilde{\underline{D}} - \underline{D}/\kappa)\cdot\underline{t}_z + ((k\cdot Ma)/(1+k-k\Gamma))(\underline{t}_z\cdot\nabla_s\Gamma) = 0 \quad (3.9)$$

$$\underline{n}\cdot(\tilde{\underline{D}} - \underline{D}/\kappa)\cdot\underline{t}_\theta + ((k\cdot Ma)/(1+k-k\Gamma))(\underline{t}_\theta\cdot\nabla_s\Gamma) = 0 \quad (3.10)$$

$$\nabla_s\cdot(\Gamma\underline{v}) = (Pe\cdot h'/R')^{-1}\underline{n}\cdot\nabla C = \Phi(1+k)\underline{n}\cdot\nabla C \quad (3.11)$$

$$\nabla_s\cdot(\Gamma\underline{v}) = \nu^*(1+kC)(C(1+k)/(1+kC) - \Gamma) \quad (3.12)$$

In the above $\underline{D}$ denotes the rate of strain tensor ($\underline{D} = \nabla\underline{v} + (\nabla v)^t$) and the dimensionless groups appearing are defined as follows:

$$Bo = (\rho'_{(o)} - \rho'_{(g)})g'R'^2/(\mu'_{(o)}U')$$

$$k = \beta'C'_\infty/\alpha'$$

$$Ma = R'T'\Gamma'_\infty/(\mu'_{(o)}U')$$

$$h' = \Gamma'_o/C'_\infty = k\Gamma'_\infty/((1+k)C'_\infty)$$

$$\Phi = (D'\alpha')/(\beta'U'\Gamma'_\infty)$$

$$\nu^* = \alpha'U'/R'$$

where g' is the gravitational acceleration constant. Note that as written in (3.11) the group multiplying the diffusive flux to the surface $((h'/R')Pe)^{-1}$, can be formulated as a function of k (and therefore the bulk concentration) and the k-independent parameter Φ. Boundary conditions are also formulated on the leading and trailing aqueous-air interfaces ($\partial V^{\ell}_{(a/g)}$ and $\partial V^{t}_{(a/g)}$). These equations add to

the nondimensional formulation the aqueous-air capillary number ($Ca_{(a/g)} = \mu'_{(a)}U'/\gamma'_{(a/g)}$) and the ratios of the Langmuir constants for adsorption onto the aqueous-air interface to those for adsorption onto the aqueous-oil interface ($\tilde{\Gamma}'_\infty/\Gamma'_\infty$, $\tilde{\beta}'/\beta'$ and $\tilde{\alpha}'/\alpha'$). Finally on the oil-air interface, there is no surfactant adsorption and the boundary conditions on that surface add only the oil-air capillary number $Ca_{(o/g)} = \mu'_{(o)}U'/\gamma'_{(o/g)}$ to the list of dimensionless groups.

The specification of the governing equations is completed with the formulation of integral constraints which set the size of the gas and aqueous slugs to the values formed in the experimental apparatus, and equate the volumetric flow rate of oil in a laboratory frame to the rate at which oil is introduced by an infusion pump. The slug constraints are straightforward and introduce the variables λ, the ratio of the characteristic axial length of the repeating unit of the flow train to the tube radius and ϵ, the void fraction of gas in the repeating unit. These variables are defined below:

$$\lambda R' = (V'_{(g)} + V'_{(a)})/(\pi R'^2)$$

$$\epsilon = V'_{(g)}/(V'_{(g)} + V'_{(a)})$$

The volumetric flow rate of oil in the train-fixed reference frame is termed the leak rate, $q'_{\ell k}$, and is in a direction opposite to the train flow. This rate is given dimensionally by $q'_{\ell k} = \int_{\partial V_c} \underline{n}\cdot\underline{\tilde{v}}'\, da'$,

where ∂V_c is any cross sectional area perpendicular to the tube axis and through which oil flows, and $\underline{n}$ is the normal to that surface directed opposite to the train flow. The volumetric flow rate in the laboratory fixed frame (i.e. the oil pump infusion rate) is denoted by q'_{oil} and is easily shown to be equal to $-q'_{\ell k}$ added to the volume of oil in the unit cell ($V'_{(o)}$) divided by the time which transpires for a unit cell to pass a fixed point in the laboratory frame. Nondimensionalizing the expression for q'_{oil} by the nominal aqueous flow rate ($\pi R'^2 U'$) yields the final dimensionless group $\Omega = q'_{oil}/(\pi R'^2 U')$.

From the arguments presented in Sec. 2, it is clear that the central equations with regard to the surfactant influence on the surface mobility of the aqueous-oil interface (the only interface which significantly affects the pressure drop) are 3.11 and 3.12. In the limit in which ν^* becomes large, the sublayer and the surface are in equilibrium. In addition, when $(Pe(h'/R'))^{-1}$ ($= \Phi(1+k)$) becomes large, the diffusive flux to the surface ($\underline{n}\cdot\nabla C$) tends to zero and the bulk concentration becomes uniform. This fact, taken together with the sorption equilibrium, insures that the surface concentration is uniform and the surface is mobile. However, these conditions are unnecessarily conservative since the characteristic length scale for surface convection is $O(R'\lambda(1-\epsilon))$ rather than order (R') and that for bulk diffusion is of order ($R'Pe^{-1/2}$) owing to the diffusion boundary layer rather than R'. Using these more accurate scalings for the slug flow, the conditions for mobility become: (i) $\nu = \alpha' R'\lambda(1-\epsilon)/U' \gg 1$ and (ii) $(R'/h')Pe^{-1/2} = \Phi(1+k)Pe^{1/2} \gg 1$.

3.3 Materials and Methods

The surface adsorbers which were dissolved in the aqueous phase were Triton-X 100, obtained from Aldrich Chemical Co. and bovine serum albumin, obtained from Sigma Co. The fluorocarbon oil of which the annular oil film is comprised is obtained from the 3M Co.(FC-43). Both the surfactant, protein and the oil were used without modification. The water with which the aqueous solutions were made was purified via a Millipore water purification system with Organex filters to remove organic impurities. The teflon tubing which serves as the test section was obtained from Alltech Associates (FEP, nominal ID of 1.5 and 1.0mm).

A series of runs were undertaken in which solutions of varying concentration of surfactant are used to form the aqueous slug in the three phase slug flow geometry. The pressure drop required to drive the flow at each concentration was measured over the course of a run. Each day the first run was one in which the aqueous slug consisted of pure water. The pressure drop for this run was used as a benchmark and provided a check for excessive impurities in the system. Subsequent runs were run in order of increasing surfactant concentration. At the end of each day the tubing was flushed out for several hours using pure water.

The experiments were undertaken in the following manner. Three phase flow is established in the system using a surfactant solution at some bulk concentration. $\Delta P'$, the pressure drop over the test section is monitored until it reaches some steady value at train velocity $U'=1.15cm/s$. U' and $\Delta P'$ are then recorded over a 45-60 minute time period, with the $\Delta P'$ at the time that each air slug

passes the second velocity detector being recorded along with that slug's average velocity over the test section. Between runs the system is flushed out for several hours with purified water if the following run is to be one with a lower concentration of surfactant than its predecessor.

The dimensionless groups can be divided into two classes, those that are related to the effect of surfactant, and those which are independent of surfactant effects. Those in the surfactant independent group are ϵ, λ, Ω, κ, and the capillary numbers. The values at which these groups are held fixed in the experiments reported herein are tabulated in Table 1. The viscosity ratio κ remains constant as all experiments are undertaken using the same fluorocarbon oil. The ratio of oil to aqueous flow rates within the system, Ω, is held fixed by fixing the rate at which oil is introduced into the system by the infusion pump, U' being held constant for all experiments reported herein. The void fraction ϵ and the aspect ratio λ are established as follows: The length of a unit cell in the test section is fixed by fixing the distance between the solenoid valve and the first detector at the extreme upstream end of the apparatus. This length is checked by making sure that the correct number of unit cells appear between the LED emitter-detectors which monitor the average velocity over the test section. The void fraction is established by measuring the volume of liquid in several hundred unit cells, and adjusting the distance between the two detectors at the extreme upstream end of the system until the desired void fraction is attained. All of these adjustments are made before fluorocarbon oil is introduced to the

system, as ϵ and λ are defined to be the void fraction and aspect ratio in the absence of an oil film.

The surfactant dependent groups are ν^*, Ma, $\Phi(1+k)$, and k. For each surfactant Ma and Φ do not change with C'_∞, whereas k is concentration dependent. Therefore as the bulk concentration of surfactant is varied, both k and $\Phi(1+k)$ will increase simultaneously. To verify remobilization, it is necessary to check that the pressure drops return to clean surface values as the bulk concentration and, in particular, $\Phi(1+k)Pe^{1/2}$ becomes large.

4. Results and Discussion

4.1 Clean Surface Results

4.1.1 Interfacial Shapes

The interfacial shape assumed by a single long gas or liquid slug suspended in Poiseiulle flow in a capillary tube has been detailed asymptotically at low capillary numbers by Bretherton (1961) as well as Park and Homsy (1983); numerical solutions for small to intermediate Ca have been undertaken by Shen and Udell (1985), Reinelt and Saffman (1985), Martinez and Udell (1988) and Ratulowski and Chang (1988). For small Ca, the leading edge of the slug is nearly hemispherical in shape. This hemispherical region is attatched via a transition region to a long cylindrical region of nearly constant wetting layer thickness. This cylindrical region, in turn, is connected to a flared region just before the trailing end of the slug, which is distended in the direction opposite to the flow and has a radius of curvature which is greater than the tube radius.

In Plate 1A and 1B photographs of the leading and trailing ends of an aqueous slug in three phase slug flow are shown in the .155cm ID tube at 30X magnification for clean surface conditions. In these photographs, the gas slug appears dark and the aqueous segment appears clear. The oil around the liquid segment appears as a dark line, while the oil in the three phase contact region forms an inclusion which is shaded light grey. Note that the leading edge of the aqueous slug depicted in Plate 1A appears nearly hemispherical except where the aqueous-air slugs adjoin. Importantly, the trailing edge of the aqueous slug has a flared region as was observed by Bretherton for single slugs in fluid filled capillaries. It is not clear whether or not the gas slug also flares at its trailing end because of the similar shading of the gas slug and its surrounding oil film. While the exact details of the aqueous-air interface configuration are not clear from the photographs, it is probable that these interfaces are bent in the direction of flow so as to accomodate the pressure gradient.

Consider the points at which the three phases meet, i.e. the ring where the oil fillet meets the ring of contact of the aqueous and gas segments. The interfacial tensions at the gas-oil interface and at the aqueous-oil interface are such that they nearly balance the interfacial tension at the air-aqueous interface in the absence of added surfactant. Neglecting line tension effects, the spreading coefficient S' which determines whether oil will spread between the air and aqueous slugs is given by :

$$S' = \gamma'_{(a/g)} - (\gamma'_{(o/g)} + \gamma'_{(a/g)}) \quad (4.1)$$

In the above equation, the interfacial tensions under clean surface conditions are: $\gamma'_{(a/g)}$=72.3 dynes/cm, $\gamma'_{(o/g)}$=16 dynes/cm and $\gamma'_{(a/o)}$=59 dynes/cm. Some impurities were present in the oil phase which caused the interfacial tension at the aqueous-oil interface to decrease to a value of $\gamma'_{(a/o)}$=55 dynes/cm at steady state. Using these values in the above equation gives an S' value of 1.3 dynes/cm, taking into account the impurities in the oil phase. A positive spreading coefficient indicates that the oil would spread between the aqueous and air slugs, i.e. S'> 0 insures that the contact angle along this ring of three phase contact is zero. Oil fails to spread between the aqueous and gas segments due only to volumetric constraints; when the rate at which oil is introduced into the system is high enough, the gas and aqueous slugs are separated by oil lamellae, and assume shapes very similar to those observed by Bretherton for single slugs. Oil also spreads between the gas and aqueous slugs when the flow is stopped, again forming oil lamellae. The slugs then assume shapes with hemispherical regions at both the leading and trailing ends, connected by long cylindrical regions. As the tube is oriented horizontally throughout the test section, this shape persists until the oil drains from the top of the slugs due to the combined actions of bouyancy and capillary suction.

In the presence of the surfactant Triton-X 100, the balance of interfacial tensions at the ring of three phase contact changes in such a manner to insure that the contact angle along this ring remains zero. At just below the CMC for Triton-X 100, $\gamma'_{(a/g)}$= 31

dynes/cm, $\gamma'_{(g/o)}$= 16 dynes/cm (unchanged as added surfactant is insoluble in the oil phase and does not adsorb appreciably at this interface) , and $\gamma'_{(a/o)}$= 12.3 dynes/cm. Using the Young-Dupre equation, the spreading coefficient S' is found to be 2.7 dynes/cm. Once again, oil spreads between the aqueous and air segments if the oil rate is brought sufficiently high as well as when the flow is stopped. Positive values of S' are realized throughout the range of bulk concentrations considered, as may be verified fron the equilibrium surface tension data of Triton X-100 as presented in Figs.(A1) and (A2) of the appendix.

4.1.2 Clean Interface Pressure Drop Results

All of the pressure drop data presented in this and the remaining sections (4.2 and 4.3) refer to the pressure drop per unit cell averaged over the course of a single run, nondimensionalized with the surface tension scaling $\gamma'_{(o/a)}/ R'$. In Fig. (4) the pressure drops required to drive the purified water benchmark runs in capillary tubing of two different inner diameters is presented against tube age, i.e. the number of days which have elapsed since a series of surfactant experiments was begun. The triangles represent pressure drop data for .1555cm ID runs and the squares .097cm ID runs. The average over all the runs was .35. All of the pressure drops reported in the figure fall within a ±10% range of this value, which confirms the nondimensionalization structure chosen. Note that after it becomes impossible to sufficiently clean the tube to get the benchmark value for the pressure drop, (i.e. after the

tubing was exposed to highly elevated concentrations of surfactant or protein) the tubing is discarded.

As stated above, the average nondimensional pressure drop per cell over all runs in both series was .35; this number specifies the pressure drop over a pair of aqueous and air slugs in a unit cell nondimensionalized with the surface tension scaling $\gamma'_{(o/a)}/R'$. There are three principal contributions to this pressure drop: the capillary contributions due to the difference in curvature at the leading and trailing edges of the air and aqueous slugs and the pressure drop due to the recirculation of fluid within the aqueous segment itself. The expression found by Bretherton to describe the pressure drop over a single long gas slug in a fluid filled capillary tube at low capillary number is used to estimate the capillary contributions to the pressure drop ($\Delta P'_c$) over a unit cell. Bretherton's expression is

$$\Delta P'_c/(\gamma'_{(o/n)}/R') = 4.52\ (3Ca_{(o/n)})^{2/3}, \quad (4.2)$$

where $\gamma'_{(o/n)} = \gamma'_{(o/a)}$ if the pressure drop over the aqueous slug is being estimated, and $\gamma'_{(o/n)} = \gamma'_{(o/g)}$ if that over the gas slug is being estimated. In equation (4.2) the capillary number $Ca_{(o/n)}$ is defined using the interfacial tension $\gamma'_{(o/n)}$. The capillary contribution to the nondimensional pressure drop over the aqueous slug is .095, that over the gas slug (scaled with the interfacial tension at the aqueous-oil interface $\gamma'_{(o/a)}$) is equal to .062. The

pressure drop due to the recirculation of the liquid in the aqueous segment ($\Delta P'_v$) can be estimated by neglecting the ends of the aqueous slug, and equating the net aqueous flow rate within the slug to zero. The expression for the pressure drop which results, nondimensionalized with the surface tension scaling stated above is :

$$\Delta P'_v/(\gamma'_{(o/a)}/R')=(8\kappa(1-\epsilon)/(\kappa\xi^2+2(1-\xi^2))(\mu'_{(a)}U'/\gamma'_{(o/a)})(\lambda) \quad (4.3)$$

where κ is the viscosity ratio of the oil to the aqueous solution, ξ is equal to $(1-\bar{h}'/R')$, where $\bar{h}'$ is the average thickness of the annular oil film surrounding the aqueous segment. Bretherton's asymptotic analysis at low Ca may be used to estimate the film thicknesses around the slugs. For long gas slugs, Bretherton found the film is determined by the hydrodynamics of the leading edge and transition regions. Using his expression, $\bar{h}'/R'=1.337Ca^{2/3}$, an average film thickness around the gas slug of 25 microns is calculated; the film thickness about an aqueous slug is expected to be on this order. The appropriate values for the void fraction ϵ, the viscosity ratio κ, the aspect ratio λ, the aqueous slug viscosity $\mu'_{(a)}$, and the slug velocity U' are detailed in Table 1. Using these values in the above expression the nondimensional pressure drop due to the internal circulation of liquid within an aqueous slug is .07. The sum of the estimates of the three contributions to the pressure drop is .23, clearly on the same order of magnitude as the pressure drop of .35 reported in the clean interface experiments above.

The estimates for the capillary contributions to the pressure are calculated using the results of Bretherton's analysis of a single gas slug in a liquid filled capillary. The shapes assumed by the aqueous and gas slugs differ from those assumes by an isolated slug, as the aqueous and gas slugs adjoin at either end. This is probably not a major source of error as Ratulowski and Chang (1989) indicate in their numerical study that the pressure drop realized across a single gas slug which adjoins gas slugs at either end in a liquid filled capillary does not differ significantly from that across an isolated gas slug. More significant errors in estimating the pressure drop across a unit cell in the three phase slug flow arise due to the volumetric constraint on the oil phase and the presence of surface active contaminants in either liquid phase. The oil is introduced in the three phase slug flow at a low, constant rate. The thickness of the film in the three phase slug flow is less than that realized in the two phase flow, which has no volumetric constraint on the continuous phase. Surface active contaminants present in either liquid phase adsorb along the aqueous-oil interface and reduce the surface velocity. The decrease in the leak rate concomittant with a decrease in surface velocity, along with the volumetric constraints on the oil lead to an increased shear along the cylindrical region of the aqueous slug. This contribution to the pressure drop is underestimated by equation (17.), which assumes a perfectly mobile interface and the Bretherton film thickness.

4.2 Triton X-100 Results

The equilibrium and sorption kinetic properties of Triton X-100 as obtained from pendant drop tensiometry are described in Appendix A which is a condensation of a larger effort by Lin et al. (1989). In Figure (5) data from the series of runs using Triton-X 100 in the aqueous phase in tubes of .1555 cm ID and .097 cm ID respectively is presented. The abscissa in the figures is $\Phi(1+k)Pe^{1/2}$, the group which measures the ratio of the rates of bulk diffusion and surface convection. Data to evaluate the parameters in this group are presented in Appendix A. As C'_∞ is varied from 0 through 10^{-3}wt%, ($\Phi(1+k)Pe^{1/2}<.035$), the nondimensional pressure drop increases monotonically to a maximum value which is approximately five times greater than that required to drive the clean flow. In this concentration range the group $\Phi(1+k)Pe^{1/2}$ increases monotonically, but is always less than 1.0. This small value reflects the fact that the bulk diffusion barriers are significant and thus at steady state surfactant has accumulated at the rear stagnation zone with little exchange with the bulk (i.e. $\nabla_s\cdot(\Gamma\underline{v}_s)\rightarrow 0$). The Marangoni surface traction which arises due to the surfactant accumulation reduces the surface velocity since the traction is opposite to the flow. Since the surface velocity toward the rear stagnation zone is decreased in the long cylindrical section of the aqueous slug, the net hydrodynamic drag on the slug is increased. The slug or train velocity is maintained at a constant value during the experiments, so the pressure drop driving the flow must increase in order to overcome this increased drag opposing the flow. This is why $\Delta P'$

increases from the clean value. As C'_∞ is increased the bulk diffusion barriers begin to be reduced. In this concentration range, however, as C'_∞ increases the increased adsorption causes the surface velocity to be reduced along a larger region of the cylindrical surface, accounting for the increase of $\Delta P'$ with C'_∞.

As bulk concentration is increased in the range of 10^{-3} to 2 wt% ($.035 \leq \Phi(1+k)Pe^{1/2} \leq 72$) the pressure drop required to drive the flow decreases fivefold due to the elimination of diffusion gradients in the bulk. The group $\Phi(1+k)Pe^{1/2}$ varies from .035 to 72, indicating that within this bulk concentration range diffusion barriers in the sublayer to the interface have been completely eliminated. Note that the CMC for Triton-X 100 corresponds to a value of $\Phi(1+k)Pe^{1/2}$ of .15; 70% of the relaxation in pressure drop therefore takes place at concentrations above the CMC, and in the presence of micelles. The advent of micellization does not alter the physicochemical picture, however, because the exchange kinetics between monomer and micelle is very fast (cf. Joos and Rillearts (1981)), and therefore both bulk gradients of micelle and monomer disappear as the bulk concentration is increased.

Since the clean surface pressure drop is recovered, the surface concentration is uniform and the interface is tangentially mobile. An interface that is completely tangentially mobile with uniform surface concentration in the absence of diffusion barriers can only be obtained if no desorption barriers exist. The ratio of desorption rate to that of surface convection, $\nu = \alpha' R' \lambda (1-\epsilon)/U'$, is independent of concentration and was found in the Appendix to be

bounded from below by .2. If ν were on this order, however, asymptotic arguments presented in the second section indicate that the clean surface pressure drop would not be recovered at elevated bulk concentration. Thus the reduction of the pressure drop to that required to drive the clean flow at elevated C'_∞ therefore indicates that Triton-X 100 has desorption kinetics faster than the .05 sec^{-1} lower bound inferred from the pendant drop experiments of Appendix A.

A surfactant laden interface in the absence of bulk diffusion barriers in which surfactant adsorbs and desorbs freely behaves as if it were a clean interface in the tangential stress balance. The interface, however, is more easily deformed as the surface tension at these high concentrations is significantly less than that in the absence of surfactants. This will affect the capillary contribution to the pressure drop over the aqueous slug. Using the pressure drop expression obtained by Bretherton, the ratio of the pressure drop for the uniformly populated surface to that required to drive the clean flow should be the ratio of the interfacial tensions of the two surfaces to the 1/3 power. The interfacial tension at the aqueous-oil interface at and above the CMC is about 12 dynes/cm. The ratio of the pressure drop required to drive the uniformly populated interface to that required to drive the clean flow as predicted by the Bretherton expression is .6. Therefore the capillary contribution to the pressure drop realized over the length of an aqueous segment at the highly elevated surfactant concentrations is .054. The contributions to the pressure drop due to the capillary forces over the air segment and due to the internal

circulation in the aqueous segment remain the same, as surfactants are not present at the air-oil interface and the viscosity of the aqueous solution remains constant throughout the concentration range considered. Therefore the pressure drop over a unit cell at the lower interfacial tension is estimated to be .184, or .84 times that required to drive the clean flow. In our experimental apparatus the pressure drop required to drive the concentrated surfactant solutions was less than that required to drive the clean flow in only one of the two series of experiments reported. The average nondimensional pressure drop at $\Phi(1+k)Pe^{1/2} = 72$, which corresponds to a C'_∞ of 2wt%, is .32, which is .91 times that required to drive the clean flow. Note that this agreement is only in the average sense: the pressure drop at this elevated k value decreased only for the .097cm ID tubing. In the .097cm ID tube the pressure drop required to drive the 2wt% solution of Triton-X 100 is .28, which is .8 times that required to drive the clean flow. The pressure drop required to drive the flow at this concentration in the .1555cm ID Triton-X 100 series was .36, which is approximately the same as the clean interface pressure drop.

4.3 Protein Results

In order to recover clean surface behavior at large $\Phi(1+k)Pe^{1/2}$, the ratio of desorption to convection, ν, has to be large as well. In the event that $\nu \leq O(1)$ clean surface behavior for large $\Phi(1+k)Pe^{1/2}$ is not possible. The experimental results of Sec. 4.2 indicate that $\nu >> 1$ for Triton-X 100, as clean interface behavior is recovered. In order to confirm that this observed

relaxation of tangential stresses at the interface was due to the sorption kinetics of Triton-X 100 , the protein B.S.A. in solution was used to form the aqueous phase in the three phase slug flow.

The sorption kinetics of proteins has been investigated by MacRitchie and Alexander (1962), Graham and Phillips (1978), Ter Minassian-Saraga (1980),and Guzman, et al.,(1986). Graham and Phillips as well as MacRitchie and Alexander postulate that proteins, once adsorbed at fluid-fluid interfaces, become denatured; that is that the adsorption is irreversible ($\nu \to 0$). Guzman, et. al. and Ter Minassian-Saraga assert that it is not neccesary to postulate irreversible adsorption to explain the existing protein sorption kinetic data; the data can be explained in terms of extremely slow desorption kinetics, i.e. desorption time scales on the order of several hours. All of these investigators also report the formation of multilayers at the fluid-fluid interfaces of concentrated protein solutions. Protein molecules align themselves in layers beneath the layer adsorbed at the interface. Thus, the desorption behavior of proteins differs markedly from that of the surfactant Triton-X 100. In light of the above arguments, for the three phase slug flow with protein solutions as the aqueous segment, the ratio of convective to desorptive time scales, ν, is clearly much less than O(1).

The protein used was Bovine Serum Albumin (B.S.A.). The Langmuir kinetic constants for B.S.A. are found by Guzman et al. to be $\Gamma'_\infty = 4.63\text{x}10^{-12}\text{mol/cm}^2$ and $\beta'/\alpha' = 7.33\text{x}10^{10}\ \text{cm}^3/\text{gmol}$. The B.S.A., crystallized and lyophilized, was used as obtained from Sigma Chemical Co. Solutions of B.S.A. were made in a buffer

solution of sodium phosphate dibasic and potassium phosphate monobasic with pH of 7.0 and ionic strength of .16 . Hydrion dry buffer was used as obtained from Micro Essential Laboratory, Inc.; no preservative was added to the solutions which were made fresh daily in order to avoid impurities and degradation of the protein.

In Fig.(6) a graph of the nondimensional pressure drop per cell vs $\Phi(1+k)Pe^{1/2}$ for a series of experiments in which B.S.A. was used to form the aqueous phase in the three phase slug flow is presented. (In evaluating the parameter Φ, a value of 10^{-6} cm^2/sec is used for the diffusion coefficient of the protein.) The experiments were undertaken in .1555cm I.D. tube. Note that the intercept for zero weight percent is $\approx$ .6 , much higher than the intercept of .35 obtained in the clean water runs reported for Triton-X 100. This difference was attributed to the presence of impurities in the buffer. Note also that the pressure drop per cell for the protein increases throughout the values of $\Phi(1+k)Pe^{1/2}$ reported until at a value of 1 the pressure drop appears to become constant at a value of $\approx$ 2, and shows no subsequent decrease with increasing $\Phi(1+k)Pe^{1/2}$. Data taken by Graham and Phillips indicates that the $5x10^{-4}$ wt% is the onset of multilayer formation for B.S.A., which corresponds to a value of $\Phi(1+k)Pe^{1/2}$ = .0025. Multilayer formation and slow desorption most likely prevent the free interface behavior from being remobilized, as is explained below.

The initial increase in the pressure drop required to drive the flow with increasing C'_∞ can be explained as before. Protein adsorbs onto the interface and is convected along the length of the cylindrical region by interfacial convection. Since desorption is

either slow or impossible, protein accumulates in this region, giving rise to Marangoni tractions which resist the flow, increasing the drag. As C'_∞ of protein is increased, the increased adsorption allows the surface velocity to be retarded along more of the cylindrical region of the aqueous slug, accounting for the increased pressure drop throughout the region of $\Phi(1+k)Pe^{1/2}<1$ reported in Figure (6).

For B.S.A. at range of $\Phi(1+k)Pe^{1/2}>1$, diffusion barriers in the sublayer to the surface should have dissipated appreciably but the pressure drop required to drive the flow remains elevated. In this concentration range the surface distribution of adsorbed surfactant has reached some sorption controlled steady state. The interface is probably not tangentially immobile, however, as the pressure drop required to drive a long cylindrical segment with no tangential mobility through a capillary tube is given by: $4\kappa(1-\epsilon)\lambda\mu'_a U'/(\sigma'(1-\xi^2))$, where $\xi=1-\hat{h}'/R'$. If the oil film thickness $\hat{h}'$ is estimated as before from the Bretherton expression, the sum of the pressure drop for the tangentially immobilized cylindrical region and the capillary contributions for the aqueous and air segments given nondimensionally is 3.33. The Bretherton film thickness exceeds that realized in the three phase slug flow, due to volumetric constraints on the oil phase, and the decrease in the leak rate when adsorbed surfactant acts to retard surface velocity. The thickness of the wetting layer in the three phase slug flow when the surface velocity is retarded is probably about 10μ (cf. Chapter 4). The estimated pressure drop over a unit cell for a completely stagnated aqueous-oil interface in the presence of a 10μ film thickness is 8.1

nondimensionally. Clearly this exceeds the pressure drop of 2.1 realized at the highest pressure drops in this series of experiments.

5. Conclusions and Implications

In this study it was demonstrated that the interfaces of moving fluid particles can remain unhindered in the presence of adsorbed surfactant if the surfactant has fast desorption kinetics, and is present in concentrations high enough that bulk diffusion barriers have been eliminated. The flow which was used in this experimental study is a three phase capillary slug flow, in which the retarding effects of adsorbed surfactant on surface velocity are strongly felt due to the volumetric constraints on the wetting phase. Surfactants were dissolved in the aqueous phase of the three phase slug flow. The remobilizing surfactant used in this study is the polyethoxyether Triton-X 100; pendant drop tensiometry studies of this surfactant showed it to be a good candidate for remobilization. At highly elevated concentrations of Triton-X 100, the three phase slug flow behaved hydrodynamically as it would in the absence of added surfactant, save that it had a uniform, reduced surface tension. As a counter example, the slow desorption kinetic protein B.S.A. was dissolved in the aqueous phase. Even at concentrations where bulk diffusion barriers of B.S.A. had been eliminated, the pressure drop required to drive the three phase slug flow remained at its elevated value, indicating that both fast desorption kinetics and the elimination of diffusion barriers in the bulk are necessary for a surfactant to remobilize a retarded surface flow.

The major implication of this study concerns the remobilization of fluid-fluid interfaces in fluid particle flows . The commonly observed effect of surfactants as impurities in multiphase fluid systems is an increase in the drag opposing the flow, resulting in a decreased particle velocity. A well known example is the retardation of the terminal velocity attained by moving fluid droplets in an infinite medium where a surfactant is present in trace amounts in either the droplet or bulk phase (c.f. Levich (1962)). Within the context of this study, the following reasons can be posited for the observed reduction in terminal velocity. If the surface active agent is present in either low enough concentration that the group $\Phi(1+k)Pe^{1/2}$ is small, i.e. there are diffusion barriers in the bulk, surface concentration gradients will develop. If the surface active agent has slow desorption kinetics, surface concentration gradients will again develop. In either of the above cases, the results of this study indicate the possibility that if a surfactant with fast sorption kinetics is added at high enough concentration, it will preferentially adsorb on the fluid interfaces, preventing the adsorption of the retarding surface active agent and allowing the droplet to settle at the nonretarded terminal velocity.

The idea of competitive adsorption as a means of remobilization of the interface has applications in dropwise mass transfer, where surface remobilization leads to enhanced interphase mass transfer. Other areas of application include the stability of foams and emulsions, and foam and liquid slug flows in porous media. The drainage rates of the film between the dispersed phases in foams and

emulsions can be accelerated by increased mobility of the interface, leading to accelerated breakdown of the foam or emulsion. In the case of multiphase slug transport in pores, the pressure drop required to drive the flow can be reduced by addition of sufficient amounts of surfactant with fast sorption kinetics.

Appendix A

Triton-X 100 Equilibrium and Kinetic Sorption Characteristics

The fast sorption surface adsorber used in this study is the nonionic commercial surfactant Triton-X 100. It is a polyethoxy-ether, and is soluble in water and insoluble in fluorocarbon oil. The structure of Triton-X 100 is C_8H_{17}- (C_6H_4) -$(OCH_2CH_2)_n$-OH , with n between 9 and 10. The aim of this appendix is to give the equilibrium adsorption properties of Triton-X 100, and to present arguments establishing lower bounds on its kinetic constants.

A.1 Equilibrium Properties

The equilibrium interfacial tensions of fluorocarbon oil FC-43 against aqueous surfactant solutions are reported in Figure A.1. The interfacial tensions were obtained by pendant drop tensiometry in conjunction with digital imaging as described briefly below. (Details are given in Lin et al. (1989). c.f. also Girault et al. (1984), Chiwetelu et al. (1988), Huh and Reed (1983), and Rotenberg, Boruvka and Neumann (1983).)

The measurement of interfacial tensions by pendant drop tensiometry entails the formation of a droplet of one fluid in a chamber filled with a second. The droplet, which is suspended from a supporting needle, assumes an axisymmetric shape which is governed by the balance of interfacial tension to gravity forces as expressed by the Young-LaPlace equation, below.

$$\Delta P' = \gamma'\left(\frac{1}{R_1'} + \frac{1}{R_2'}\right) \qquad \text{(A.1a)}$$

where R_1' and R_2' are the principal radii of curvature, γ' is the interfacial tension and $\Delta P'$ is the pressure difference across the interface. All primed quantities are dimensional. With gravity being the only external force the pressure difference can be expressed as

$$\Delta P' = \Delta P_0' + \Delta\rho' g' z' \qquad \text{(A.1b)}$$

with

$$\Delta P_0' = 2\gamma'\frac{1}{R_0'} \qquad \text{(A.1c)}$$

where $\Delta\rho'$ is the density difference of the two fluids, z' is the vertical coordinate measured up along the axis of symmetry of the droplet from the drop apex, g' is the gravitational constant, and R_0' is the radius of curvature at the origin, i.e. at the apex of the droplet.

Let x' be the horizontal coordinate whose origin is also located at the drop apex and define ϕ, the turning angle of the drop, according to:

$$\frac{dx'}{dz'} = \tan\phi$$

Expressing x' and z' as parametric functions of the arc length s' such that

$$\frac{dx'}{ds'} = \sin\phi \qquad\qquad \frac{dz'}{ds'} = \cos\phi$$

the Young-Laplace equation can be recast as:

$$\frac{d\phi}{ds'} = -\frac{\sin\phi}{x'} + \frac{2}{R_0'} + \Delta\rho' g' z'/\gamma'$$

subject to the boundary conditions $\phi(0)=z'(0)=x'(0)=0$.

Nondimensionalizing s', x', and z' with R_0' the above equations become:

$$\frac{dx}{ds} = \sin\phi \qquad \text{(A.2a)}$$

$$\frac{dz}{ds} = \cos\phi \qquad \text{(A.2b)}$$

$$\frac{d\phi}{ds} = 2 + \frac{z}{a} - \frac{\sin\phi}{x} \qquad \text{(A.2c)}$$

subject to $\phi(0)=z(0)=x(0)=0$. In the above, a, the capillary number is defined to be $a = \Delta\rho' R_0'^2 g'/\gamma'$. The Young-LaPlace equations in the form of equations (A.2) can be integrated numerically to give the theoretical droplet shape for some value of the capillary number a.

Consider an oil droplet formed in an aqueous surfactant solution. The droplet's shape will change with time as surfactant molecules diffuse through the bulk and adsorb onto the interface until the equilibrium surface concentration, and thus the equilibrium surface tension and shape are attained. The droplet's shape at formation and subsequent shape changes are video-recorded

over time. Drop imaging is undertaken using a modified Rame-Hart goniometer and a Data Translation digitizing board (DT2861) with a 512x512 pixel resolution. Each of the video images are digitized, generating a set of experimental points which locate the position of the interface. These points are used as input to an objective function which is the sum of the minimized distances between the theoretical curves generated by integrating equations (A.2) and the experimental curves obtained from the digitized video images. The objective function is a function of four parameters which are: $q_1=X_0'$, $q_2=Z_0'$, $q_3=R_0'$, $q_4=a$. X_0' and Y_0' locate the origin of the experimental curve relative to that of the theoretical curve. The objective function is minimized with respect to these four parameters. From the value of a and R_0' which minimize the objective function the value of γ', the interfacial tension, can be found.

Using the above technique, equilibrium interfacial tension measurements were made for aqueous solutions of Triton-X 100 against fluorocarbon oil. The surfactant was obtained from Aldrich Chemical Co. and used without modification. The fluorocarbon oil was obtained from the 3M Co., (FC-43). The water used was purified using a Millipore water purification system with Organex filters to remove organic impurities. Note that the pure water surface tension obtained using this apparatus is 72.3 dynes/cm. The Langmuir constants, Γ_∞' and β'/α', for the interfacial tension data at the Triton-X 100 solution -FC43 interface were calculated by minimizing the square error of the surface pressure recorded at concentrations below the critical micelle concentration to the Langmuir adsorption

isotherm. The Langmuir coefficients for Triton-X 100 were found to be $\Gamma'_\infty = 2.17 \times 10^{-10}$ gmol/cm^2 and $\beta'/\alpha' = 3.79 \times 10^{10}$ cm^3/gmol. The Langmuir isotherm which corresponds to these constants is shown as the solid line at concentrations less than the critical micelle concentration in Fig. A1. Note that the critical micelle concentration for Triton-X 100 at the aqueous-oil interface occurs at about 1.85×10^{-7} gmol/cm^3.

A.2 Kinetics

The transient surface tensions of a freshly formed droplet in surfactant solution are measured using pendant drop tensiometry as described above. The kinetic data reported herein are at the aqueous-air interface of Triton-X 100 solutions. The kinetic behavior at this interface should be similar to that at the aqueous-oil interface.

The equilibrium surface tension data for aqueous Triton-X 100 solutions at the aqueous-air interface and the solid curve indicating the fit of the Langmuir adsorption isotherm to the experimental data are reported in Figure A2. Note that the CMC for Triton-X 100 at the aqueous-air interface is about 1.7×10^{10} gmol/cm^3, very close to the CMC at the aqueous-oil interface. The Langmuir kinetic constants were found to be $\Gamma'_\infty = -3.08 \times 10^{-10}$ gmol/cm^2 and $\beta'/\alpha' = 1.22 \times 10^{9}$ cm^3/gmol. $\beta' C'_\infty/\alpha'$ at 2.2×10^{-8} gmol/cm^3 is 26.32. This gives an equilibrium surface concentration at this concentration of 2.97×10^{-10} gmol/cm^2. Van Hunsel, Bleys and Joos (1986) report an equilibrium surface concentration at this bulk

concentration of Triton-X 100 of 2.5×10^{-10} gmol/cm^2. This agreement supports the experimental results obtained.

The equations which govern the mass transfer of surfactant in nondimensional form are:

$$\frac{\partial^2 C}{\partial z^2} = \frac{\partial C}{\partial t} \qquad \text{(A.4a)}$$

$$\frac{\partial \Gamma}{\partial t} = k_a\left(\frac{\Gamma'_\infty}{\Gamma'_0} - \Gamma\right)C - k_d\Gamma \qquad \text{(A.4b)}$$

subject to the boundary and initial conditions :

$$\begin{aligned} &\frac{\partial \Gamma}{\partial t} = \frac{\partial C}{\partial z} && (z=0,t) \\ &C = 1 && (z=\infty,t) \\ &\Gamma = 0 && (z,t=0) \\ &C = 1 && (z,t=0) \end{aligned} \qquad \text{(A.4c)}$$

In the above equations

$$C = C'/C'_\infty \qquad \Gamma = \Gamma'/\Gamma'_0 \qquad t = t'/(h'^2/D')$$

$$k_d = \alpha'/(D'/h'^2) \qquad k_a = \beta' C'_\infty/(D'/h'^2) \qquad k = \beta' C'_\infty/\alpha' = k_a/k_d$$

$$\Gamma'_0/\Gamma'_\infty = k/(1+k)$$

where Γ'_0 is the surface concentration in equilibrium with C'_∞, the bulk surfactant concentration, and D' is the diffusivity in the

bulk. h', the adsorption depth, is defined to be $h' = \Gamma_0'/C_\infty'$. In the above equations planar coordinates have been adopted because h' is of order 10^{-2}cm and R', the drop radius, is of order .1cm. This gives $\frac{h'}{R'} \ll 1$, allowing curvature to be neglected.

Short time experimental data of the surface tension as a function of nondimensional time for a bulk concentration of 1.55×10^{-8}gmol/cm^3 is presented by the symbols in Fig. A3; each symbol represents the time history of a single bubble. Also presented in the figure are numerical solutions of the transport equations for k=18.8 (this corresponds to a bulk concentration of 1.55×10^{-8}gmol/cm^3) and four different values of k_a (1, 10, 100 and the diffusion controlled regime $k_a \to \infty$; note k_d is fixed once a value of k_a is selected by the equilibrium ratio β'/α'). A value of 3.8×10^{-6}cm^2/sec, derived from the studies of Joos (1981), was used for the diffusion coefficent of Triton X-100. The solution algorithim used to solve (A.4) is adopted from the studies of Miller (1982). From Fig. A4 it is clear that k_a is at least as large as 10^2, and this translates to a lower bound of k_d of 5 or α' of .05 sec^{-1}. The article by Lin et al. gives a more comprehensive set of data on the sorption kinetics of Triton X-100 by the pendant drop method, and also describes in detail the numerical algorithim used for the solution of Eqs. A.4.

Having established bounds on the kinetic constants of adsorption and desorption, the ranges covered by the dimensionless groups $k\nu$ and ν, can be estimated. The parameter $k\nu$, defined to be

$\beta' C_\infty' R' \lambda (1-\epsilon)/U'$ gives the ratio of the rate of adsorption to the rate of convection on the surface of the liquid slug and ν, given by $\alpha' R' \lambda (1-\epsilon)/U'$ is similarly the ratio of the rate of desorption to tha rate of convection. Using the parameters of this study, $k\nu$ is found to vary between 0 and 10^2 at the CMC and ν is equal to or larger than .2. Therefore the adsorption rate becomes much faster than the convection rate as the CMC is approached. A more rigorous lower bound cannot be found for the desorption rate because the faster relaxations of the drop interfacial tension at higher bulk concentrations cannot be resolved using pendant drop tensiometry as the adsorptive time scales are on the same order as the time required to form the pendant drop. Note, however, that in order to be consistent with the experimental results of this study ν must be considerably larger than the conservative lower bound established by these experiments.

Surfactant transport processes
on the surface of a moving drop

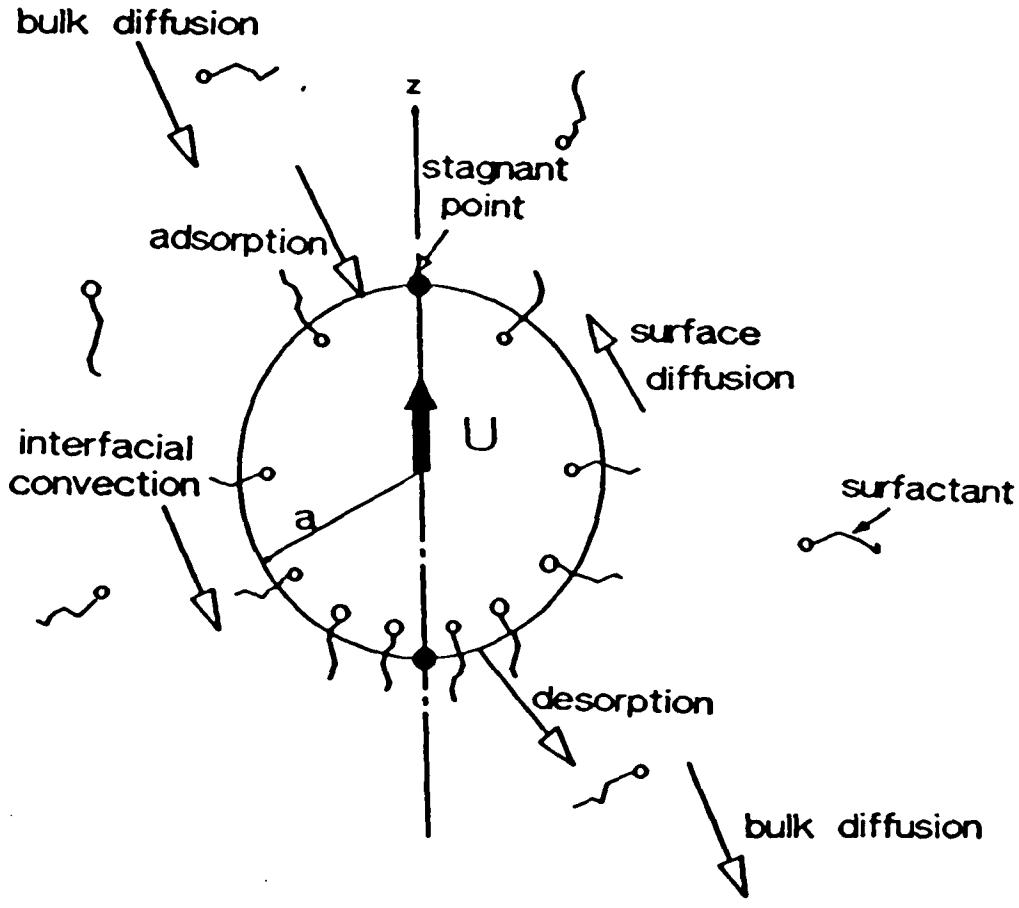

FIGURE 1.

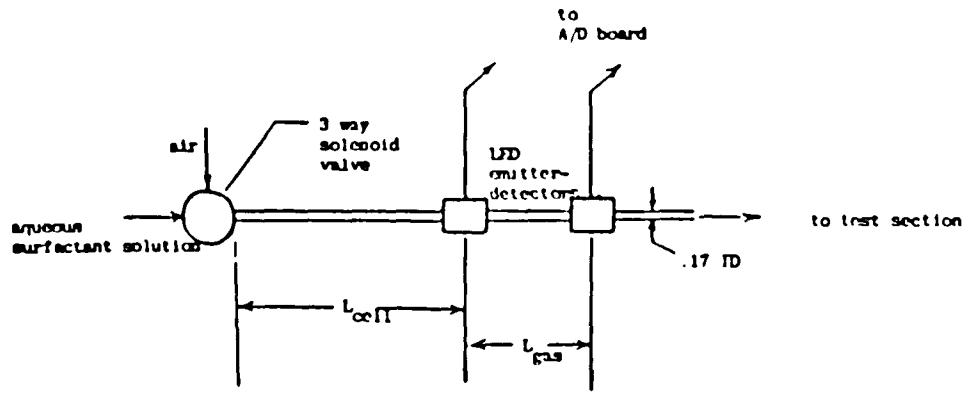

FIGURE 2.A

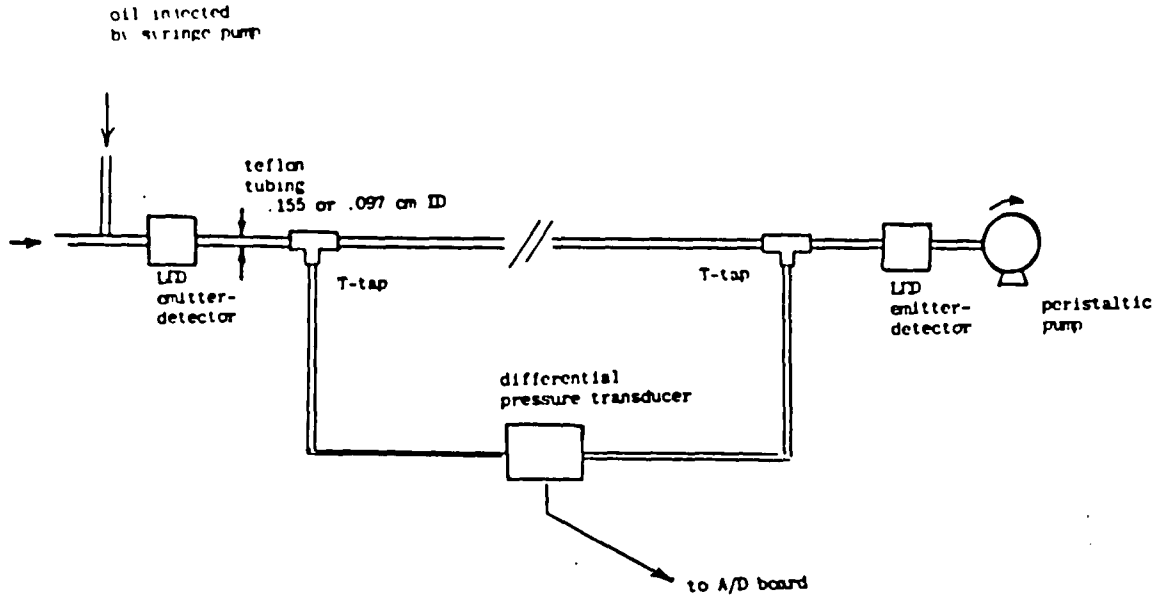

Figure 2.B

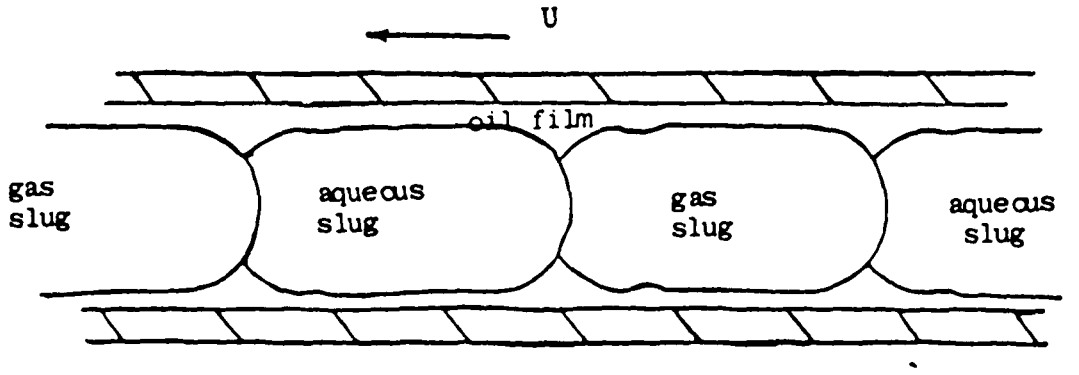

FIGURE 3.

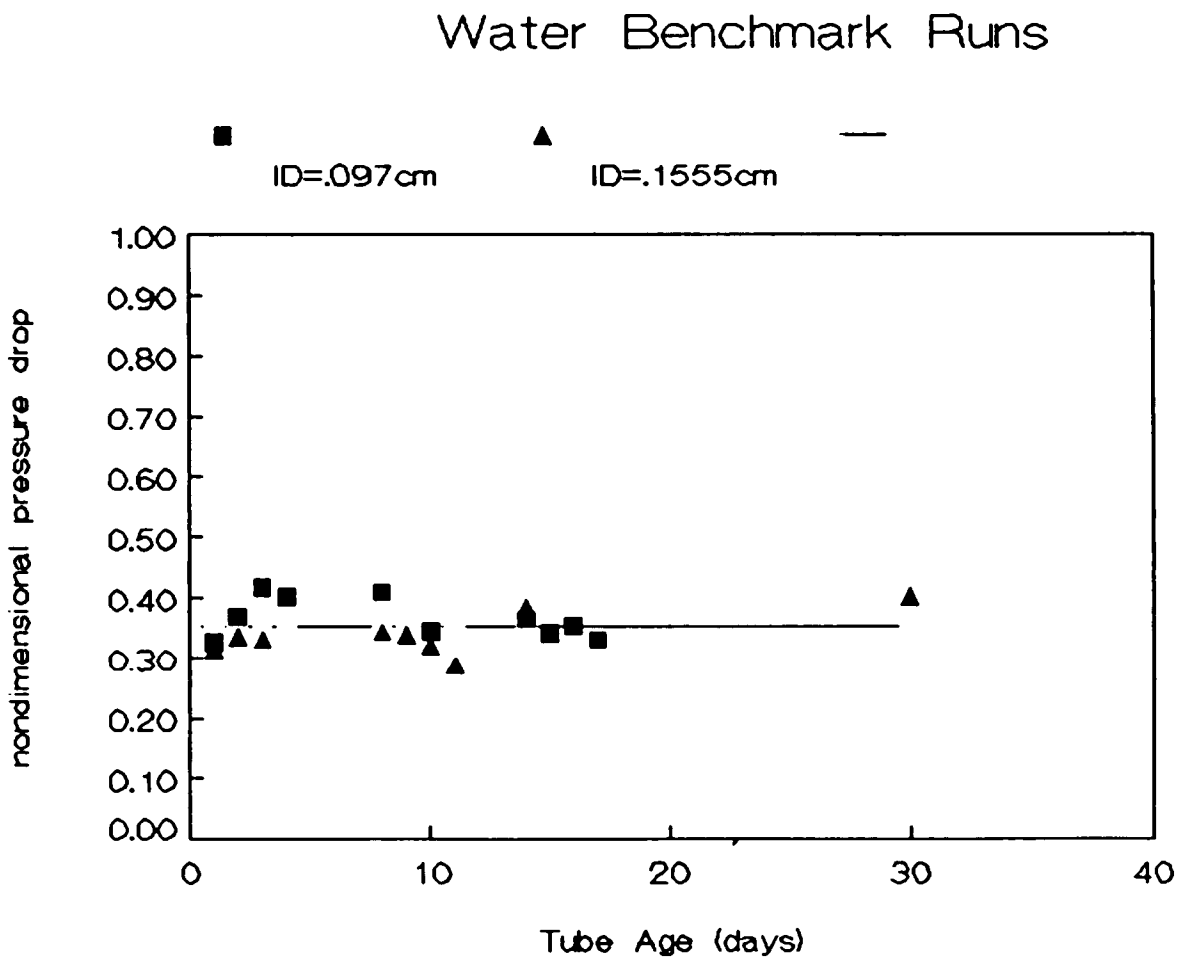
Water Benchmark Runs
ID=.097cm
ID=.1555cm
nondimensional pressure drop
1.00
0.90
0.80
0.70
0.60
0.50
0.40
0.30
0.20
0.10
0.00
0
10
20
30
40
Tube Age (days)

FIGURE 4.

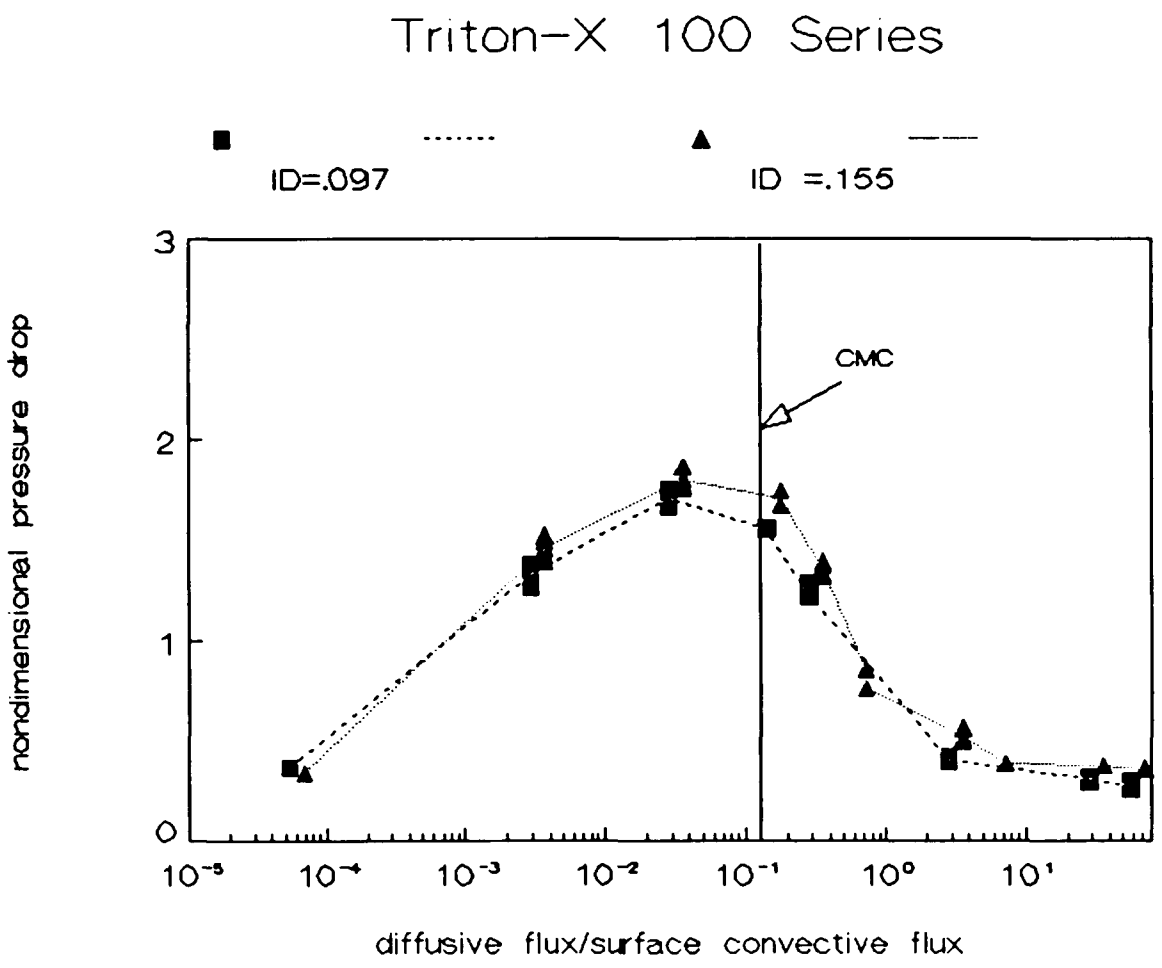
Triton-X 100 Series
ID=.097
ID =.155
CMC
nondimensional pressure drop
diffusive flux/surface convective flux
0
1
2
3
10^{-5}
10^{-4}
10^{-3}
10^{-2}
10^{-1}
10^{0}
10^{1}

FIGURE 5.

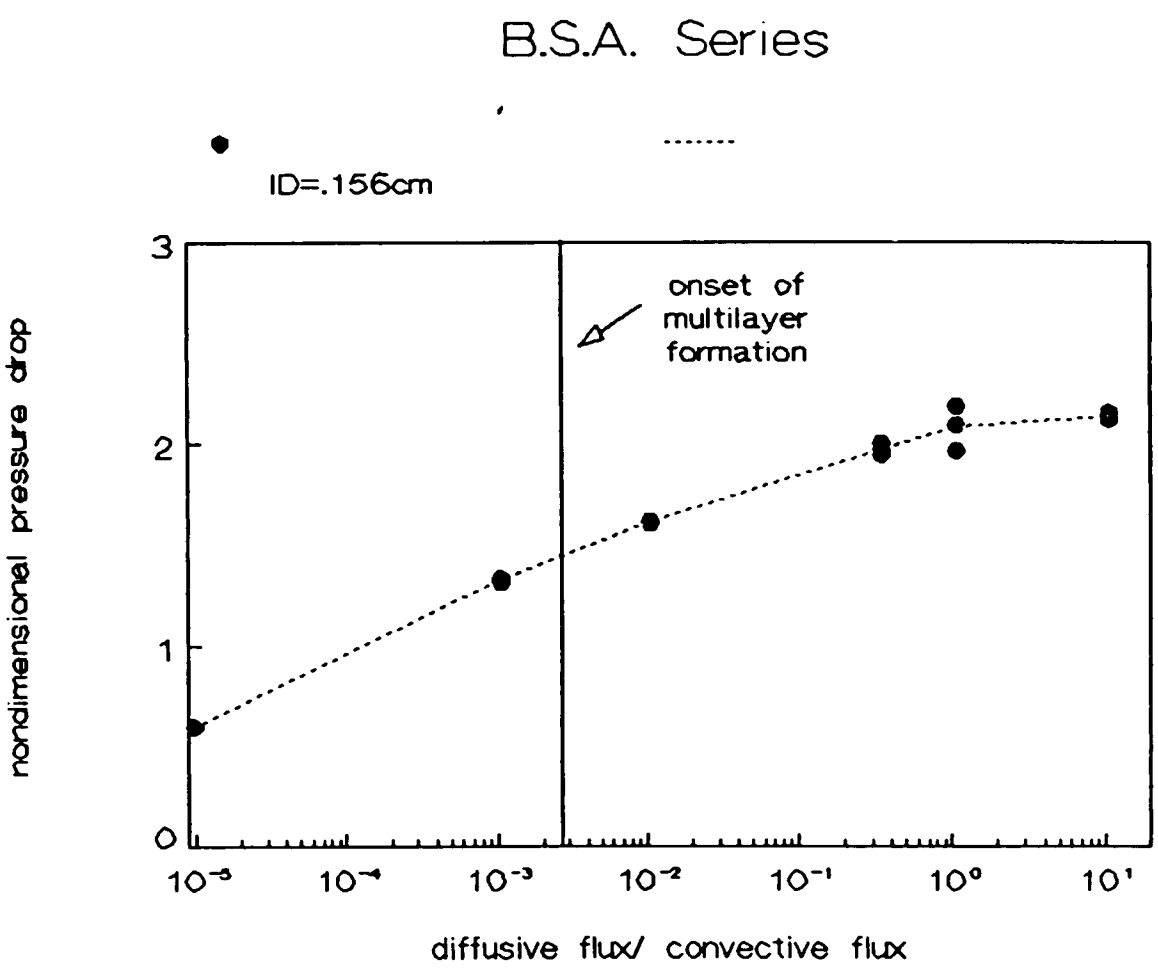
B.S.A. Series
ID=.156cm
onset of
multilayer
formation
nondimensional pressure drop
diffusive flux/ convective flux
0
1
2
3
10^{-5}
10^{-4}
10^{-3}
10^{-2}
10^{-1}
10^{0}
10^{1}

FIGURE 6.

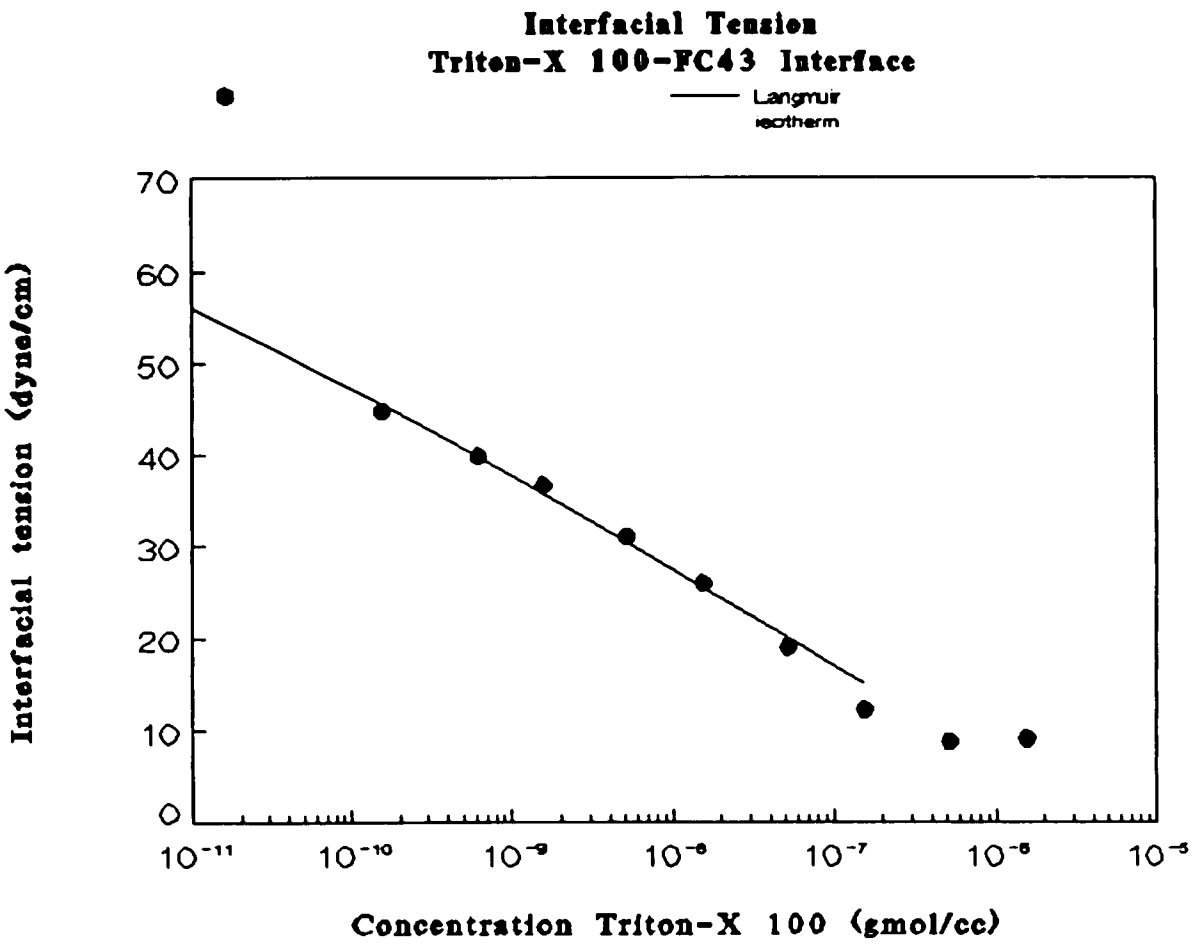
Interfacial Tension
Triton-X 100-FC43 Interface
Langmuir isotherm
Interfacial tension (dyne/cm)
70
60
50
40
30
20
10
0
10^{-11}
10^{-10}
10^{-9}
10^{-8}
10^{-7}
10^{-6}
10^{-5}
Concentration Triton-X 100 (gmol/cc)

FIGURE A1.

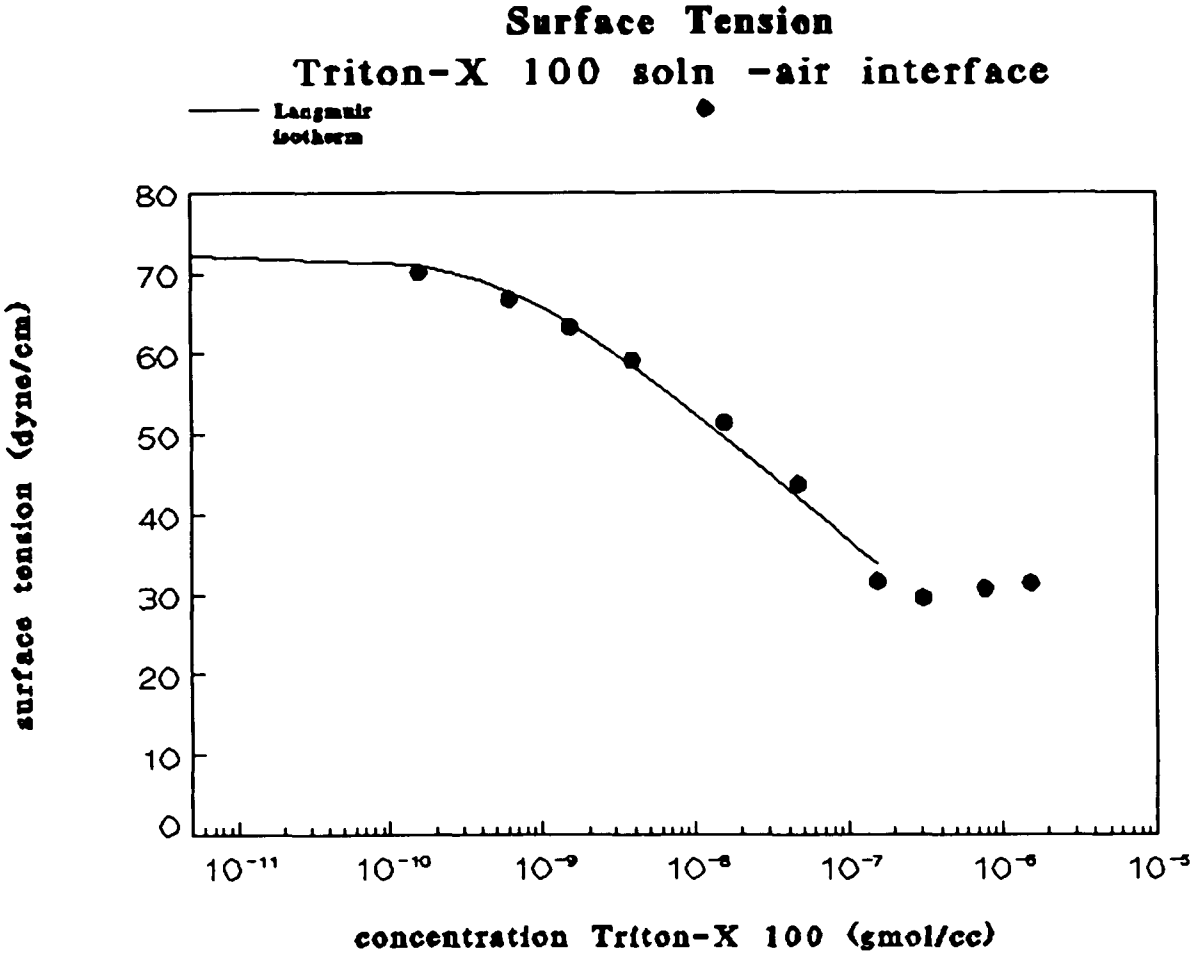
Surface Tension
Triton-X 100 soln -air interface
Langmuir isotherm
surface tension (dyne/cm)
80
70
60
50
40
30
20
10
0
10^{-11}
10^{-10}
10^{-9}
10^{-8}
10^{-7}
10^{-6}
10^{-5}
concentration Triton-X 100 (gmol/cc)

FIGURE A2.

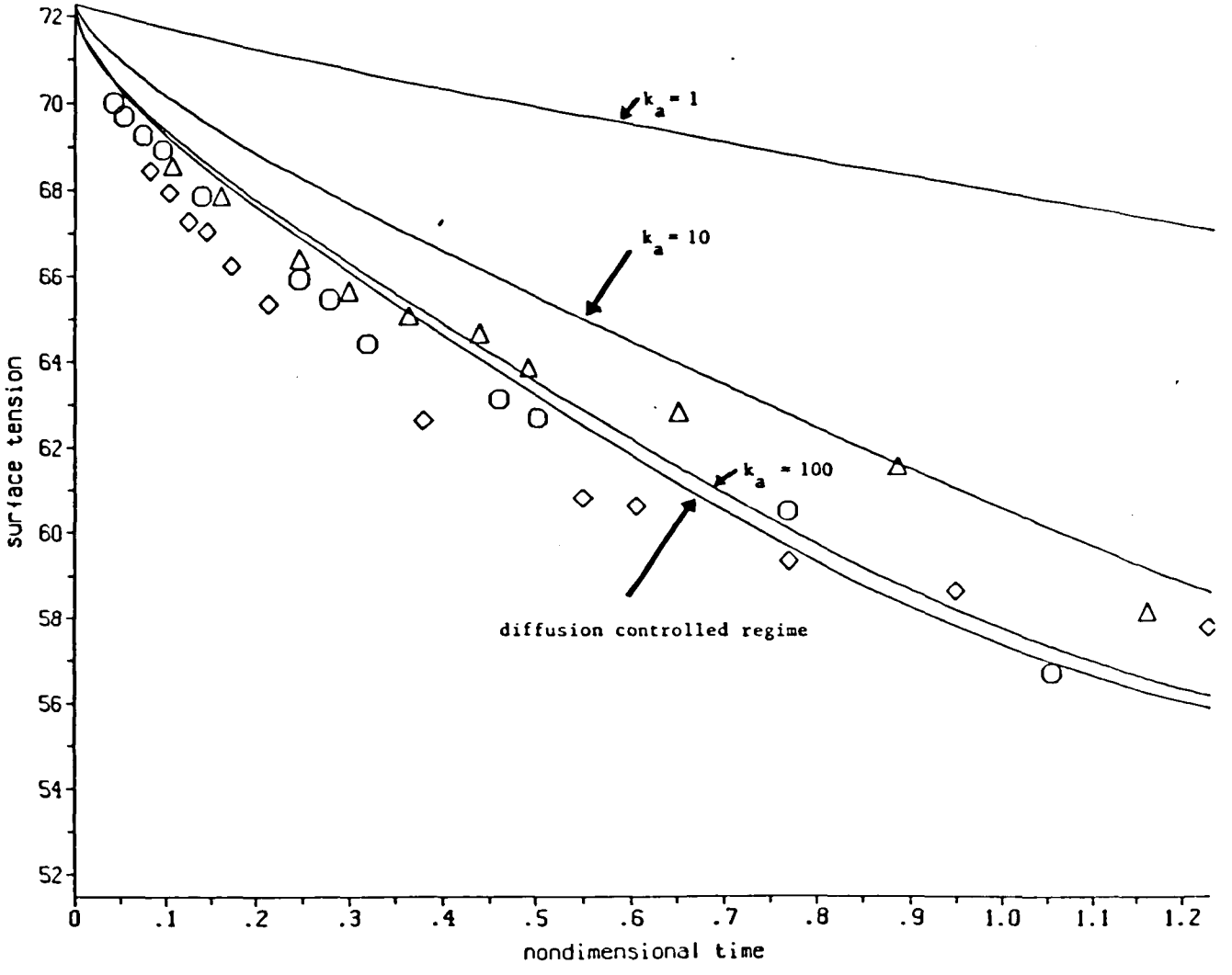
72
70
68
66
64
62
60
58
56
54
52
surface tension
k_a = 1
k_a = 10
k_a = 100
diffusion controlled regime
0
.1
.2
.3
.4
.5
.6
.7
.8
.9
1.0
1.1
1.2
nondimensional time

Figure A3

Table 1

Surfactant Independent Dimensionless Groups

group name	symbol	TRX-100 .097cmID	TRX-100 .155cmId	BSA .155cmID
void fraction	ϵ	.43	.42	.42
aspect ratio	λ	81.5	81.5	85.0
viscosity ratio	κ	5.9	5.9	5.9
oil:aqueous flow rate	Ω	.0033	.0032	.0033
Capillary numbers (held fixed for all experiments)				
oil-aqueous:	$Ca_{(o/a)} = 1.02 \times 10^{-3}$			
oil-gas:	$Ca_{(o/g)} = 3.80 \times 10^{-3}$			
aqueous-gas:	$Ca_{(a/g)} = 1.42 \times 10^{-4}$			

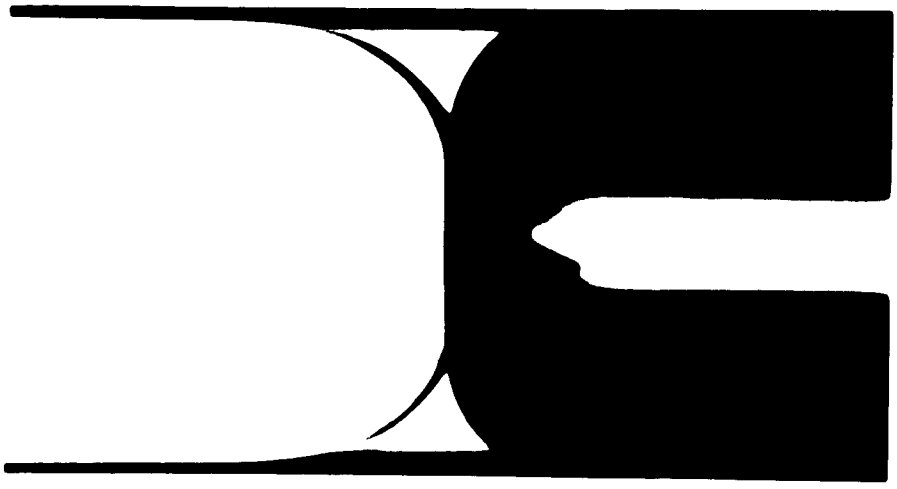

PLATE 1A.

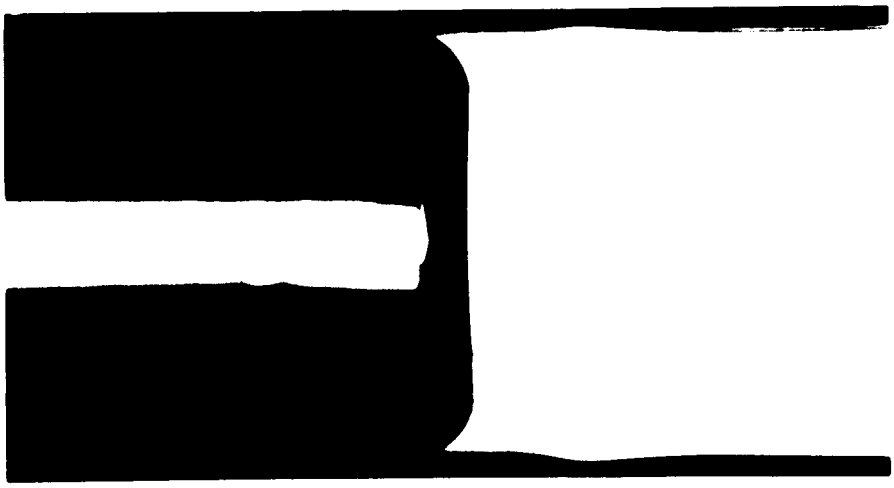

PLATE 1B.

Chapter 3

The Remobilization of Surfactant Laden Fluid Particle Interfaces By The Competitive Adsorption of a Freely Exchanging Surfactant

1. Introduction

This is the second of a two part study on the remobilization of fluid particle interfaces stagnated by adsorbed surfactant. (The first part of this study (Stebe et al. (1989)) is hereafter referred to as (I.).) The retardation of surface velocity by surfactant adsorption in fluid particle flows has been established in many studies (cf., for example, the monograph by Levich (1962) and his later review article (Levich (1969)). The physicochemical basis for the effect was first outlined by Frumkin and Levich (1947), and may be explained as follows. Consider the simple fluid particle flow in which a droplet is moving in an unbounded, otherwise quiescent continuous fluid, surfactant present in either the droplet or continuous phase. In the frame moving with the drop velocity, the surface convection is directed from the leading pole, a diverging stagnation point, towards the trailing pole, a converging stagnation point. Surfactant molecules in the sublayer to the droplet interface kinetically adsorb onto the drop interface, depleting the sublayer of surfactant molecules. This depletion sets up a diffusive flux of surfactant from the bulk to the sublayer. Adsorbed surfactant molecules are swept by surface convection to the convergent stagnation point, where they can desorb into the sublayer and diffuse through the sublayer to the bulk. It is the balance of

these transport processes as they occur in series which determines the steady state distribution of surfactant along the fluid particle interface. In the event that desorption or diffusion through the sublayer to the bulk is slow compared to the rate at which surfactant is swept to the rear pole by surface convection, surfactant will accumulate there. At steady state there will be some higher surface concentration within this region than elsewhere on the interface. This surface concentration gradient gives rise to a surface tension gradient, the surface tension at the rear pole being less than elsewhere on the droplet interface. The resulting stress, a Marangoni tension, acts to oppose and hence reduce the surface velocity. This retards the fluid particle velocity as it increases the drag exerted by the continuous phase on the particle.

In the first part of this study it was shown that the surface velocity of a fluid particle can remain unretarded in the presence of a single adsorbed surfactant if the instrinsic desorption rate of the surfactant (a quantity independent of bulk concentration) is fast when compared to convection, and the surfactant is present at high enough bulk concentration. As conjectured in (I.), as the bulk concentration is increased both the rate of adsorption and diffusion between the bulk and the sublayer increase with an increase in bulk concentration; at high enough concentrations these transport processes become fast in comparison to convective transport of surfactant along the surface. With sorptive and diffusive barriers now all absent, a uniform surface concentration is established as surfactant freely adsorbs and desorbs from the interface. The fluid particle flow behaves hydrodynamically as it would if no adsorbed

surfactant were present, save that it has a reduced, uniform surface tension.

Surface active impurities are ubiquitous, and usually retard fluid particle flows, presumably because they are present in concentrations low enough that diffusion barriers exist and possibly because their desorption rate is slow in contrast to the prevailing surface convection rate. In this communication it is demonstrated that fluid particle flows so stagnated by some adsorbed surface active contaminant can be rendered tangentially mobile by the competitive adsorption of a freely exchanging surfactant. The idea behind competitive adsorption is as follows: Consider a surfactant which desorbs quickly in comparison to the transport rate by surface convection, and which is added to a fluid particle flow containing surface active impurities. If the fast desorption remobilizing surfactant is present in high enough concentrations so that its adsorption is fast and no diffusion barriers exist to hinder its free exchange between the bulk and the droplet interface, it will preferentially adsorb onto the interface, preventing the adsorption of the retarding impurity and allowing the fluid particle flow to behave as it would in the absence of surfactant. The focus of this study is to verify these ideas experimentally by using a specially designed periodic three phase capillary slug flow for which the pressure required to drive the flow at a constant velocity is extremely sensitive to the mobility of the slug interface.

This study is divided into four sections. In the first, the physicochemical conditions for remobilization by competitive adsorption are structured quantitatively using the Langmuir

adsorption kinetics to describe the kinetic exchange of surfactant, and boundary layer arguments to formulate the bulk mass transfer. The slug particle flow used to experimentally verify these ideas is described in the second section, along with a discussion of the experiments undertaken and the experimental protocol. The results of the competitive adsorption experiments are discussed in the third section. The fourth and final section consists of conclusions and a discussion of the applications of these ideas.

2. Physicochemical Criteria for Remobilization

Consider a fluid particle, either a droplet or a bubble, settling in an unbounded, continuous, otherwise quiescent fluid in which a single surfactant has been dissolved. In (I.) it was shown that for surfactants with fast desorption rates, such a flow could be made to behave hydrodynamically as it would in the absence of surfactant if the bulk concentration is high enough. The criteria for this surfactant laden, free surface condition may be established as follows.

The kinetic exchange rate of surfactant between the interface and the sublayer can be expressed in the Langmuir formalism as:

$$Q' = \alpha' \left(\frac{\beta'}{\alpha'} C_s' (\Gamma_\infty' - \Gamma') - \Gamma' \right) \qquad (2.1)$$

In (2.1), α' and β' are the desorption and adsorption rate constants, respectively, C_s' is the sublayer concentration, and Γ' and Γ_∞' are the surface concentration and the maximum packing density of surfactant molecules on the interface. From (2.1) the surface

concentration in equilibrium with the bulk concentration C'_∞ far from the drop interface is given by: $\Gamma'_0=\Gamma'_\infty k/(1+k)$, where $k=\beta' C'_\infty/\alpha'$. (Note that in (2.1) and henceforth, all dimensional quantities are primed, while nondimensional quantities are not primed.) This kinetic formalism can be used to scale the sorption kinetics along a fluid particle with a perimeter perpendicular to the particle motion of order ℓ' and an area of order ℓ'^2. The rate at which surfactant molecules adsorb from the sublayer to the interface is $O(k\alpha'\Gamma'_0\ell'^2)$; the rate at which they desorb is $O(\alpha'\Gamma'_0\ell'^2)$.

The rate of diffusion through the bulk depends upon the relationship between the convective and diffusive fluxes through the bulk; this relationship is characterized by a bulk Peclet number $Pe=U'\ell'/D'$, D' being the bulk diffusivity of surfactant. Mass transfer in liquids is usually within the regime of large Peclet number. Within that regime, the diffusive flux of surfactant normal to the interface takes place in a boundary layer of thickness δ'. In this layer, the diffusive flux is balanced by a convective flux along the interface. The maximum diffusive flux for a droplet or bubble occurs for a perfectly mobile interface, and from scaling arguments it can be established that δ' is of $O(\ell' Pe^{-1/2})$. The rate (through the area ℓ'^2) at which surfactant diffuses through the sublayer of thickness δ' is therefore $O(D'C'_\infty\ell' Pe^{1/2})$.

The rate of convection of surfactant along the perimeter ℓ' is $O(U'\ell'\Gamma'_0)$, where U' is the drop velocity. Thus the rate of

desorption to convection, defined here as ν is equal to $\alpha'\ell'/U'$ and is seen to be independent of bulk concentration. The rate of diffusive mass transfer through the sublayer of thickness δ' to the rate of surface convection is equal to $(Pe^{-1/2}\ell'/(\Gamma_o'/C_\infty'))$. If desorption is fast compared to the rate of surface convection, i.e. if $\nu>1$, the distribution of surfactant along the droplet interface is diffusion controlled. A diffusion controlled surfactant will accumulate at the trailing pole of the droplet if the rate at which surfactant diffuses through the sublayer to the bulk is less than the rate at which surfactant is swept to the rear pole by surface convection, i.e. if $Pe^{-1/2}\ell'/(\Gamma_o'/C_\infty') < 1$. If, however, this group is large, indicating that diffusive mass transfer is not rate limiting, surfactant will not accumulate at the converging stagnation point in the flow.

In order that the group $Pe^{-1/2}\ell'/(\Gamma_o'/C_\infty')$ be made large experimentally, the ratio of Γ_o'/C_∞' , which appears in the denominator is of interest. This ratio is the adsorption depth h', which is the distance normal to the interface which contains as much surfactant as that adsorbed on the interface at equilibrium per unit area. A surface can accomodate only a finite number of surfactant molecules. As bulk concentration is increased the surface concentration approaches some constant value, given by the maximum packing per unit area Γ_∞'. Clearly then, as the bulk concentration is increased over several orders of magnitude, h' must approach zero. As the adsorption depth becomes small, the ratio of diffusive

to surface convective fluxes becomes large, indicating that diffusive fluxes are no longer rate limiting.

In summary, if desorption is fast (ν>1) a surfactant's distribution is diffusion controlled. For such a surfactant, if diffusive mass transfer is slow compared to surface convection ($Pe^{-1/2}\ell'/(\Gamma_o'/C_\infty') < 1$) surfactant will accumulate at converging stagnation points in the flow, retarding the surface velocity. If, however, diffusive mass transfer is made fast compared to surface convection ($Pe^{-1/2}\ell'/(\Gamma_o'/C_\infty') > 1$) by decreasing the adsorption depth (increasing C_∞'), surfactant will not accumulate at the rear pole of the droplet, but will rather diffuse back into the bulk. A uniform surface concentration in equilibrium with the uniform subsurface concentration will be realized along the droplet interface, and no retarding stresses will develop.

Consider now the case in which a droplet is settling in a continuous fluid which contains a surface active contaminant. It is presumed that the impurity retards the surface velocity because it is present in low concentration and therefore diffusion barriers exist ($Pe^{-1/2}\ell'/h' < 1$) and possibly because desorption is slow (ν < 1). If a surfactant with fast desorption is added to the solution in high concentration, it will compete with the contaminant for adsorption onto a freshly created surface. Since the rate of adsorption is proportional to the bulk concentration, the fast desorption surfactant should populate the interface in preference to the comtaminant. If it is present in high enough concentrations, it

will swamp the interface (i.e. its maximum packing concentration Γ'_∞ will be approached) preventing any substantial adsorption of the surface active impurity. As no surface active contaminant is able to adsorb, the hydrodynamics of the droplet interface under these conditions are as those of a droplet in the presence of a single, fast desorbing surfactant present in highly elevated concentrations: Surfactant is distributed uniformly along the drop interface and no surface tension gradients arise to retard the flow. In this manner the competitive adsorption of a fast desorbing kinetic surfactant can prevent the adsorption and subsequent retarding influence of a surface active impurity.

3. Materials and Methods

The concept of remobilizing a surface retarded by the adsorption of a contaminant by the competitive adsorption of a remobilizing surfactant was verified experimentally in a three phase capillary slug flow. The flow consists of a train of alternating air and aqueous slugs surrounded by an annular fluorocarbon oil film, which in turn encoats the inner wall of a teflon capillary tube. A schematic of the interfacial configurations of the flow regime is given in Fig. 1. The flow is drawn through the tube at a constant velocity. Surface active molecules dissolved in the aqueous phase adsorb along the aqueous-fluorocarbon oil interface, and are swept by surface convection to the trailing end of the cylindrical region of the aqueous slug. If barriers to desorption

or diffusive mass transport exist, adsorbed molecules accumulate in this region and retard the surface velocity.

This flow regime was selected because the pressure drop required to drive the train is very sensitive to the mobility of the aqueous-fluorocarbon oil interface. There are two primary reasons for this sensitivity. First, when surfactants retard the aqueous slug interfacial velocity, the shear stress in the wetting layer increases markedly because the layer is so thin. Secondly, when the surface mobility is retarded, the leakrate of oil (i.e. the flow rate of oil in the frame moving with the train velocity) is reduced. The leakrate (q'_{lk}) is related to the oiling rate (q'_{oil}) by the relation:

$$q'_{lk} = V'_{(o)}/T' - q'_{oil} \qquad (2.2)$$

where T' is the time required for one unit cell to travel past a fixed point in the laboratory frame and $V'_{(o)}$ is the amount of oil in a unit cell. As the leak rate decreases, the amount of oil surrounding a unit cell must also decrease as q'_{oil} is held fixed. To reduce $V'_{(o)}$, the amount of oil in the inclusion between the air and aqueous slugs can be reduced, or, the film can thin. In any case, the fact that the oiling rate is fixed precludes the appreciable thickening of the annular oil film which would relieve the excessive shear in the film region. Thus with a decrease in the surface mobility, the shear in the wetting layer increases markedly, and the pressure drop required maintain a constant train velocity increases commensurately.

The experimental apparatus used to create the slug flow is described in detail in (I.); only a brief description will be included here. At the upstream end of the experimental system is a flow cell which creates the aqueous and air segments in a manner independent of the flow rate through the system. A three way miniature solenoid valve (Lee Co.) is configured so as to draw either air or aqueous reagent. The solenoid valve is attatched to a piece of glass tubing (ID=1.7mm), along whose length, at known distances from the solenoid valve, are located two LED emitter-detector pairs. These pairs are attatched to relay circuits which allow them to direct the solenoid valve to draw from either the air or aqueous sources. The glass tube is initially filled with the aqueous solution. An air segment is drawn into the tube. When the aqueous-air interface at the leading end of the air segment passes the first LED emitter-detector pair, the solenoid valve begins to draw air. When the same aqueous-air interface passes the second LED emitter-detector pair, the solenoid valve draws from the aqueous source. The distance between the solenoid valve and the first detector therefore determines the length of a unit cell; the distance between the two detectors determines the length of the air segment. The glass tubing is attatched to a length of teflon tubing. At the union of the two tubes is a teflon "T" fitting, through which the fluorocarbon oil (FC43, 3M Corp.) is introduced at a constant rate by action of a syringe infusion pump (Sage Instruments). Since the fluorocarbon oil preferentially wets the inner wall of the teflon tube, the oil spreads along the wall as it is drawn through the teflon tube along with the aqueous and air

slugs formed at the front end of the system. In this manner the three phase slug flow is established.

The average velocity of a unit cell over the test section of teflon tubing (Alltech Assoc., FEP, nominal ID of 1.5 mm) is monitored via two LED emitter-detector pairs. The pressure drop over the test section is measured using a diaphragm type differential pressure transducer (Validyne). The pressure is tapped at either end of the test section by "T" taps attatched to fluid-filled lines which lead to either side of the pressure transducer chamber. Pressure and velocity data, taken online during each run, is collected using an A/D board (Data Translation DT2805) in an IBM P.C..

At the beginning of each series of experiments, the ID of the teflon test section is established by volume displacement. The aspect ratio and void fraction (L'/R' and $V'_{(g)}/(V'_{(g)}+V'_{(aq)})$) are established at 85 and .4 respectively. Each series of experiments was undertaken holding these two groups, along with the oil introduction rate and the train velocity held constant. For each run, the three phase flow is established using whichever aqueous surfactant solution is of interest. The pressure drop and average velocity are monitored until a steady state has been established along the test section of the tubing. The pressure drop and average velocity are then recorded for 60 minutes. The aqueous source is then changed, and the process begun again. At the end of each day the system is flushed for several hours with purified water.

In each series of experiments, two surface adsorbers were dissolved in the aqueous phase. The first surface active agent,

whose concentration was not varied, was present as a "contaminant". Its sorption kinetics or diffusion mass transport barriers were such that this first surface active agent hindered the surface velocity, requiring a high pressure drop to draw the three phase slug flow through the capillary tube. The second surface active agent in each experimental series was one with fast desorption kinetics present at high enough concentrations so that it freely exchanged between the bulk and the surface (adsorption and bulk diffusion fast in comparison to the rate of convection).

The remobilizing surfactant employed was Triton X-100, a polyethoxyether with a structure $C_8H_{17}\text{-}(C_6H_6)\text{-}(OCH_2CH_2)_n\text{-}OH$ (n between 9 and 10). A series of experiments presented previously in (I.), and reviewed in Sec. 4, established that at high concentrations of surfactant the interface was completely mobile. It was therefore concluded that for Triton X-100 the desorption rate was fast in comparison to the convective rate in those experiments, and that at high concentrations diffusion barriers are effectively removed by diminishing adsorption depths.

Two surface adsorbers are used as contaminants. The first is the protein bovine serum albumin (BSA). Several lines of evidence indicate BSA exhibits a slow desorption rate. First, proteins adsorbed onto interfaces usually denature (MacRitchie and Alexander (1962), Graham and Phillips (1978), Ter Minassian-Sarga (1980) and Guzman et al. (1986)), and this change in structure certainly hinders the desorption back into solution. Second, in regard to BSA, fundamental studies by Graham and Phillips (1978) using radiolabelling techniques established that at elevated

concentrations ($>10^{-3}$ wt percent) BSA begins to form multilayers, a development which would also act to slow the desorption rate. Finally more direct evidence comes from the recent studies by Carbonell *et al*. (1989) which established that radiolabelled BSA exchanges with an unlabelled bulk with a time constant of the order of hours.

The second adsorber used as a contaminant was the surfactant Brij-35, a polyethoxyether like Triton X-100, only with a structure $C_{12}H_{25}$-$(OCH_2CH_2)_{23}$-)-OH. Results of pressure drops on the three phase flow to be presented in Sec. 4 indicate that this surfactant retards surface flow at intermediate concentrations because of bulk diffusion gradients.

Both the Brij-35 and the Triton X-100 were used as obtained from Aldrich Chemical Co. The protein B.S.A., crystalllized and lyophillized, was used as obtained from Sigma Chemical Co.. The protein was dissolved in buffer solutions of sodium phosphate dibasic and potassium phosphate monobasic with a pH of 7.0 and an ionic stength of .16. The buffer, Hydrion dry buffer, was used as obtained from Micro-essential Laboratory, Inc. No preservative was added to the solutions, which were made fresh daily in order to avoid impurities and the degradation of the protein solutions. The water with which the aqueous solutions were made was purified using a Millipore water purificaton system with Organex filters to remove organic impurities.

In the first series of experiments, the concentration of B.S.A. in solution was held fixed at 10^{-4}weight percent. Two additional

B.S.A.-Triton-X 100 series are reported herein, with B.S.A.'s concentration held fixed at 10^{-2} and .1 weight percent. One series of experiments using Brij-35-Triton-X 100 solutions is also reported. The concentration of Brij-35 was held fixed at $5x10^{-3}$ weight percent, a concentration at which the ratio of the rate of diffusive to convective mass transport of Brij-35 through the sublayer to the bulk is much less than one, indicating that diffusive mass transfer of Brij-35 is rate limiting. In all four series of experiments, the concentration of Triton-X 100 was varied over several orders of magnitude from no added Triton-X 100 to 1 weight percent of the remobilizing surfactant.

4. Results and Discussion

For clarity of presentation and ease of comparison, the results are best cast in nondimensional form. The theoretical basis for the hydrodynamic analysis of the three phase flow is the unit cell consisting of an air-aqueous slug pair along with its surrounding oil film. A nondimensionalization of the governing equations and the boundary conditions for this cell is given in (I.). The resulting nondimensional groups which prescribe the flow can be divided into two sets. The first set includes nondimensional groups which are independent of surfactant effects; the second set includes those which describe the influence of surfactants. The surfactant independent groups are:

$$\kappa = \mu'_{(o)}/\mu'_{(a)} \qquad \chi = \rho'_{(o)}/\rho'_{(a)} \qquad Re = R'U'\rho'_{(a)}/\mu'_{(a)}$$

$$Ca_{(o/a)} = \mu'_{(o)}U'/\gamma'_{(o/a)} \qquad Ca_{(o/g)} = \mu'_{(o)}U'/\gamma'_{(o/g)}$$

$$Ca_{(a/g)} = \mu'_{(a)}U'/\gamma'_{(a/g)} \qquad Bo = (\rho'_{(o)} - \rho'_{(g)})g'R'^{2}/(\mu'_{(o)}U')$$

$$\lambda R' = (V'_{(g)} + V'_{(a)})/(\pi R'^{2}) \qquad \epsilon = V'_{(g)}/(V'_{(g)} + V'_{(a)})$$

$$\Omega = q'_{oil}/(\pi R'^{2}U')$$

In the above the superscripts (a), (g) and (o) identify properties of the aqueous, gas and oil phases, respectively. The spaces occupied by the oil, gas and aqueous phases in the unit cell are denoted by $V'_{(o)}$, $V'_{(g)}$ and $V'_{(a)}$, respectively, the oil induction rate is denoted by q'_{oil}, and the gravitational acceleration by g'. The variables μ' and ρ' denote viscosity and density, R' denotes the tube radius, and U' the train velocity. The clean interfacial tensions of the oil-aqueous, oil-gas and aqueous-gas surfaces are denoted by $\gamma'_{(o/a)}$, $\gamma'_{(o/g)}$ and $\gamma'_{(a/g)}$, respectively. The meanings of the dimensionless groups are clear; note in particular that the gas void fraction and aspect ratio of a unit cell is given by ϵ and λ, respectively, and the ratio of the volumetric flow rate of oil to the nominal aqueous flow rate is given by Ω. The values at which theses groups are fixed for each series of experiments are given in Table 1.

The surfactant related groups are, neglecting the adsorption at the aqueous-air interface which does not significantly influence the pressure drops realized:

$$Pe_{(i)} = U'R'/D'_{(i)} \qquad k_{(i)} = \beta'_{(i)}C'_{\infty_{(i)}}/\alpha'(i)$$

$$Ma_{(i)} = R'T'\Gamma'_{\infty_{(i)}}/(\mu'_{(o)}U')$$

$$\nu_{(i)} = \alpha'_{(i)}/(U'/R') \qquad \Phi_{(i)} = (D'_{(i)}\alpha'_{(i)})/(\beta'_{(i)}U'\Gamma'_{\infty_{(i)}})$$

where the subscript (i) indicates that such a group exists for each surface active agent dissolved in the source. In arriving at these dimensionless surfactant related groups for each of the surface active species in the flow, it was assumed that the surface adsorbers act independently in reducing the surface tension. With this assumption within the Langmuir formalism a modified Frumkin's equation can be developed for the oil-aqueous interfacial tension:

$$\gamma'_{(o/a)}(C'_{\infty(i)}) - \gamma'_{(o/a)} = \Sigma\, R'T'\Gamma'_{\infty(i)} \log\,(1-\Gamma'_{(i)}/\Gamma'_{\infty_{(i)}}) \qquad (3)$$

For each series of experiments, the pressure drop per unit cell is reported for each run. The pressure drop is nondimensionalized using a surface tension scaling of $\gamma'_{(o/a)}/R'$.

For the aqueous slugs of the three phase flow, the scaling of the ratio of the desorption rate to the convection rate through the perimeter perpendicular to the flow must be revised from that presented in the first section in order to account for the long aspect ratio of the slug. The correct scaling is $\alpha'\Gamma'_o R'^2\lambda(1-\epsilon)/(\Gamma'_o U'R')$. Surface active impurities will exert a drag opposing the flow if their kinetics of desorption are slow, or, if they have barriers to diffusive mass transport. In terms of the dimensionless

groups presented above, this is true if $\nu < 1$ or $\alpha'\Gamma_o'R'^2\lambda(1-\epsilon)/(\Gamma_o'U'R') < 1$ for the surface active agent. The purpose of the experiments is tc verify that interfaces stagnated by adsorbed surface active impurities become mobile when ν and $(\ell'/h')Pe^{-1/2}$ for the remobilizing surfactant are large. For remobilization the following conditions are required for the remobilizing surfactant:

$$\alpha'R'\lambda(1-\epsilon)/U' > 1$$

$$\Phi(1+k)Pe^{1/2} - Pe^{-1/2}(\ell'/h') > 1$$

where the adsorption depth condition has been rewritten in terms of the nondimensionalizations appearing above. The first condition is independent of concentration and only a characteristic of the surfactant. The second group increases with bulk concentration, and can be made to be much larger than one .

4.1 Mobile Interfaces in the Presence of Single Surfactant Adsorption

In the first part of this study, (I.), a series of experiments with solutions of Triton-X 100 in purified water as the aqueous slug phase were undertaken. In those experiments, as in the experiments to be discussed in this communication, the concentration of the Triton-X 100 solutions was varied through a range of concentrations where there are barriers to diffusive mass transport ($\Phi(1+k)Pe^{1/2}<1$) to concentrations for which these barriers have been eliminated ($\Phi(1+k)Pe^{1/2}>1$). Numerical values for the parameters necessary to evaluate $\Phi(1+k)Pe^{1/2}$ are found from the equilibrium adsorption

curve for Triton-X 100 (c.f. (I.)) to be $\beta'/\alpha' = 1.2 \times 10^{9} cm^3/gmol$ and $\Gamma'_{\infty} = 2.17 \times 10^{-10} gmol/cm^2$. The diffusion coefficient is inferred from the studies of Joos et al. (1979) and is taken to be $3.8 \times 10^{-6} cm^2/sec$.

The pressure drop per unit cell when plotted against $\Phi(1+k)Pe^{1/2}$ shows the following trends (see Fig. (2); the square and triangular data points indicate experiments run in .097 mm and .155 mm tubing, respectively). Throughout the concentration range where the ratio of the two rates of mass transport are between 6×10^{-5} and 3.5×10^{-2} the pressure drop required to drive the three phase slug flow increased monotonically. Within this concentration range barriers to diffusive mass transfer are important. As the bulk concentration of Triton-X 100 is increased throughout this range, more surfactant adsorbs and is distributed nonuniformly along the cylindrical slug interface, exerting a traction resisting the flow. As the bulk concentration of Triton-X 100 increases still further, through the range where $\Phi(1+k)Pe^{1/2}$ is increased from 3.5×10^{-2} to ≈ 2, the pressure drop decreases monotonically, attaining a pressure drop equal to that required to drive the three phase slug flow in the absence of added surfactant. Throughout this range, the barriers to diffusive mass transport of Triton-X 100 are disappearing, allowing the free exchange of Triton-X 100 between the bulk and the slug interface. Further increases in bulk concentration of Triton-X 100, for which the ratio of fluxes varies between 2 to 70 do not effect the pressure drop required to drive

the flow, as throughout this range, surfactant is exchanging freely between bulk and interface. These results indicate that Triton-X 100 has fast sorption kinetics, since if significant desorption barriers existed ($\nu<1$), remobilization of the aqueous-oil interface would not have been realized even in the absence of diffusion barriers.

Experiments with only Brij-35 dissolved in the aqueous phase indicate that the desorption rate of this surfactant is also fast. In Fig. (3) the nondimensional pressure drop per unit cell, nondimensionalized by surface tension scalings, is plotted as a function of increasing $\Phi(1+k)Pe^{1/2}$ for Brij-35. In evaluating the group $\Phi(1+k)Pe^{1/2}$ for Brij-35 , essentially a dimensionless concentration, the values for β'/α', Γ'_∞ and D' from the Triton-X 100 study are used as the sorption kinetics of these surfactants are similar. For $\Phi(1+k)Pe^{1/2}$ within the range of $5x10^{-5}$ to .14 , the pressure drop required to move the slug train at constant velocity increases with increasing $\Phi(1+k)Pe^{1/2}$, indicating that the Brij-35 is adsorbing along and accumulating at the trailing end of the aqueous-oil interface and acting to retard the flow. As $\Phi(1+k)Pe^{1/2}$ for Brij-35 is increased to values greater than .14, however, the pressure drop required to drive the flow decreases from its peak value, attaining a value close to that required to drive the clean flow for $\Phi(1+k)Pe^{1/2}$ larger than 10. As the barriers to diffusive mass transfer within the aqueous slug are eliminated, the surface of the aqueous slug moves as it would in the absence of surfactant, and

the pressure drop on the order of that required to drive the clean flow is recovered. Further increases in $\Phi(1+k)Pe^{1/2}$ cause no change in the pressure drop required to drive the flow, as the barriers to diffusive mass transfer have already been eliminated.

4.2 BSA- Triton-X 100 Competitive Adsorption Results

The three series of experiments in which mixtures of BSA, held at fixed concentration, and Triton-X 100, whose concentration was varied through a range of concentrations where barriers to diffusive mass transfer are important to concentrations where these barriers have been eliminated are reported in Fig. (4). Consider first the pressure drops required to drive the three phase slug flow with no Triton-X 100 present in the system. The nondimensional pressure drop per unit cell required to drive the buffer solution in the absence of any BSA or Triton-X 100 is .6. The slow desorber BSA acts to retard the surface velocity, increasing the drag opposing the flow. The pressure drop required to drive the flow in the presence of the stagnating adsorbed protein is significantly higher than the no added BSA flow: a pressure drop of 1.26 is required to drive the three phase slug flow with an aqueous concentration of 10^{-4} weight percent BSA, no Triton-X 100 present. A pressure drop of 1.56 is realized when the 10^{-3} weight percent BSA solution is used to form the aqueous slug, and a pressure drop of 1.9 is needed to drive the three phase flow when 10^{-1} weight percent BSA solutions are used to form the aqueous slug phase. These data points are the mantissa intercepts in Fig. (4).

As Triton-X 100 is added to the system at low concentrations, Triton-X-100 has barriers to diffusive mass transfer and acts to retard the aqueous -oil interface along with the BSA. Consider first the 10^{-4} weight percent BSA -Triton-X 100 results. As the concentration of Triton-X 100 is increased from zero, the pressure drop increases monotonically until,at $\Phi(1+k)Pe^{1/2}$ of $3.5x10^{-2}$ it attains some peak value. Within this range of $\Phi(1+k)Pe^{1/2}$ diffusive flux of Triton-X 100 is still rate limiting. Triton-X 100 is adsorbing along the aqueous-oil interface, establishing some nonuniform surface concentration. As the concentration of Triton-X 100 within this range is increased, the stagnating effect grows more pronounced. Increasing the concentration of Triton-X 100 increases the ratio of diffusive to surface convective mass transport rates, $\Phi(1+k)Pe^{1/2}$. When this group is within the range of .035 to 36, there is a monotonic decrease in pressure drop required to drive the flow. At $\Phi(1+k)Pe^{1/2}$ of 36 a pressure drop of .28 is reached , a pressure drop less than that required to drive the buffer solution in the absence of added surface active species.

The 10^{-3} weight percent BSA-Triton-X 100 series shows similar behavior, although the pressure drop required to drive the flow at this concentration of BSA initially remains constant with increasing Triton-X 100 concentration. The stagnating influence of BSA at this concentration is such that at the lowest bulk concentrations of Triton-X 100, there is not enough Triton-X 100 present to appreciably increase the surface retarding effect of the adsorbed protein molecules. As the ratio of diffusive to surface convective

fluxes is increased above $3.6x10^{-3}$ to 36, the same behavior as was found for the 10^{-4} weight percent BSA series is found. The pressure required to drive the flow first increases then decreases monotonically. At $\Phi(1+k)Pe^{1/2}$ of 36 the pressure drop required to drive the flow is .36, roughly equal to that required to drive the 10^{-4} weight percent BSA solution at this concentration of Triton-X 100.

Finally, the 10^{-1} weight percent BSA-Triton-X 100 series is also reported in Fig. (4). At this concentration, the equilibrium measurements of Graham and Phillips indicate that BSA forms multilayers under the protein molecules already adsorbed on the aqueous-oil interface. The surface velocity of the aqueous-oil interface should be completely stagnated under these conditions. The addition of another surface active agent in regimes where it should act to retard surface velocities should therefore have no effect. Between $\Phi(1+k)Pe^{1/2}$ of $3.5x10^{-2}$ and 36, however, as the Triton-X 100 comes to dominate the surface behavior of the system, the 10^{-1}weight percent BSA curve coincides with those of the other two BSA series experiments. The fast sorption kinetic surfactant Triton-X 100 was able to remobilize a completely stagnated interface by competitive adsorption.

4.3 Brij-35-Triton-X 100 Series Results

In a series of experiments, Brij-35 is used as a surface active "contaminant"; the concentration of Brij-35 was held fixed at $5x10^{-3}$

weight percent, the bulk concentration which coincides with the peak pressure drop required to drive the flow. Once again the concentration of Triton-X 100 is varied through a range in which barriers to diffusive mass transfer are important to concentrations at which these barriers have been eliminated. The data from this series of experiments is presented in Fig. (4). The abscissa in this graph is $\Phi(1+k)Pe^{1/2}$ for Triton-X 100.

As in the BSA series in which BSA was present at .1 weight percent, the interface of the aqueous slug is stagnated to such an extent that the addition of Triton-X 100 at concentrations where is should act to oppose the flow has no effect. For $\Phi(1+k)Pe^{1/2}$ between $6x10^{-5}$ and .035, therefore, the pressure drop required to drive the flow remains constant. As $\Phi(1+k)Pe^{1/2}$ is increased above this value, however, through the range of .035 to 3.55, the pressure drop required to drive the three phase slug flow with Brij-35-Triton-X 100 solutions comprising the aqueous phase decreases to the pressure drop required to drive the clean flow.

5. Conclusions and Applications

In this communication, data which indicates that a surfactant which exchanges rapidly between the bulk and the interface can remobilize the interface of a fluid particle flow which has been stagnated due to the presence of a surface active contaminant is presented. Remobilization was demonstrated using a three phase slug flow in which the changes in the mobility of the aqueous-fluorocarbon oil interface significantly affected the pressure drop

required to drive the slug train at a constant velocity. Two surface active agents were used as surface active "contaminants": the protein BSA, which has slow desorption kinetics and the commercial surfactant Brij-35, which has fast sorption kinetics but can act to hinder surface velocities if it is present at concentrations where barriers to its diffusive mass transport exist. The remobilizing surfactant was Triton-X 100. In all series of experiments reported, when the barriers to diffusive mass transport for Triton-X 100 were eliminated, the pressure drop required to drive the three phase slug flow was reduced to the value required to drive the flow in the absence of surface active agents. Regardless of the exchange barriers of the retarding surface active impurity, then, competitive adsorption can remobilize the stagnated interfaces in fluid particle flows, allowing them to behave hydrodynamically as they would in the absence of adsorbed surface active agents.

The concepts demonstrated here have implications in many technologies, both established and emerging. Some examples are discussed below.

In general, the presence of surface active contaminants in fluid particle flows acts to hinder surface velocity, and therefore, in the case of constant driving forces, particle velocity. In microgravity environments, the removal of gas bubbles from solution by application of a temperature gradient can be significantly hindered by the presence of surface active impurities (c.f. Kim and Subramaniam (1989)) because the thermocapillary force is on the same order of magnitude as the Marangoni force due to gradients in surface concentration. Competitive adsorption of surfactants that

exchange quickly between the interface and the bulk in microgravity environments would allow the expedient removal of gas bubbles or liquid drop impurities.

The rate of drainage of thin films is hindered by surface active impurities. The competitive adsorption of a fast sorption kinetic surfactant speeds the draining of such films by allowing the surface of the film to move as if no adsorbed surfactant were present. As lifetimes of foams and emulsions is dependent on the rate at which the films which form between the dispersed phase drain, the competitive adsorption result is of interest in the control of the lifetimes of foams and emulsions. Accelerating the rate of drainage of a thin film hindered by surface active contaminants also enhances the attatchment of bubbles to ore particles in froth flotation.

In liquid-liquid displacements, as in tertiary oil recovery where water is forced through oil filled pores, and in the transport of foams through porous media, the remobilization of interfaces has application. (c.f. Barthes-Biesel et al. (1987), Ratulowski and Chang (1989), Ginley and Radke (1989), Schwartz et al. (1986), and Gauglitz and Radke (1986)). If the surface velocity of the displacing phase in liquid-liquid extraction is stagnated, the shearing in the wetting phase will lead to a thickening of the annular film formed by the wetting phase around the displacing phase. This increase in film thickness leads to a decrease is the efficiency with which the wetting phase is displaced from the pore. Alternatively, however, the increased resistance lends mobility

control to the displacing phase, and thus remobilization may be used to obtain a suitable balance.

In interphase mass transfer, in which a liquid or gas is bubbled through a continuous phase in order to remove a solute from either phase, the efficient contacting of the two fluids is of great importance. In the event that surface active impurities are present, the surface velocity of the droplets will be hindered. The vortices in the droplots, when viewed in the frame moving with the drop velocity will be shifted forward, leading to less effective contacting of the two fluids (c.f. Beitel and Heideger (1971)). The remobilization of this interface should lead to a more efficient contacting of the two phases, enhancing mass transfer as long as the increased resistance due to the uniform coverage of fast sorption kinetic surfactant is less than the resistance due to shifted vortices in the hindered flow case.

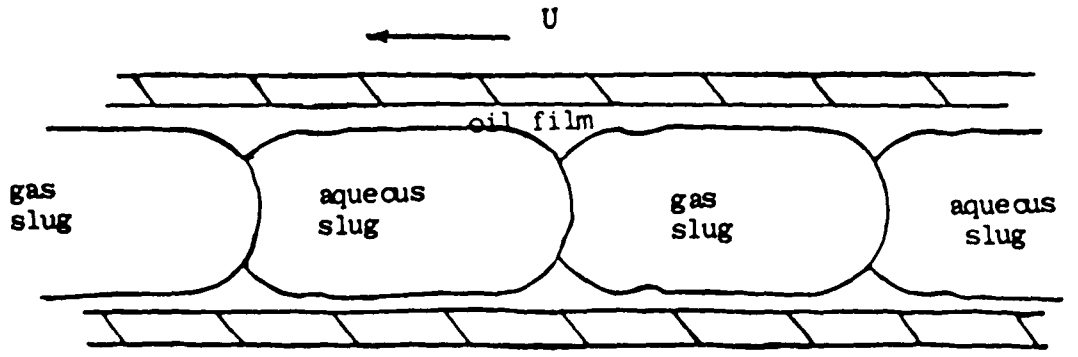

FIGURE 1.

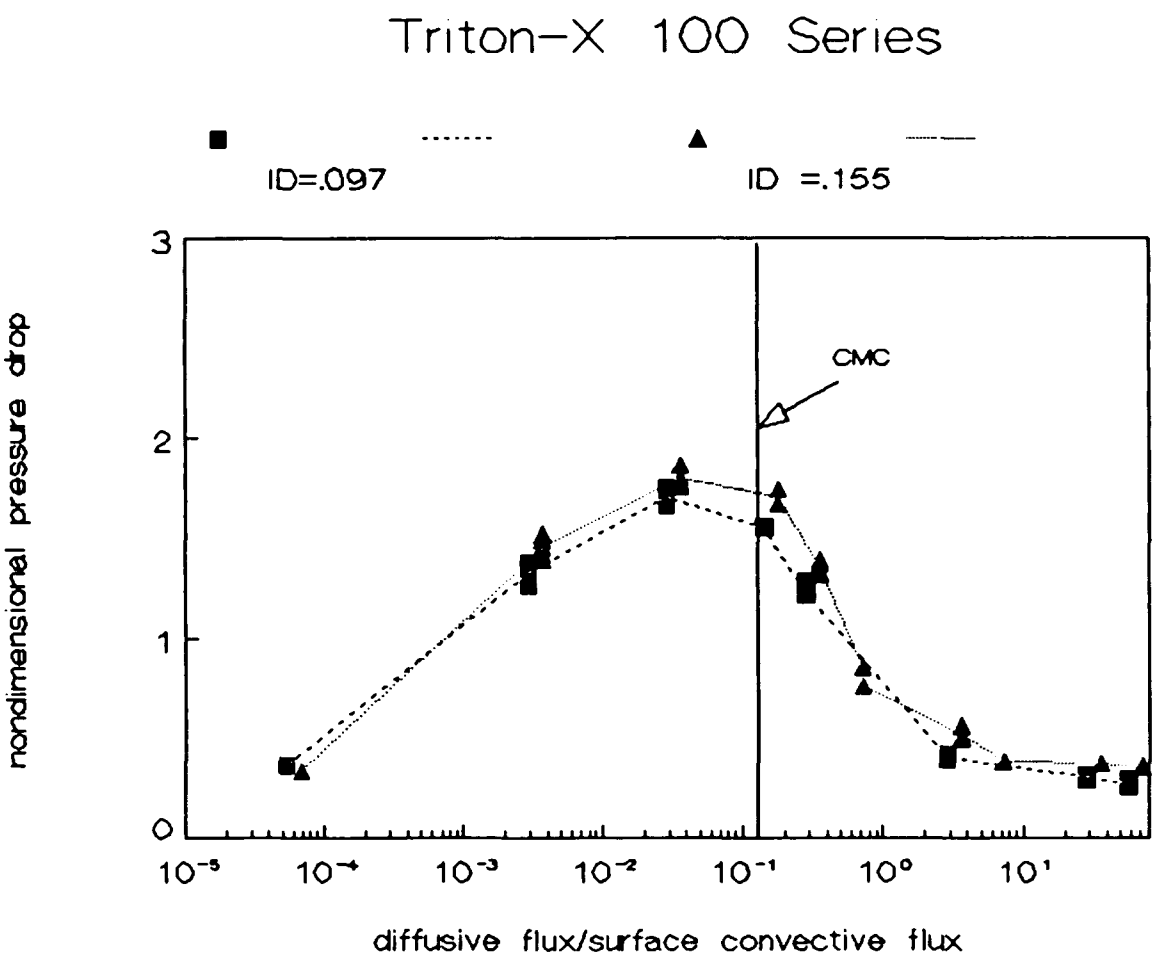
Triton-X 100 Series
ID=.097
ID =.155
CMC
nondimensional pressure drop
diffusive flux/surface convective flux
0
1
2
3
10^{-5}
10^{-4}
10^{-3}
10^{-2}
10^{-1}
10^{0}
10^{1}

FIGURE 2.

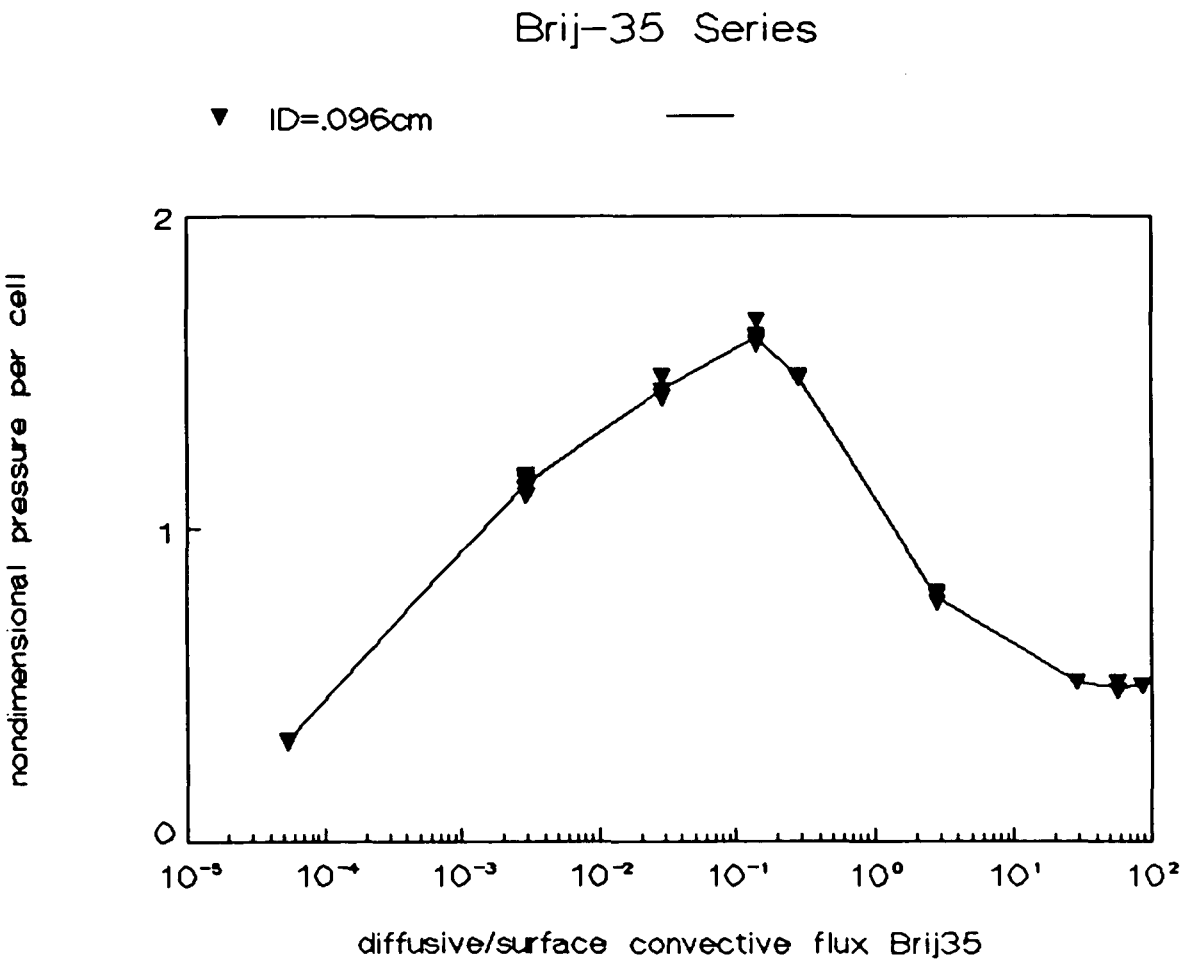
Brij-35 Series
▼ ID=.096cm
nondimensional pressure per cell
2
1
0
10^{-5}
10^{-4}
10^{-3}
10^{-2}
10^{-1}
10^{0}
10^{1}
10^{2}
diffusive/surface convective flux Brij35

FIGURE 3.

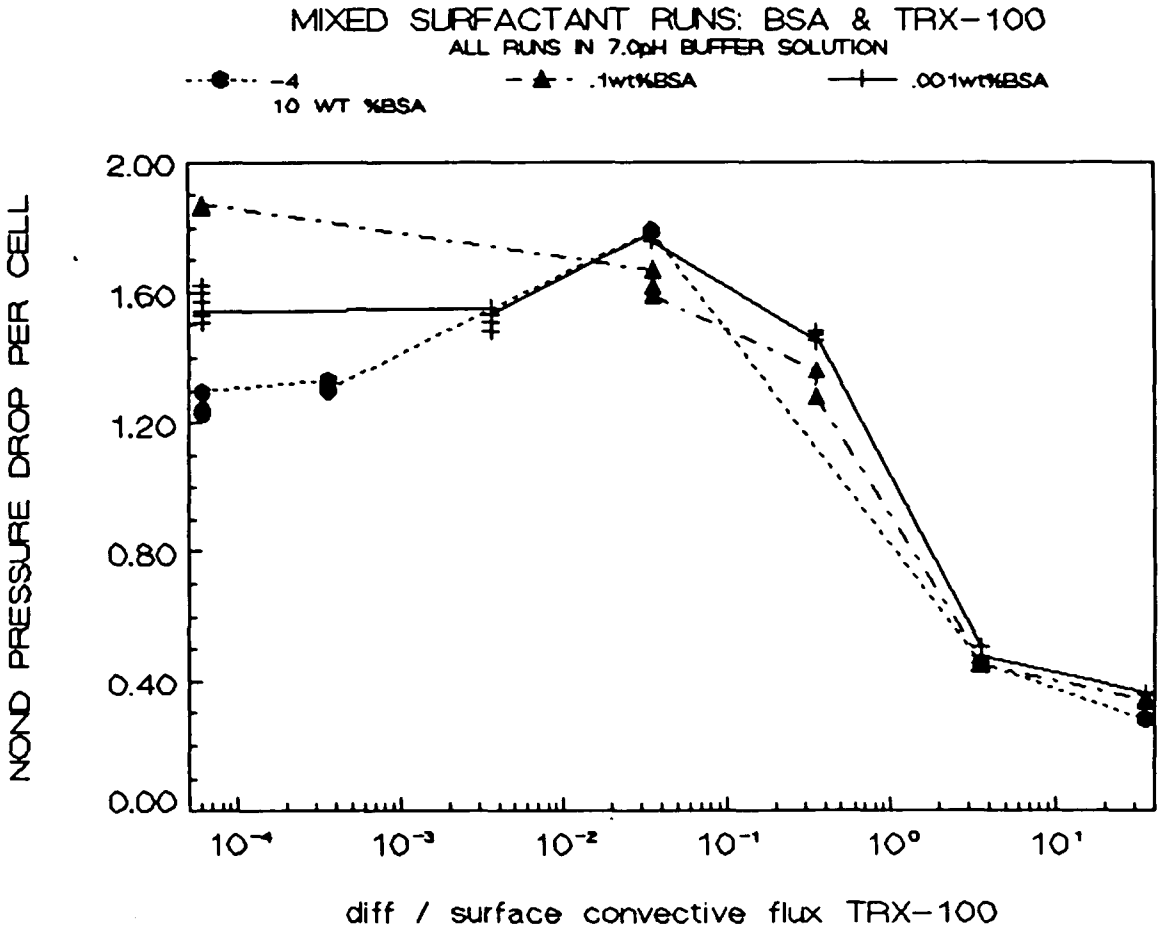
MIXED SURFACTANT RUNS: BSA & TRX-100
ALL RUNS IN 7.0pH BUFFER SOLUTION
-4
10 WT %BSA
.1wt%BSA
.001wt%BSA
NOND PRESSURE DROP PER CELL
2.00
1.60
1.20
0.80
0.40
0.00
10^{-4}
10^{-3}
10^{-2}
10^{-1}
10^{0}
10^{1}
diff / surface convective flux TRX-100

FIGURE 4.

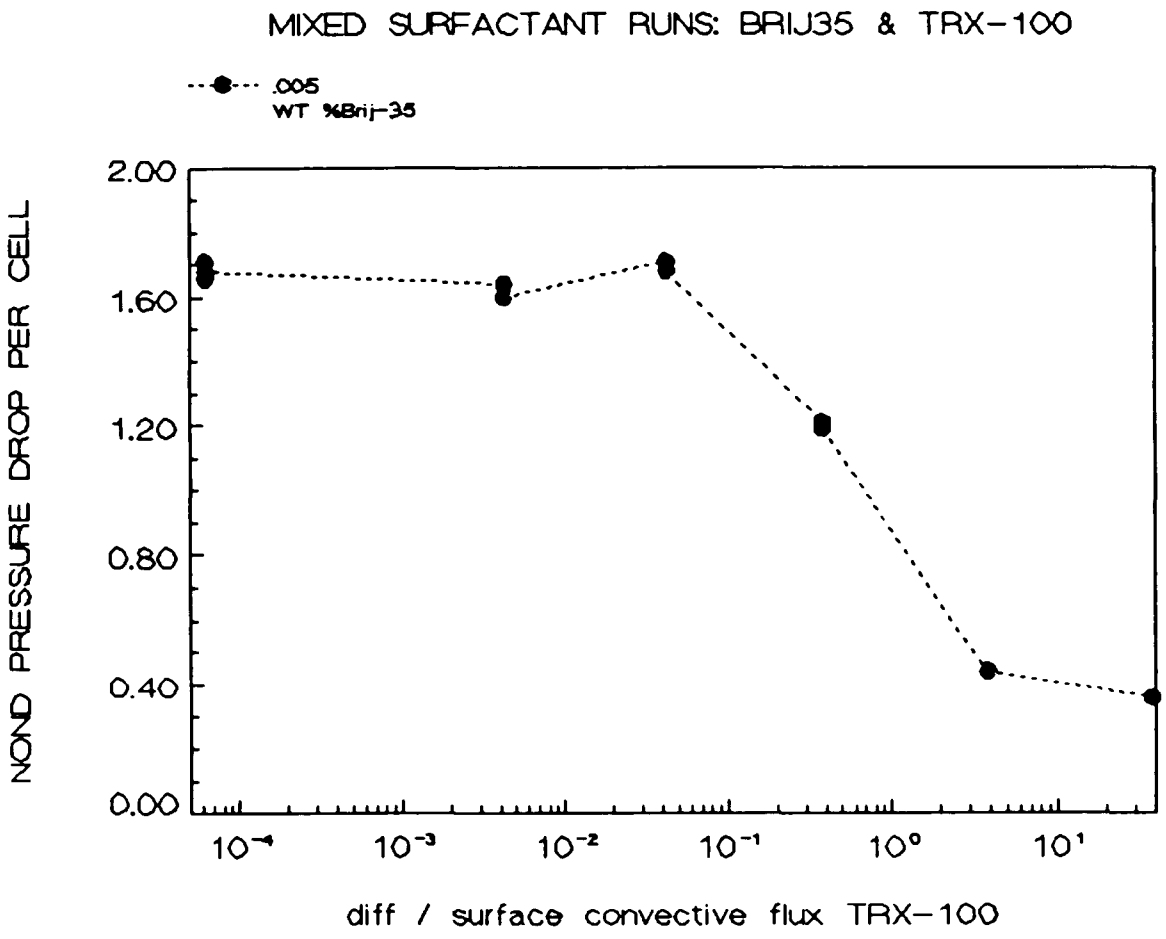
MIXED SURFACTANT RUNS: BRIJ35 & TRX-100
.005
WT %Brij-35
NOND PRESSURE DROP PER CELL
2.00
1.60
1.20
0.80
0.40
0.00
10^{-4}
10^{-3}
10^{-2}
10^{-1}
10^{0}
10^{1}
diff / surface convective flux TRX-100

FIGURE 5.

Table 1

Surfactant Independent Dimensionless Groups

		BSA-TRX 10^{-4}WT% BSA	BSA-TRX 10^{-3}WT% BSA	BSA-TRX 10^{-1}WT% BSA	BRIJ-TRX $5x10^{-3}$WT% BRIJ-35
void fraction	ϵ	.43	.44	.44	.43
aspect ratio	λ	82	82.1	81	84
viscosity ratio	κ	5.9	5.9	5.9	5.9
oil:aqueous flow rate	Ω	.0033	.0032	.0033	.0033

Capillary numbers (held fixed for all experiments)

oil-aqueous: $Ca_{(o/a)} = 1.02x10^{-3}$

oil-gas: $Ca_{(o/g)} = 3.80x10^{-3}$

aqueous-gas: $Ca_{(a/g)} = 1.42x10^{-4}$

Chapter 4

Scope of Future Research

1. Measurement of Wetting Layer Thicknesses

A technique has been developed for the accurate, noninvasive measurement of the film formed by the wetting phase in slug flows. The method of measurement is applicable to films which are on the order of a few percent or larger of the tube radius. The method entails using absorbance data and the Beer-Lambert law for finding the path length of a beam of monochromatic light. Measurement of the film thickness performed in previous studies used volume displacement methods (cf. Fairbrother and Stubbs (1935), Taylor (1961) and Cox (1962)), or the measurement of the changing length of an aqueous slug as it passed through an initially dry capillary tube (cf. Bretherton (1961) and Schwartz et al. (1986)). Other investigators have measured wetting layer thicknesses by measuring changes in resistivity due to the wetting layer left on a capillary tube wall by a passing slug of electrolytic solution (cf. Marchessault and Mason (1960) and Chen (1986)). The direct measurement of film thickness from magnified photographs of the capillary tube, a method used by Goldsmith and Mason (1963) for slug flows at large capillary numbers, is applicable only to films which are of $O(100\mu)$ or larger. The volume displacement and changing aqueous slug length methods for establishing the film thickness are cumbersome. The resistivity method works well for film thicknesses large enough that grooves and irregularities in the glass capillary

tube used have a negligible effect on the conductivity changes observed in the absence and then presence of the wetting layer; however, this method is applicable only to wetting layers formed by electrolytic solutions.

The absorbance method for measuring wetting layers described herein is applicable to slug flows in capillary tubes which transmit light. The slug phase and wetting layer must have approximately the same index of refraction so that the impinging light beam is not appreciably bent as it passes from one phase to another.

2. The Absorbance Method for Measuring Wetting Layers

The absorbance method for measuring the wetting layer left by the continuous phase in slug flows in capillary tubes relies on the repeated use of the Beer-Lambert law. A solute is dissolved in either the continuous (wetting) phase or in the slug phase. In the expressions for the film thickness derived below, it is assumed that the solute is present only in the slug phase. Similar expressions can be derived if the solute is dissolved only in the wetting phase.

Consider a capillary tube filled with the slug phase fluid. From the Beer-Lambert law the absorbance of monochromatic light across this tube is given by:

$$\log (I'_{sl}/I'_i)=\epsilon'_{sl}D' \qquad (2.1)$$

where I'_i is the intensity of the light which impinges on the fluid within the tube; I'_{sl} is the intensity of the light after it has

passed through the slug fluid, ϵ'_{sl} is the extinction coefficient in the slug phase and D' is the tube diameter.

The absorbance across a capillary tube filled with the slug phase in which solute at concentration C' has been dissolved is given by :

$$\log (I'^{*}_{sl}/I'_{i}) = \epsilon'_{sl} D' + \epsilon'_{d} C' D' \qquad (2.2)$$

where I'^{*}_{sl} is the intensity of the light after it has passed through the solution, and ϵ'_{d} is the extinction coefficient due to the solute dissolved in the slug phase .

The absorbance of light across a tube containing the slug fluid surrounded by an annular film of thickness h' formed by the wetting phase with no solute present in the slug phase is given by:

$$\log(I'_{slf}/I'_{i}) = \epsilon'_{f} 2h' + \epsilon'_{sl}(1-2h'/D')D' \qquad (2.3)$$

while the absorbance of this system with the slug phase containing solute at concentration C' is:

$$\log(I'^{*}_{slf}/I'_{i}) = \epsilon'_{f} 2h' + \epsilon'_{sl}(1-2h'/D')D' + \epsilon'_{d} C'(1-2h'/D')D' \qquad (2.4)$$

where the intensity of the light after passing through the system is I'^{*}_{slf}. In equations (2.3) and (2.4) ϵ'_{f} is the extinction coefficient of the film formed by the wetting phase.

From equations (2.1)-(2.4) the following expressions can be obtained:

$$\log(I'^{*}_{sl}/I'_{sl}) = \epsilon'_d C' D' \qquad \text{(i)}$$

$$\log(I'^{*}_{slf}/I'_{slf}) = \epsilon'_d (1-2h'/D') D' C' \qquad \text{(ii)} \qquad (2.5)$$

$$\log(I'^{*}_{slf}/I'^{*}_{sl}) = 2h'(\epsilon'_f - \epsilon'_{sl}) - \epsilon'_d C' 2h' \qquad \text{(iii)}$$

Using these expressions, the film thickness of the wetting phase in a capillary tube of known inner diameter can be obtained and checked graphically. The absorbance across the tube containing only the slug phase is measured. A series of absorbance measurements across the tube filled with a solution of the slug fluid and solute at varying concentration are obtained. The absorbance of the pure slug fluid is subtracted from the absorbance at each concentration. A graph of these differences plotted against concentration should be linear with slope $\epsilon'_d D'$, according to equation 2.5(i).

The absorbance of the pure slug phase in a tube in which the wetting layer has been established is then measured. Again, a series of absorbance measurements across the tube containing a solution of the slug fluid and solute at varying concentration are made, this time in the tube containing the wetting layer as well. The difference of the absorbance at each concentration and the absorbance in the absence of solute, both in the presence the wetting layer, when graphed against the concentration of solute

should again be linear, this time with slope $(1-2h'/D')D'\epsilon'_d$. (cf. equation 2.5(ii)). Using the extinction coefficient found from the graphical solution of equation 2.5(i), the film thickness h' can be found from this slope.

In order to graphically evaluate equation 2.5(iii), the absorbance of the slug fluid solutions in the absence of the wetting layer are subtracted from the absorbances of the solutions with the film present at each concentration. These values should also be linear in C', with a slope of $-2h'\epsilon'_d$. The film thickness obtained from this slope should agree with that obtained from 2.5(ii), providing an internal check for the reliability of each measurement.

3. Materials and Methods

The absorbance method for measuring the wetting layer left by the continuous phase in slug flows has been used to measure the thickness of the annular fluorocarbon oil film which wets the inner wall of a teflon capillary tube in a three phase capillary slug flow. The flow consists of a train of alternating air and aqueous segments which are drawn through a teflon tube whose inner wall is encoated with a fluorocarbon oil film. The flow is periodic, with an air-aqueous slug pair and its surrounding fluorocarbon oil film being treated as a unit cell. The aspect ratio of the unit cell, $2L'/D'$, was held fixed at 85, and the void fraction $(V'_{(g)}/(V'_{(a)}+V'_{(g)}))$ was held fixed at .4. In these expressions L' is the length of a unit cell; D' is the inner diameter of the capillary tube. The volumes of the gas and aqueous phases are denoted by $V'_{(g)}$

and $V'_{(a)}$ respectively. The flow was driven at constant velocity of 1.15cm/sec by the action of a peristaltic pump. The oil was introduced at a low, constant rate of $.23cm^3/hr$. The average thickness of the annular oil film around the aqueous slug was measured. The thickness of the film around the air slug could not be resolved as the light was scattered by the gas phase.

The three phase slug flow is established at the upstream end of the system and drawn under suction through the test section. The test section consists of a length of precision drawn teflon capillary tubing (Technicon, ID=.159cm) which is threaded through a flow cell in a UV photometer (Knauer Inc.). The downstream end of the teflon tubing is attatched to a peristaltic pump (LKB Productor), which drives the flow at a constant velocity under suction. The average velocity of a unit cell is monitorred using a pair of LED emmiter-detectors at either end of the teflon test section.

The flow cell in the UV photometer through which the teflon capillary tube is threaded is designed so that the tubing is centered in the path of a beam of monochromatic light. The light beam passes through a small slit (of $O(100\mu)$) and passes through a full diameter of the tube before passing through a second slit of the same dimensions and impinging on the photodiode. The wavelength of the light used in the experiments reported herein was 253nm.

Aqueous solutions of .001N perchloric acid were used to form the aqueous phase. Potassium dichromate was used as the solute, and dissolved in various concentrations in the acidic solvent. This solution was chosen because its spectral properties are well

documented (cf. Burke and Mavrodineanu) and the solute does not dissolve appreciably in the fluorocarbon oil used to form the wetting phase (FC-70). Absorbance data taken by scanning spectrophotometry of FC-70 saturated with $K_2Cr_2O_7$ blanked against FC-70 in the absence of solute shows a strong peak at 216nm, and only slight absorbance over the other wavelengths scanned including 253nm, the wavelength of the light used in these experiments . This represents the worst case, as it is of oil which is saturated with potassium dichromate. In this series of experiments, the oil comes in contact with relatively dilute solutions of $K_2Cr_2O_7$, which adsorb strongly at 253nm.

The perchloric acid and potassium dichromate were used as obtained from Aldrich Chemical Co. The water used to make to aqueous solutions was purified using a Millipore water filtration system with Organex filters to remove organic impurities. Solutions of $K_2Cr_2O_7$ in .001N perchloric acid at concentrations from 0 to 500 mg/kg solution were used to form the aqueous phase.

For each film thickness measurement a clean length of teflon tubing was threaded into the flow cell. The absorbance in the absence of an oil film of .001N perchloric acid solution along with a series of absorbance measurements at varying concentrations of solute in the aqueous solution were taken. After the three phase slug flow was established through the system and allowed to come to steady state, each of the absorbance measurements was repeated in the presence of the annular oil film. The appropriate differences in absorbances were taken so that equations (2.5 i-iii) apply; from

best fit of the lines of these absorbance ratios plotted against concentration, the film thickness for that slug flow was found.

4. Results

Four film thickness measurements are reported herein. The first three measurements are of the annular oil film surrounding the aqueous slug in the three phase slug flow, the aqueous phase consisting of .001N perchloric acid solutions of varying concentration of $K_2Cr_2O_7$. The fourth film thickness reported is the thickness of the fluorocarbon oil film around the aqueous phase in which the surfactant Triton-X 100 has been dissolved at a bulk concentration of 10^{-3} weight percent. At this bulk concentration barriers exist to the diffusive transport of Triton-X 100 through the sublayer to the aqueous-oil interface to the bulk. Triton-X 100 adsorbs along the cylindrical aqueous-oil interface and collects near the converging stagnation ring at the trailing end of the slug. Surface tension gradients along the length of the aqueous slug result due to the gradients in surface concentration; these gradients in surface tension exert a stress which opposes the surface velocity. Since the velocity of the flow is kept constant, this results in an increased shear in the thin oil film. This change in the system's hydrodynamics should result in a different annular oil film thickness than that in the absence of surfactant.

4.1 Film Thickness Around an Aqueous Slug with No Surfactant

The average film thickness of the wetting layer around an aqueous slug in the three phase slug flow was measured using the

absorbance method. The extinction coefficient ϵ'_d of the solute potassium dichromate in the aqueous phase was found to be 14.93 and 14.95 $(g\ cm/kg)^{-1}$ (see Figs (1a) and (1b)). The difference in the absorbances of the dichromate solutions at each concentration and the absorbance of the .001N perchloric acid solvent , both in the presence of the wetting phase, were plotted against concentration. From the slope of this line, values for the film thickness were found (see Figs(2a,b,c). For two of the three data runs reported herein, the absorbance of the dichromate solutions in the absence of the wetting layer was subtracted from the absorbance of the dichromate solutions in the presence of the wetting layer at each concentration. The slope of that data when plotted against concentration provides a check for the film thickness. (see Fig.3a and 3b). The third data set reported was run on the same tube used for the second run. The same extinction coefficient was used for Run 3 as was used for Run 2. Since the wetting layer is not easily removed from the wall of the tubing, it was not possible to obtain the absorbance of the film-free tube for that run, and no check for the film thickness was computed. The data is presented in Table 1.

4.2 Film Thickness Around an Aqueous Slug with Surfactant

The film thickness measured around the aqueous slug containing the surfactant Triton-X 100 was found by the same procedure as described above. The extinction coefficient was found from the absorbances of the potassium dichromate solutions and the absorbance of the solute free perchloric acid in the absence of an oil film. The three phase slug flow was established in the test section and

the film thickness allowed to reach a steady value. The absorbance of the perchloric acid solution and the absorbance of the solute containing aqueous solutions were all taken in the presence of the wetting layer. This body of data allowed the evaluation of the thickness of the wetting layer from both equation 2.5(ii) and 2.5(iii), providing a check for the reliability of the data reported. The extinction coefficient graph is given in Fig.(4). The value of the extinction coefficient is found to be 14.4(g cm/kg)$^{-1}$, in good agreement with the data in Table 1. The film thickness h' was found to be 15.1μ around the surfactant containing aqueous slug from equation 2.5(ii) (see Fig(5a)) and h'_{check} is found to be 18.5μ from equation (2.5iii). (see Fig. (5b))

4.3 Discussion

Most previous studies of wetting layers in slug flows have studied the wetting layer left by a continuous phase in a two phase slug flow. Using a matched asymptotic expansion, Bretherton (1961) and later Park and Homsy (1984) showed that the thickness of a wetting layer around an inviscid semi-infinite slug is $h'_B/R' = 1.337(Ca)^{2/3}$ where R' is the tube radius (.078cm) and Ca, the capillary number is $\mu'_w U'/\sigma'$, where μ'_w is the viscosity of the wetting phase, U' is the slug velocity and σ' is the surface tension at the interface. The interfacial tension of the fluorocarbon-oil interface is $\approx$ 60 dynes/cm, the viscosity of the oil used is $\approx$ 50cp. Using these values in the Bretherton formula, the predicted film thickness is found to be 48μ, on the same order as the surfactant

free results reported herein, but greater presumably because of the oil rate constraint in the three phase flow. The implications of the volumetric constraints on the behavior of the wetting layer in the presence of adsorbed surfactant are explained below.

Consider the volumetric flow rate of oil in the reference frame which moves with the unit cell velocity, q'_{lk}:

$$q'_{lk}=-q'_{oil}+\pi\int_0^{L'}(R'^2-w'^2(z))dz/T' \qquad (2.6)$$

where q'_{oil} is the rate at which oil is introduced in the laboratory frame, L' is the length of a unit cell, and R' the tube radius. The radial location of the oil interface is given by w'(z), where z is the axial coordinate along the length of a unit cell in the frame which moves with the slug velocity. The time required for a unit cell to pass a fixed point in the lab frame is T'=L'/U', U' being the slug velocity. The integral term gives the volume of oil which surrounds an aqueous -oil slug pair. In the three phase slug flow , q'_{oil} is held constant. As surfactant adsorbs along the aqueous-oil interface in the three phase flow, viscous shearing in the oil film increases due to the tractions which develop along the interface opposing the flow. The oil which moves along with the wall in the frame moving with the slug velocity, q'_{lk}, decreases. Since q'_{oil} is held fixed, the amount of oil surrounding a unit cell divided by the time required for it to pass must also decrease according to equation (2.6). The radius and slug velocity are held fixed in these experiments. In order for this term to decrease, either the cell must elongate or the annular film must thin. The decrease in

the thickness of the wetting layer when surfactants are present can be understood in this context.

5. Proposed Study of Two Phase Slug Flows

Most prior research on capillary slug flows focussed on two phase slug flows. As yet no complete study of the effect of surfactant adsorption in such flows has been completed. It is proposed to study the effect of surfactant adsorption in such flows, with surfactant present in the continuous phase. The behavior of a two phase slug flow with surfactant dissolved in the wetting phase should differ from the three phase slug flow reported here in two respects. Since the surfactant is in the film phase, the additional resistance to mass transfer due to the thinness of the wetting layer must be included. The hydrodynamic behavior in the presence of adsorbed surfactant should also differ as there is no scarcity of the wetting phase. The film formed by the wetting layer is free to increase to relieve viscous shearing in the thin film region as tractions along the interface develop. It is expected then that the film thicknesses realized in the presence of adsorbed surfactant in the regimes where desorption or bulk diffusion is rate limiting would be greater than those realized in the absence of surfactant, in contrast to the reduction in film thicknesses realized in the three phase slug flow due to surfactant adsorption. The pressure drops realized in the two phase slug flows should be less than those realized in the three phase slug flow as the thickening of the wetting layer in the two phase flow reduces the shear in the film region.

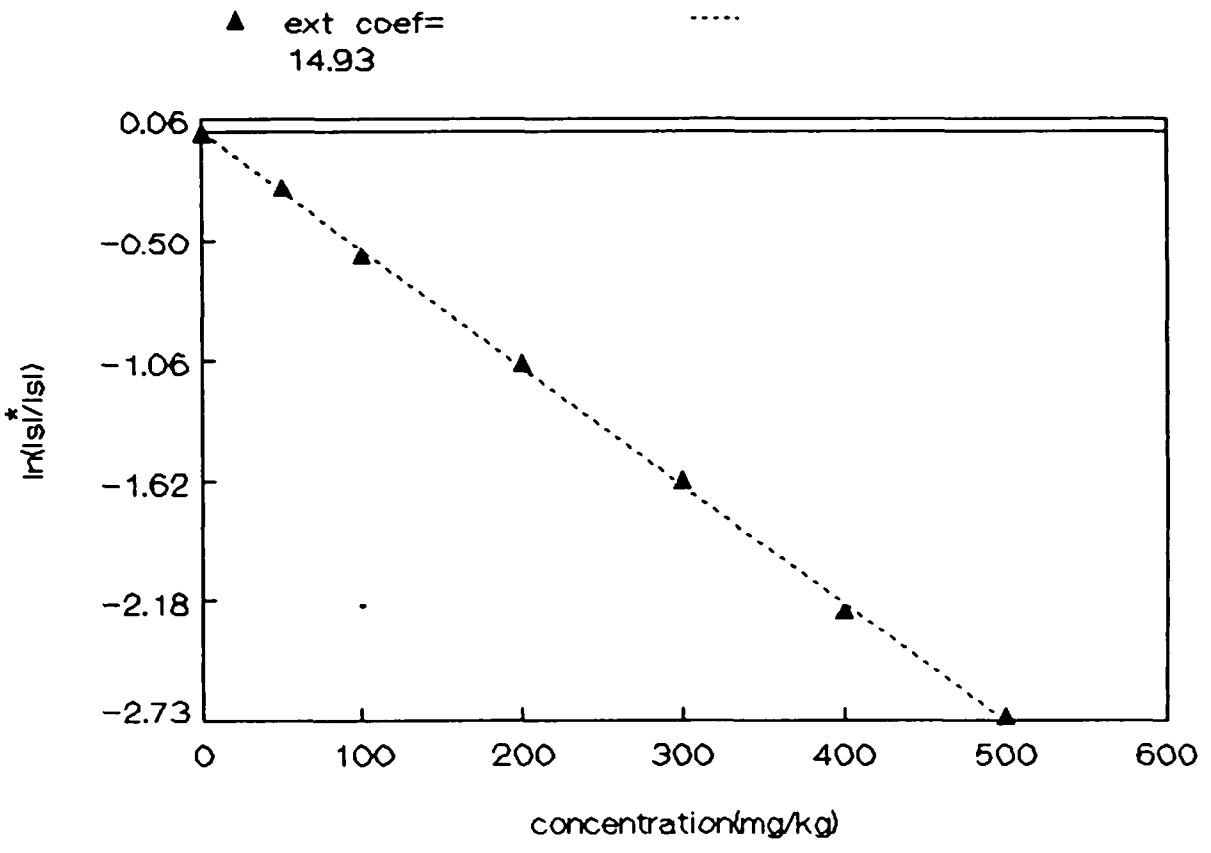
extinction coefficient Run1
ext coef=
14.93
0.06
-0.50
-1.06
-1.62
-2.18
-2.73
ln(Isl*/Isl)
0
100
200
300
400
500
600
concentration(mg/kg)

FIGURE 1A

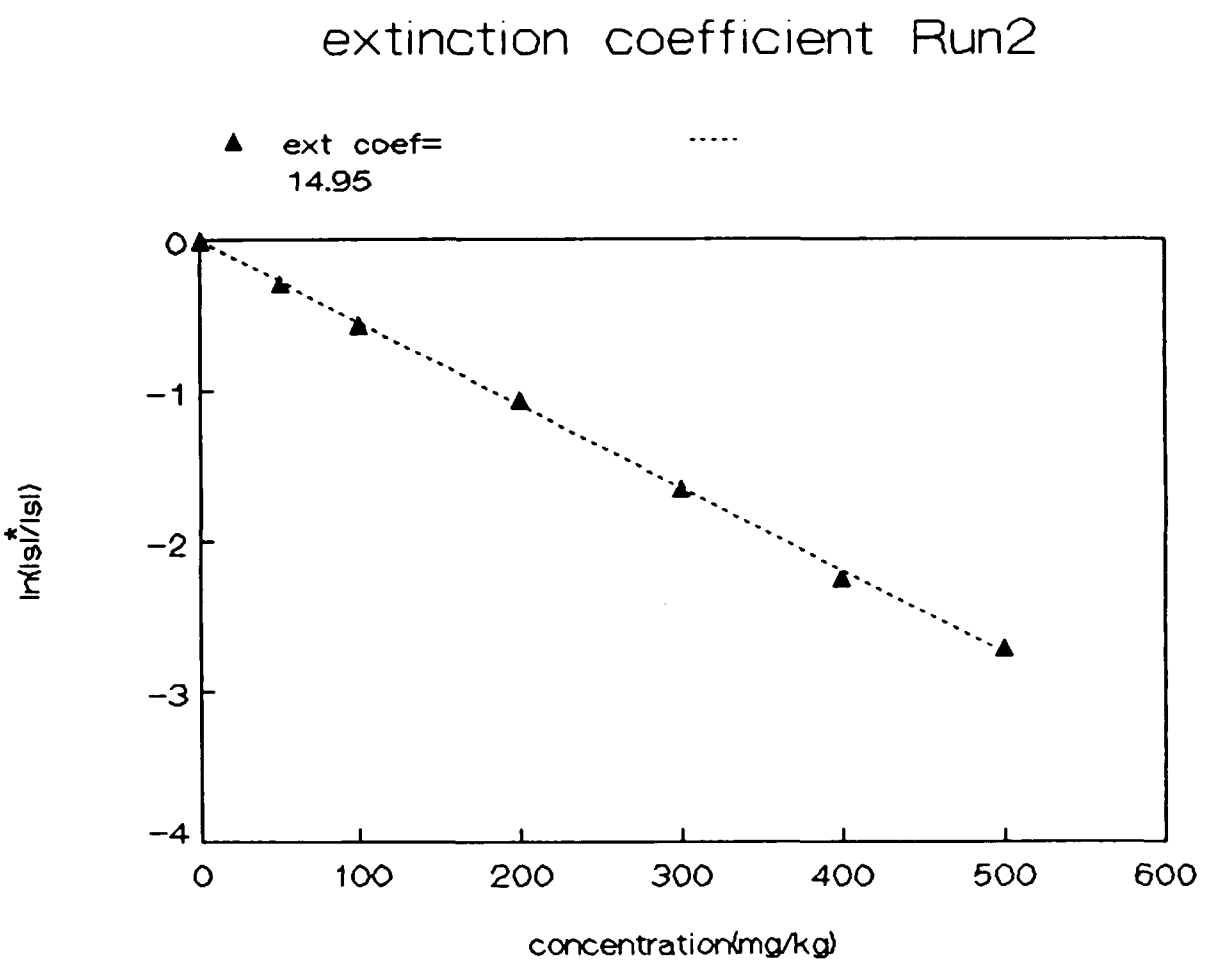
extinction coefficient Run2
ext coef=
14.95
0
-1
-2
-3
-4
0
100
200
300
400
500
600
ln(Is*I/IsI)
concentration(mg/kg)

FIGURE 1B

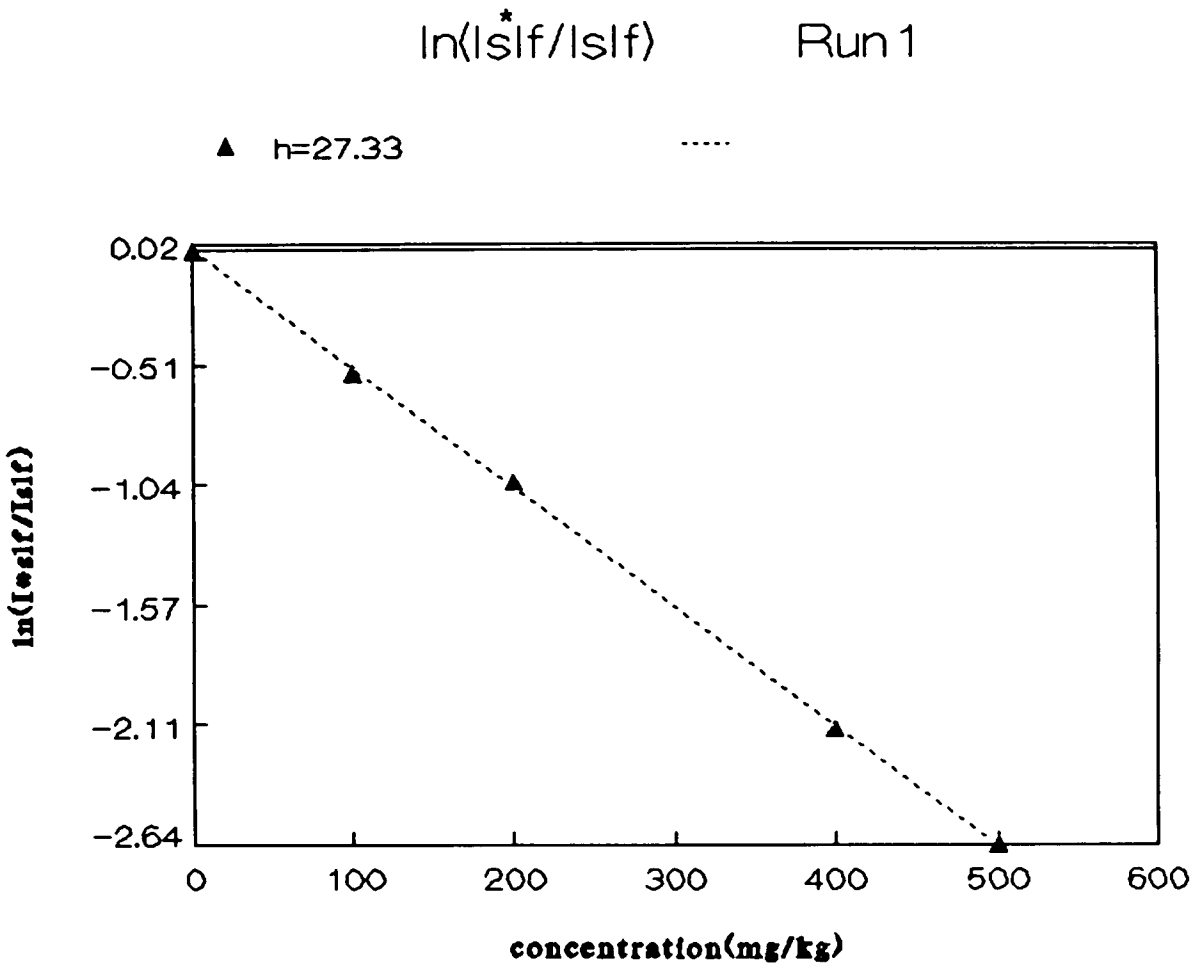
ln(Is*If/IsIf) Run 1
h=27.33
0.02
-0.51
-1.04
-1.57
-2.11
-2.64
ln(Is*If/IsIf)
0
100
200
300
400
500
600
concentration(mg/kg)

FIGURE 2A

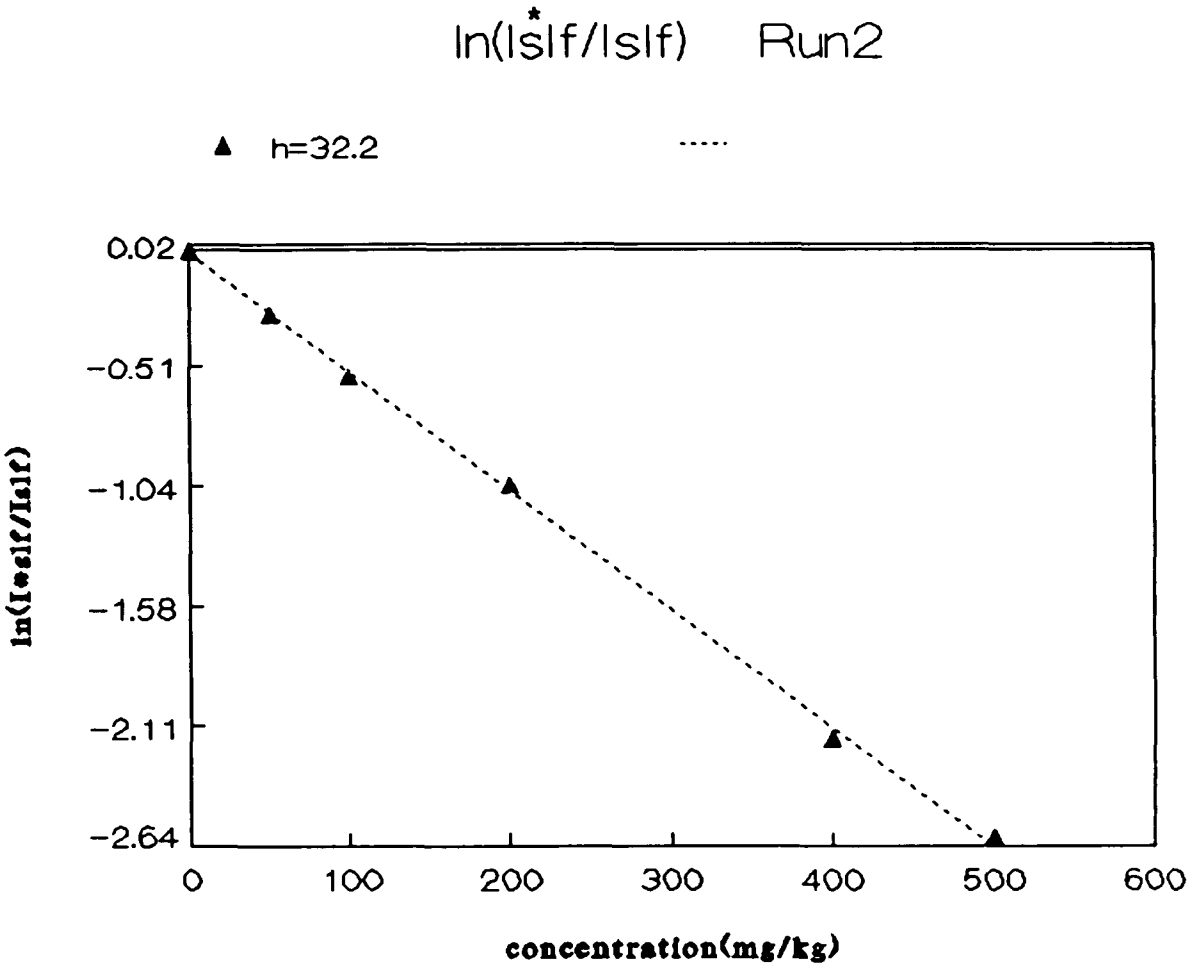
ln(Is*If/IsIf) Run2
h=32.2
0.02
-0.51
-1.04
-1.58
-2.11
-2.64
ln(Is*If/IsIf)
0
100
200
300
400
500
600
concentration(mg/kg)

FIGURE 2B

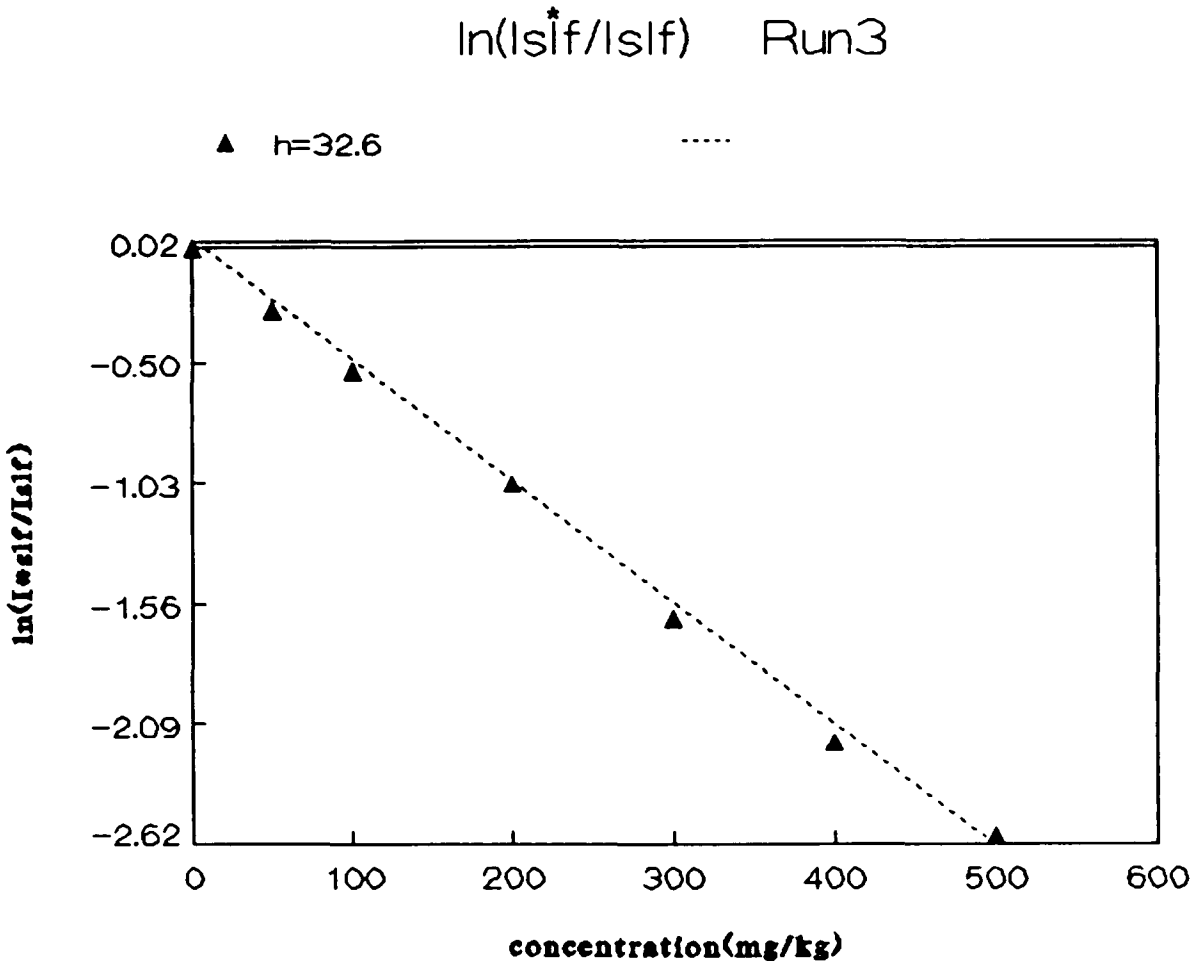
ln(Is*f/Isf) Run3
h=32.6
0.02
-0.50
-1.03
-1.56
-2.09
-2.62
ln(Is*f/Isf)
0
100
200
300
400
500
600
concentration(mg/kg)

FIGURE 2C

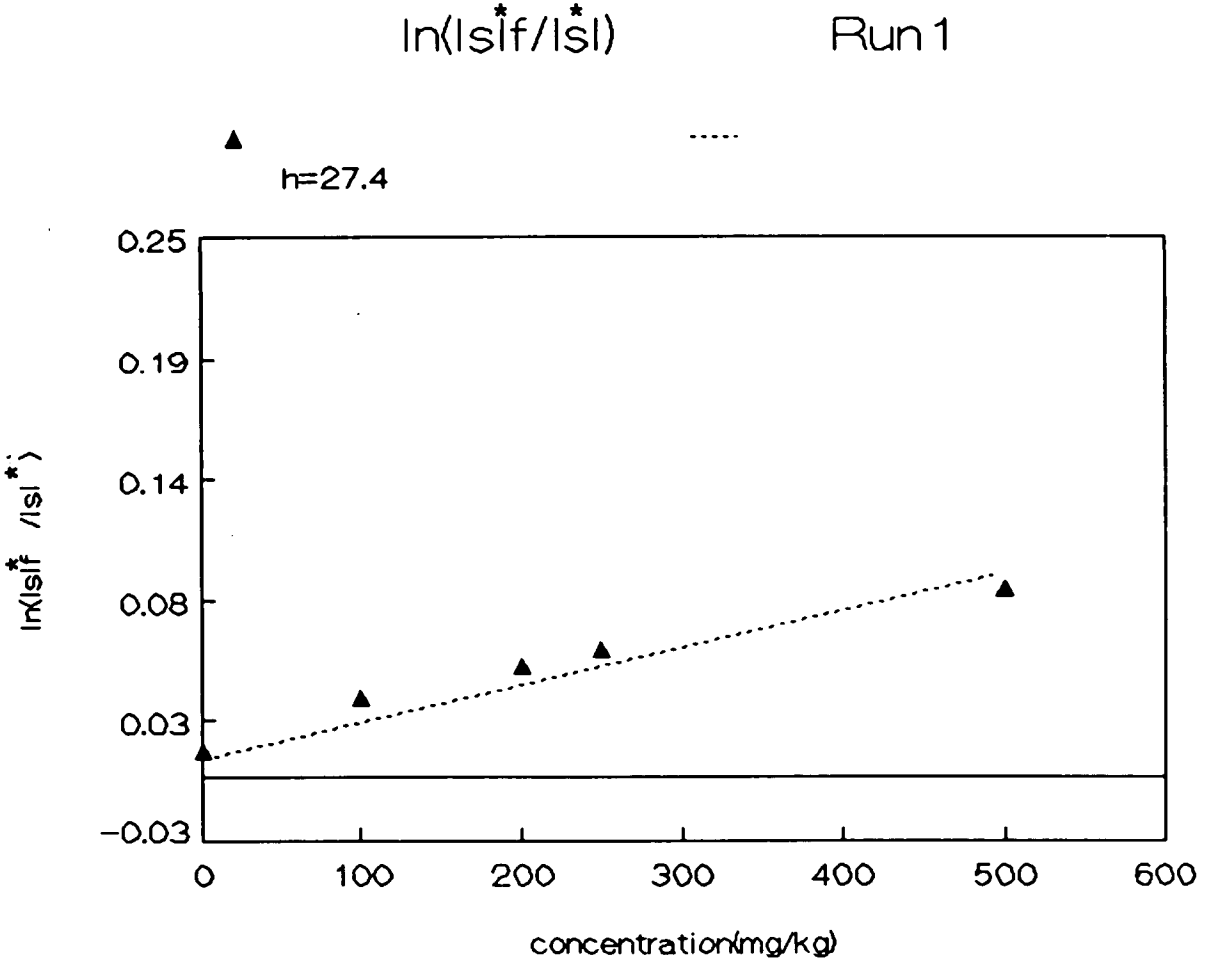
ln(Is*f/Is*l)
Run 1
h=27.4
0.25
0.19
0.14
0.08
0.03
-0.03
0
100
200
300
400
500
600
concentration(mg/kg)

FIGURE 3A

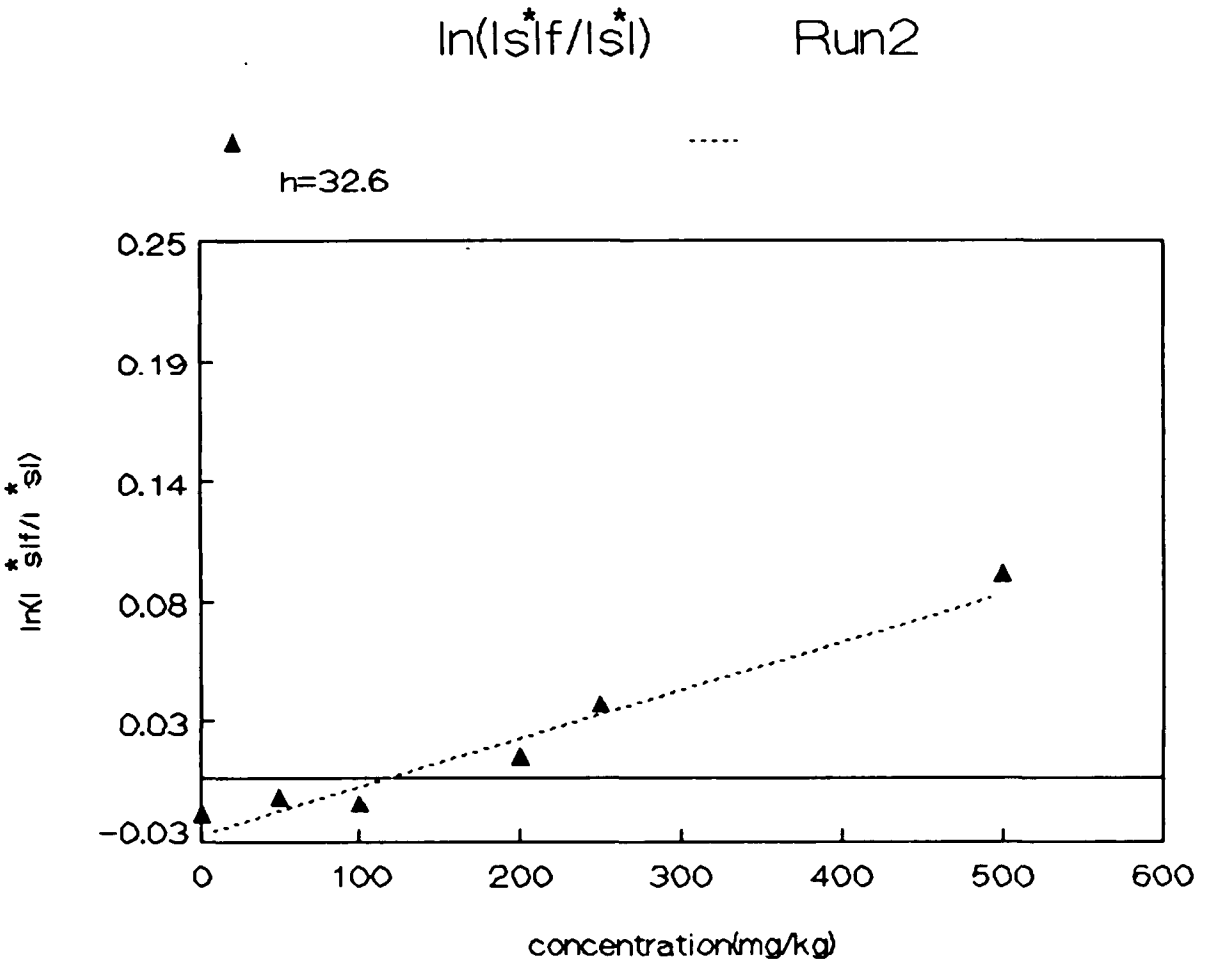
ln(Is*If/Is*I)
Run2
h=32.6
0.25
0.19
0.14
0.08
0.03
-0.03
0
100
200
300
400
500
600
concentration(mg/kg)

FIGURE 3B

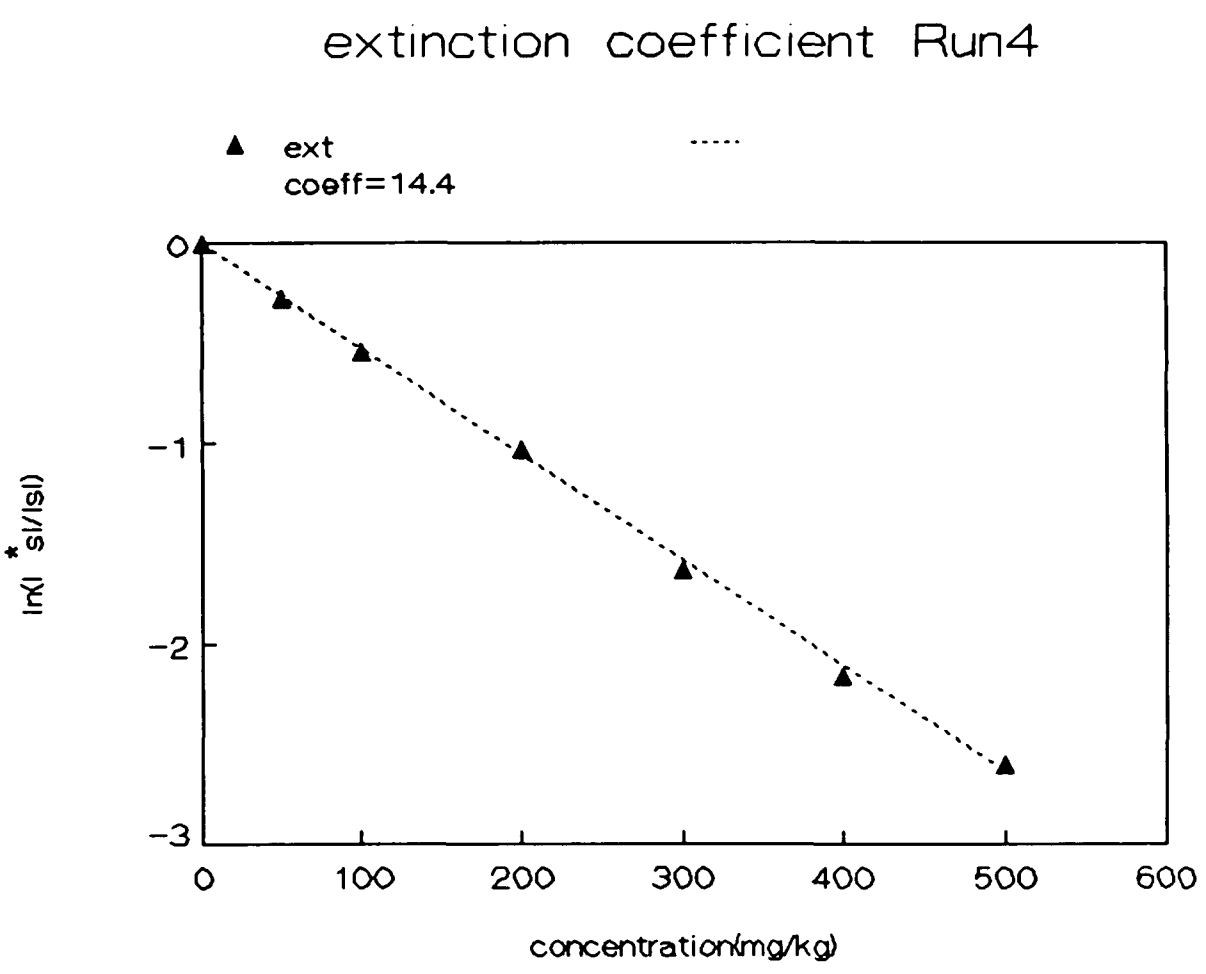
extinction coefficient Run4
ext
coeff=14.4
0
-1
-2
-3
ln(I *sI/IsI)
0
100
200
300
400
500
600
concentration(mg/kg)

FIGURE 4

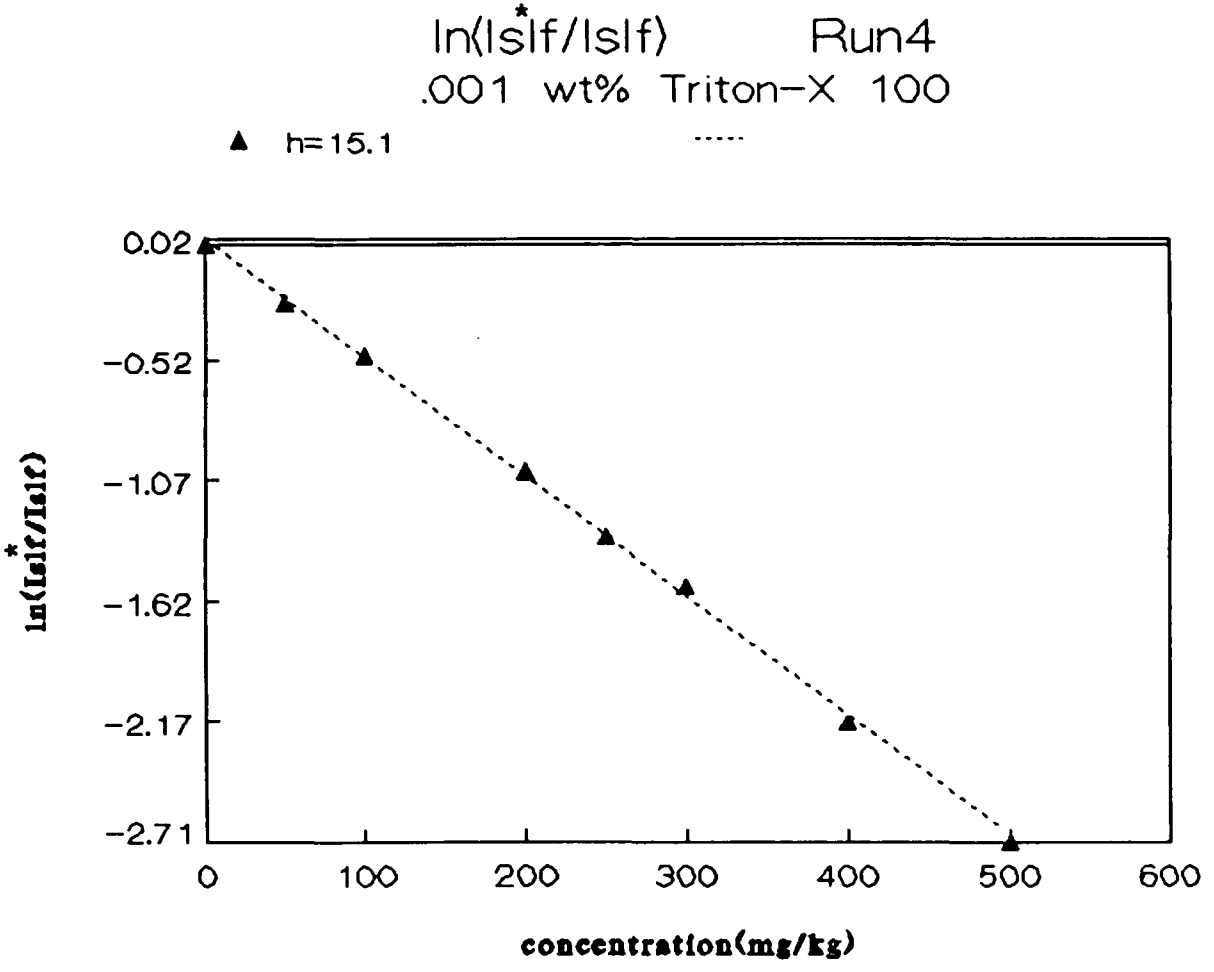
ln(Is*If/IsIf) Run4
.001 wt% Triton-X 100
h=15.1
0.02
-0.52
-1.07
-1.62
-2.17
-2.71
0
100
200
300
400
500
600
ln(Is*If/IsIf)
concentration(mg/kg)

FIGURE 5A

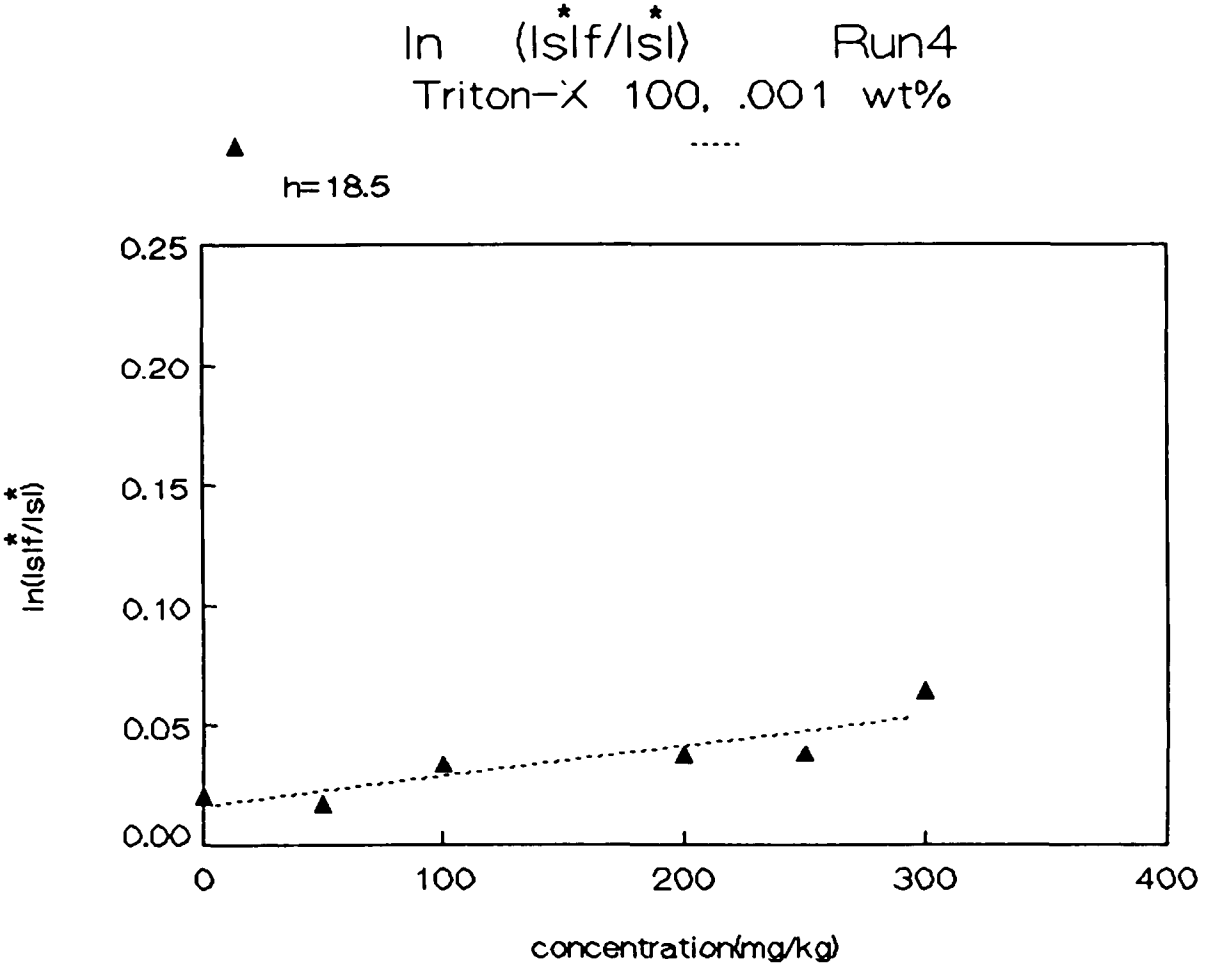
ln (Is*If/Is*) Run4
Triton-X 100, .001 wt%
h=18.5
0.25
0.20
0.15
0.10
0.05
0.00
ln(Is*If/Is*)
0
100
200
300
400
concentration(mg/kg)

FIGURE 5B

TABLE 1

Run extinction	ϵ'(g cm/kg)$^{-1}$ (eq.4.5ii) coefficient	h'	h'_{check} (eq. 4.5iii)
Run 1	14.93	27.3μ	27.4μ
Run 2	14.95	32.2μ	32.6μ
Run 3	14.95*	32.6μ	

*Runs 2 and 3 performed on same piece of tubing; the same extinction coefficient is used for both runs.

References

1. Adamczyk, Z., 1987, "Nonequilibrium Surface Tension and Mixed Sorption Kinetics," J. Colloid and Interface Sci., 120(2), 477-485

2. Adamczyk, Z., and Petlicki, J., 1987, "Adsorption and Desorption Kinetics of Molecules and Colloidal Particles," J.Colloid and Interface Sci., 118(1), 20-49

3. Agrawal,S.K. and Wasan, D.T. 1979 "The Effect of Interfacial Viscosities on the Motion of Drops and Bubbles" Chem.Eng.J.,18, 215-223

4. Aveyard, R., and Vincent, B. Prog. Surface Sci. , 8, 59 (1977)

5. Barthes-Biesel, D., Moulai-Mostefa, N., and Meister, E., 1988, "Effect of Surfactants on the Flow of Large Gas Bubbles in Capillary Tubes" in press

6. Beitel, A. and Heideger, W.J., 1971, "Surfactant Effects on Mass Transfer from Drops Subject to Interfacial Instability," Chem. Eng. Sci., 26 4, 711-717

7. Bretherton, F.P., 1961,"The Motion of Long Bubbles in Tubes," J.Fluid Mech.,10, 166-188

8. Burke, R.W., and Mavrodineanu, R. ,"Certification and Use of Acidic Potassium Dichromate Solutions as an Ultraviolet Absorbance Standard"

9. Chen, J.D., 1985, "Measuring the Film Thickness Surrounding a Bubble Inside a Capillary", 109 , 341-349

10. Chiwetelu, C.I., Hornof, V., and Neale, G.H., 1988, "The Measurement of Dynamic Interfacial Tension by Photomicropendography," J. Colloid Interface Sci., 125(2), 586-601

11. Cox, B.G., 1962, "On Driving a Viscous Fluid Out of a Tube," J.Fluid Mech., 14, 81-98

12. Davis, R.E., and Acrivos, A., 1966, "The Influence of Surfactants on the Creeping Motion of Bubbles," Chem. Eng. Sci.,21, 681-685

13. Elzinga, E.R. and Banchero, J.T., 1961, "Some Observations on the Mechanics of Drops in Liquid-Liquid Systems," AIChE J., 7, 394

14. Fairbrother, F., and Stubbs, A., 1935, "Studies in Electrodosmosis. Part IV. The Bubble-Tube Methods of Measurement," J. Chem. Sci., 1, 237-261

15. Frumpkin, A. and Levich, V.G., 1947, Zh. Fiz. Khim. 21, 1183

16. Garner, F.H. and Skelland, A.H.P., 1955, "Some Factors Affecting Droplet Behavior in Liquid-Liquid Systems," Chem Eng. Sci. , 4 , 149

17. Gauglitz, P.A., and Radke, C.J., "The Role of Wettability in the Breakup of Liquid Films Inside Constricted Capillaries", Thin Liquid Film Phenomena, AIChE Symposium Series 252, V82, (1986)

18. Ginley, G.M. and Radke, C.J., 1987, "The Influence of Soluble Surfactants on The Flow of Long Bubbles Through a Cylindrical Capillary," in press

19. Girault, H.H., Schiffren, D.J., and Smith, B.D.V., 1982, "Drop Image Processing for Surface and Interfacial Tension Measurements," J. Electroanal. Chem., 137, 207-217

20. Girault, H.H., Schiffren, D.J., and Smith, B.D.V., 1984, "The Measurement of Interfcial Tension of Pendant Drops Using a Video Image Profile Digitizer," 101(1), 257-266

21. Goldsmith, H.L., and Mason, S.G., 1963, " The Flow of Suspensions Through Tubes II. Single Large Bubbles," J. Colloid Sci., 18, 237-261

22. Graham, D.E., and Phillips, M.C., 1978, "Proteins at Liquid Interfaces" I. Kinetics of Adsorption and Surface Denaturation," J. Colloid Interface Sci., 70(3), 403-414

23. Graham, D.E., and Phillips, M.C., 1978, "Proteins at Liquid Interfaces" II.Adsorption Isotherms," J. Colloid Interface Sci., 70(3), 415-426

24. Graham, D.E., and Phillips, M.C., 1978, "Proteins at Liquid Interfaces" III. Molecular Strucures of Adsirbed Films," J. Colloid Interface Sci., 70(3), 415-426

25. Griffith, R.M., 1962, "The Effect of Surfactants on the Terminal Velocity of Drops and Bubbles," Chem Eng. Sci., 17, 1057

26. Guzman, R., Carbonell, R.G., and Kilpatrick, P.K., 1986, "The Adsorption of Proteins to Gas-Liquid Interfaces," J. Colloid Interface Sci., 114(2), 536-547

27. Harper, J.F., 1972, "The Motion of Bubbles and Drops Through Liquids," Adv. Appl. Mech., 12, 59-129

28. Harper, J.F., 1973, "On Bubbles with Small Immobile Adsorbed Films Rising in Liquids at low Re," J.Fluid Mech., 58, 539-545

29. Harper, J.F., 1982, "Surface Activity and Bubble Motion," Adv. Appl. Sci. 35, 343-351

30. Hirasaki, G. and Lawson, J.B., 1986, "SPE J. 25, 176

31. Horton, Y.J., Fritsch, T.R., and Kintner, R.C., 1965, "Experimental Determination of Circulation Velocities Inside Drops," Can. J. Chem. Eng., June 1965, 143-146

32. Huang, W.S. and Kintner, R.C. , 1969, "Effects of Surfactants on Mass Transfer Inside Drops", AIChE J., 15 ,Sept. 735-744

33. Huh, C. and Reed, R.L. , 1983, " A Method for Estimating Interfacial Tensions and Contact Angles from Sessile and Pendant Drop Shapes," J. Colloid Interface Sci., 91(2), 472-484

34. Joos, P., and Rillaerts, E., 1981, "Theory on the Decermination of the Dynamic Surface Tension with the Drop Volume and Maximum Bubble Pressure Methods," J. Colloid Interface Sci., 79(1), 96-100

35. Kim, H.S., and Subramaniam, R.S., 1988, "The Thermocapillary Migration of a Droplet with Insoluble Surfactant " Parts I&II, J. Colloid Interface Sci., accepted for publication,

36. Le Van, M.D., and Holbrook, J.A., 1982, "Retardation of Droplet Motion by Surfactant. Part I. Theoretical Development and Asymptotic Solutions" Chem. Eng. Comm., 20 , 191-207

37. Le Van, M.D., and Holbrook, J.A., 1982, "Retardation of Droplet Motion by Surfactant. Part II. Numerical Solutions for Exterior Diffusion, Surface Diffusion, and Adsorption Kinetics" Chem. Eng. Comm., 20 , 191 - 207

38. Le Van, M.D. and Newman, J., 1976, "The Effect of Surfactant on the Terminal and Interfacial Velocities of a Bubble or Drop," AIChE J., 22, 695

39. Levich, V.G., Physicochemical Hydrodynamics pp. 409-420, Prentice Hall, Englewood CLiffs, N.J., 1962

40. Levich, V.G., and Krylov, V.S. , 1969, "Surface Tension-Driven Phenomena",Annual Review of Fluid Mech., 1 , 293-316

41. Lin, S.Y., McKiegue, K., and Maldarelli, C., 1989, "The Measurement of Diffusivities and Sorption Kinetic Constants by Transient Pendant Drop Tensiometry using a Digitized Image of a Pendant Drop," J. Colloid Interface Sci. . (submitted for publication)

42. MacRitchie, F. and Alexander, A.E., 1962, "Kinetics of Adsorption of Proteins at Interfaces Part I. The Role of Bulk Diffusion in Adsorption," J. Colloid Sci., 18 , 453-457

43. MacRitchie, F. and Alexander, A.E., 1962, "Kinetics of Adsorption of Proteins at Interfaces Part II. The Role of Pressure Barriers in Adsorption," J. Colloid Sci., 18 , 458-463

44. Marchessault, R.H. and Mason, S.G., 1960, "flow of Entrapped Bubbles through a Capillary," Ind. Eng. Chem., 52,(1) 79

45. Martinez, M.J., and Udell, K.S., 1988, "Boundary Integral Analysis of the Creeping Flow of Long Bubbles in Capillaries," J. Appl. Mech. (in press)

46. Martinez, M.J., and Udell, K.S., 1988, "The Axisymmetric Creeping Motion of Drops Through Circular Tubes" J. Appl. Mech. (in press)

47. Miller, R. and Kretzschmar, G. "Numerische Losung fur ein gemischtes
Modell der diffusion-kinetik-kontrollierten Adsorption" Colloid Polymer Sci., 258 ,85 (1980)

48. Newman, J. , 1966 "Retardation of Falling Drops", Chem Eng. Sci. 22, 83- 85

49. Park, C.W. and Homsy, G.M., 1983, "Two Phase Displacement in Hele Shaw Cells: Theory," J. Fluid Mech., 139, 291-308

50. Ratulowski, J., and Chang, H.C., 1989, "Transport of Gas Bubbles in Capillaries," Phys. Fluids, 1, No.10

51. Reinelt, D.A., 1986, "The Rate at which a Long Bubble Rises in a Vertical Tube," J. Fluid Mech., 175, 557-565

52. Reinelt, D.A., and Saffman, P.G., 1985, "The Penetration of a Finger into a Viscous Fluid in a Channel and Tube", SIAM J. Sci Stat. Comp. , 6, 542-561

53. Reinelt, D.A., 1987, "Interface Conditions for Two Phae Displacement
In Hele-Shaw Cells", J. Fluid Mech., 183, 219-234

54. Rillaerts, E. and Joos, P., 1982, "Rate of Demicellization from the Dynamic Surface Tensions of Micellar Solutions," J. Phys. Chem., 86 , 3471-3478

55. Rotenberg, Y., Boruvka, L., and Neuman, A.W., 1983, "Determination of Surface Tension and Contact Angle from the Shapes of Axisymmetric Fluid Interfaces," 93(1), 169-183

56. Savic, P., 1953, "Circulation and Distortion of Liquid Drops Falling Through a Viscous Medium." Rept. MT-22, Division of Mechanical Engineering, National Research Council of Canada

57. Sadahl, S.S. and Johnson, R.E., 1982 "Stokes Flow Past Bubbles and Drops Partially Coated with Thin Films, Part I. Stagnant Cap of Surfactant Film- Exact Solution," J. Fluid Mech., 126, 237-250

58. Saville, D.A., 1973, "The Effects of Interfacial Tension Gradients on the Motion of Drops and Bubbles," Chem. Eng. J., 5 251

59. Schechter, R.S. and Farley, R.W., 1963, "Interfacial Tension Gradients and Drop Behavior", Can. J. Chem. Eng., 41, 103

60. Scheludkl, A. 1963, Kolloid Z., 191, 52

61. Schwartz, L.W., Princen, H.M., and Kiss, A.D., 1986, "On the Motion of Bubbles in Capillary Tubes," J. Fluid Mech. 172, 259-275

62. Shen, E.I. and Udell, K.S. ,1985, "A Finite Element Study of Low Reynolds Number Two-Phase Flow in Cylindrical Tubes," J. Appl. Mech., 52, 253-256

63. Taylor, G.I., 1961, "Deposition of a Viscous Fluid on the Wall of a Tube" ,J. Fluid Mech., 10, 161-165

64. Ter Minassian-Saraga, L. 1980, "Protein Denaturation on Adsorption and Water Activity at Interfaces: An Analysis and Suggestion," J. Colloid Interface Sci., 80(2), 393-401

65. Wasserman, M.L., and Slattery, J.C., 1969, "Creeping Flow Past a Fluid Globule When a Trace of Surfactant is Present," AIChE J., 15, 533-548

66. Van Hunsel, J.V., Bleys, G. and Joos, P., 1986, "Adsorption Kinetics at the Oil/Water Interface," J. Colloid Interface Sci., 114(2), 432-441